technische universität
dortmund

Study on CO$_2$ Capture Using Thermomorphic Biphasic Solvents with Energy-Efficient Regeneration

Zur Erlangung des akademischen Grades eines

Dr.-Ing.

vom Fachbereich Bio- und Chemieingenieurwesen der Universität Dortmund

Dissertation

vorgelegt von

M.Sc. Jiafei Zhang

aus

Hangzhou, V.R. China

Dortmund 2013

Abstract

Chemical absorption with amine solvent is the most dominated commercial technology adapted for CO_2 capture from power plant to mitigate the climate change and global warming issues. However, significant energy consumption and irreversible solvent degradation are the major unsolved challenges occurred in the amine-based post-combustion capture (PCC) process. It is therefore essential to develop new solvents and advanced technologies to overcome these drawbacks of conventional alkanolamines. In this paper a novel thermomorphic biphasic solvent (TBS) system has been studied as one of the alternative solutions to improve the solvent-based PCC process.

A series of screening experiments have been conducted to select suitable lipophilic amines as activating components for CO_2 absorption. The influence of molecular structure on absorption and desorption characteristics has also been investigated to predict and design potential lipophilic amine absorbents. According to the performance parameters, the selected lipophilic amines have been classified into two categories: absorption activator, for example N-methylcyclohexylamine (MCA) with rapid reaction kinetics, and regeneration promoter, for instance N,N-dimethylcyclohexylamine (DMCA) exhibiting excellent regenerability. Amine molecules with an α-carbon branch such as 2-ethylpiperidine (2-EPD) are of great interest due to their fast reaction rate and good CO_2 absorption capacity. To meet the selection criteria of the ideal solvent for chemical absorption, solvent recipes have been optimised by blending two or three amines and evaluated in a 100 mL glass bubble column with varying temperatures from 25 to 85 °C and CO_2 partial pressures between 4-100 kPa. The formulated TBS absorbents have exhibited rapid reaction kinetics, high cyclic CO_2 loading capacity, excellent solvent regenerability, moderate energy demand and low solvent degradation.

However, the undesired heterogeneous solution formed in absorber and evident volatile losses represent new challenges for lipophilic amines. With addition of a small amount of solubiliser such as 2-Amino-2-methyl-1-propanol (AMP), the phase change temperature has been increased dramatically and a homogeneous solution can thus be employed in absorption. Such solubilised biphasic solvent, e.g. a blended absorbent comprising DMCA+MCA+AMP, forms a single phase at 40 °C in the absorber and converts to two phases at an elevated temperature of 80 °C in the desorber. Therefore, a conventional absorption column can be employed for CO_2 capture using TBS without

any modification. To eliminate the issue of solvent vaporisation loss, an additional scrubbing unit with high boiling point organic solvent has been proposed to recover the vapour of lipophilic amine exhausted with the treated gas at the top of absorber. Additionally, the integration of an inter-stage cooling system into the absorption column has also been suggested for not only reducing the vaporisation losses but also enhancing the CO_2 loading capacity.

Further investigations on solvent degradation have found the thermal degradation of lipophilic amines is minor owing to the lower desorption temperature required, typically 90 °C, compared to that for conventional stripping process of over 120 °C. The oxidative degradation of absorption activators, e.g. MCA, is significant, but it is negligible for regeneration promoters such as DMCA. Ketonisation and oximation were observed as the main reactions for MCA, while methylation and demethylation occurred with DMCA. The optimised solvent recipe DMCA+MCA+AMP exhibited a good chemical stability against both thermal and oxidative degradations.

To exploit the low-value heat for solvent regeneration in place of steam stripping, preliminary studies on new desorption techniques such as nucleation, agitation, ultrasound and extraction have been conducted. Nucleation accelerates the CO_2 releasing from the rich solvent, but hardly achieves deep regeneration at 80-90 °C; while agitation and ultrasonic desorption are both comparable to the stripping method, but only have insignificant mechanical or electrical energy consumption. The energy consumption in extractive regeneration is slightly higher than other intensification techniques, but it reduces the required desorption temperature to only 60-70 °C and cuts the exergy demand further with an extended freedom for integrating the process heating network or even using waste heat for regeneration purposes.

After optimisation of the solvent recipe and adaptation of novel regeneration techniques for CO_2 capture using TBS, bench scale experiments in a 40 mm I.D. glass packed column with 1 m height random packings have been carried out to investigate the influence of amine solutions on the packing wettability. Both the pressure drop and liquid hold-up of TBS were observed to be higher than for MEA at the same gas load factor, mainly due to the higher viscosity of the CO_2 loaded TBS solution. The viscosity of lean TBS solution is lower than that of alkanolamines, but it increases dramatically after CO_2 loading and rises to more than 10 mPa·s at room temperature. TBS solution presents a lower surface tension and a smaller contact angle on various metal and plastic materials compared to MEA. This thus directly indicates a good wettability of TBS on

packings even using certain plastic materials such as high-density polyethylene (PE-HD) in the absorption column.

Several modified process flow diagrams have been developed according to the various desorption techniques. The energy consumption has also been estimated for corresponding process flowsheeting. The main saving of the regeneration energy for TBS process is not in the heat of reaction but in the sensible heat and latent heat, since the reaction enthalpies for absorption activators are even higher than for the benchmark MEA, but the lower regeneration temperature enhances the process heat integration and significantly reduces the exergy demand. The outstanding performance parameters of such TBS system together with those novel intensified and energy-effective regeneration techniques make it one of the most promising candidates to assess the technical viability in further development work for future CO_2 capture processes.

Acknowledgements

I would like to express my sincere gratitude to Professor David Agar for being my supervisor and giving advice during the whole research project and support to finalize my PhD dissertation. I am also sincerely grateful to Dr. Frank Geuzebroek, ir. Mark Senden, Dr. Xiaohui Zhang and Dr. Robert Moene from Shell Global Solutions not only for providing me this amazing opportunity to have financial support but also for their kind advice to give impetus to my research and without whom the project could not have been accomplished.

My thanks go to the staff of the Chair of TCB who have lent a hand and contributed to all of the aspect of my study, especially to Dr. Yudy Tan for his kind assistance to help me start up my research and his brilliant suggestions on this CO_2 absorption project as well as to Michael Schlüter, Julian Gies and Jerzy Konikowski for their willingness to provide me with excellent technical support. Thanks to Kachi, Robert, Yu, Wangzhong, Khuram and Jing for their remarkable contribution during their Master's theses or practical research projects.

I would also like to address my thanks to Dr. Frank Katzenberg at the Chair of BMP who has kindly provided the convenience of using the contact angle measurement apparatus, Dr. Günther Neue at the Chemistry Department who lent me the tensiometer, Dr. Siegfried Gantert at BTU-Cottbus who has helped me to carry out the ultrasonic desorption test and Mr. Phill O'Kane from Thermal Hazard Technology who has conducted the heat of absorption measurement for my referencing. Thank you to the Lanxess AG, the Raschig GmbH and the departmental mechanic workshop, who have generously provided some special chemicals and materials for my experiment.

Finally, special thanks to my beloved mother and father for their understanding and support to my many years' study abroad.

Jiafei Zhang   *Chemische Verfahrenstechnik*

Table of Contents

Jiafei Zhang   *Chemische Verfahrenstechnik*

List of Tables

List of Figures

ix

x

Abbreviation

ACV	Absorption activator
BF	Bicarbonate formation
bp.	Boiling point
BLD	Blended solvent
BS	Berl-Saddle
CCS	Carbon Capture and Storage
CF	Carbamate formation
CR	Carbamate reversion
CST	Critical solution temperature
CSTR	Continuous stirred tank reactor
DMX	Demixing
GC	Gas chromatography
HSSs	Heat stable salts
iCap	innovative CO_2 capture
IGCC	Integrated gasification combined cycle
IHB	Inhibitor
LCST	Lower critical solution temperature
LLPS	Liquid-liquid phase separation
MS	Mass spectrometry
PCC	Post-combustion carbon capture
PRM	Regeneration promoter
PST	Phase separation temperature
RR	Raschig ring
RS	Raschig super ring
TBS	Thermomorphic biphasic solvent
UCST	Upper critical solution temperature
VLE	Vapour-liquid equilibrium
WS	Wilson ring

Abbreviation for all the amines is listed in Appendix A.

Nomenclature

a	Specific surface	[m^2]
A	Surface area	[m^2]
c_i	Concentration of component i	[mol/L]
d	Diameter	[m]
C_p	Specific heat capacity	[kJ/(kg·K)]
E	Extraction coefficient	[-]
E_{vap}	Latent heat of evaporation	[kJ]

F	Specific mass flow	[kg/mol$_{-CO2}$]
F	Load factor	[Pa$^{0.5}$]
g	Gravity on Earth,	[m/s^2]
h	Height	[m]
h_{dyn}	Dynamic liquid hold-up	[m^3/m^3]
$\Delta_r H$	Heat of absorption / desorption	[kJ/mol$_{-CO2}$]
K	Capillary constant	[-]
K_c	Partition coefficient	[-]
L_v	Specific latent heat for vaporization	[kJ/kg]
m_i	Mass of component i	[kg]
M_r	Relative molecular weight	[-]
n	Number of stages	[-]
p	Pressure	[kPa] or [bar]
P	Power	[W]
Q	Heat	[kJ]
R	Reflux ratio	[-]
R	Gas constant: 8.314	[J/(mol·K)]
T	Temperature	[K] or [°C]
t	Time	[s]
u	Velocity	[m/s]
V_i	Volume of component i	[m^3]

Greek symbols

α	CO$_2$ loading capacity	[mol$_{-CO2}$/L$_{-sol}$] or [mol$_{-CO2}$/mol$_{-amine}$]
δ	Solubility parameter	[MPa$^{0.5}$]
ε	Porosity	[-]
η	Effective coefficient for extraction	[-]
θ	Contact angle	[°]
μ	Dynamic viscosity	[cP] or [mPa·s]
v	Kinematic viscosity	[cSt] or [mm^2/s]
ρ	Density	[kg/m^3]
σ	Surface tension	[mN/m]
Φ	Heat loss coefficient	[W/(m^2·K)]

Subscripts

C	Column
G	Gas
L	Liquid
P	Packing
r	Reaction
s	Sample
v	Vaporisation
w	Water
W	Wall

1 Introduction

1.1 Response to climate change

1.1.1 Reduction of CO_2 emission

Anthropogenic CO_2 emission from fossil fuels combustion is considered to be one of the main causes of global climate change. Fossil fuel-fired power plant contributes the largest worldwide CO_2 emissions. In order to mitigate the climate change, strategies such as improvement of energy efficiency, development of low CO_2 sources of energy and acceleration of CO_2 Capture and Storage (CCS) solutions have been proposed for reducing the greenhouse gas emission (IPCC, 2005; Riemer, 1996).

Due to the present extent of fossil fuels use, CCS, including capture (separation from gas mixtures and compression to supercritical conditions), transport and storage (injection, measurement, monitoring and verification), is one of the most promising technologies for emission reduction (Steeneveldt et al., 2006).

1.1.2 CO_2 capture technologies

CO_2 capture is a process of removing CO_2 produced by hydrocarbon combustion (coal, oil and gas) before its emission to the atmosphere. Both economic and energy costs are the major considerations in its use for large CO_2 sources such as power stations and industrial plants. There are three major approaches for carbon capture: post-combustion capture, pre-combustion capture, and oxy-fuel combustion process (IPCC, 2005; Stolten and Scherer, 2011).

Table 1. Typical composition of flue gases

(unit: %)	CO_2	N_2	O_2	H_2O	NO_x	SO_x	Ar
Coal-fired	12-16	75-80	2-4	10-15	400 ppm	150 ppm	0.82
Gas-fired	3-5	70-75	10-12	7-10	<50 ppm	<10 ppm	0.89

Post-combustion capture is a technology removing CO_2 from flue gas after combustion. It can be applied to conventional fossil fuel-fired power plants with an additional CO_2 capture unit, separating CO_2 from gas mixtures with N_2, O_2, water vapour and other trace gas impurities. Table 1 shows the typical composition of flue gases from coal- and gas-fired power plants (Rolker and Arlt, 2006). Because of the low CO_2 partial pressure, chemical absorption is favoured for this process, but high energy consumption for solvent thermal regeneration is the major shortcoming. Since other

1

contaminant gases such as O_2, SO_x, and NO_x can be present in flue gases, solvent degradation also becomes a challenge (MacDowell et al., 2010; Tönnies et al., 2011).

Pre-combustion capture refers to a process removing of CO_2 prior to combustion. It firstly transforms the gaseous hydrocarbon fuel (CH_4 or gasified coal) to a synthesis gas (H_2 and CO) and then converts CO to CO_2 by reacting it with H_2O to produce H_2 for combustion. By finally separating CO_2 from H_2, water vapour is the main by-product after combustion. It is applicable to natural gas- and coal-fired integrated gasification combined cycle (IGCC) power plants. However, the requirement of a gas treating chemical plant, high investment cost for building a new plant, low efficiency of H_2 burning and less flexibility are the main disadvantages.

Oxy-fuel combustion capture involves burning fossil fuel with pure oxygen in place of air, so that the flue gas consists of mainly CO_2 ($\approx$90 vol.%) and water vapour. By condensation of the water vapour, CO_2 can be easily separated for compression. However, high energy penalty for O_2 production is the significant shortcoming. The features of those capture processes are summarised in Table 2.

Table 2. Comparison of CO_2 capture technologies

Process	Separation	Typical methods
Post-combustion	CO_2 vs. N_2	***Chemical absorption*** Carbonate looping Solids adsorption
Pre-combustion	CO_2 vs. H_2	Chemical absorption Carbonate looping Membranes
	H_2 vs. CO_2	Solids adsorption Membranes
Oxy-fuel combustion	O_2 vs. N_2	Cryogenic air separation Chemical looping Membranes

1.2 Chemical absorption

1.2.1 Conventional solvents and improvements

Chemical absorption using amine-based solvents is the most promising commercial technology for post-combustion carbon capture (PCC). Amine scrubbing is presently both the preferred option and probably the only commercially mature technology for

2

1. Introduction

CO_2 removal. However, it has been estimated that the desorption step would be responsible for more than half of the overall processing costs, primarily due to the high energy consumption for the solvent regeneration (Meldon, 2011; Rao et al., 2002; Straelen and Geuzebroek, 2011; Wang et al., 2011).

Monoethanolamine (MEA), a primary amine, is the most commonly used solvent for CO_2 scrubbing and can also be employed in PCC process (Kohl et al., 1997; Rochelle, 2009), but it has several weaknesses: (a) low net CO_2 loading capacity, (b) solvent degradation, (c) corrosion and (d) high energy consumption. For reduction of reaction enthalpy and enhancement of net CO_2 capacity, N-methyldiethanolamine (MDEA) as a tertiary amine and 2-Amino-2-methyl-1-propanol (AMP) as a sterically hindered amine have also been suggested as alternative absorbents, but limited reaction kinetics is a serious shortcoming. Many research groups have thus focused on finding new absorbents for CO_2 absorption with following criteria:

- Reduced energy consumption
- High reactivity and capacity with respect to CO_2
- Minor environmental impact
- Low degradation and corrosion

A research team at the Research Institute of Innovative Technology for the Earth (RITE) in Japan screened various aqueous tertiary amine solvents to mitigate the energy requirements by lowering absorption heat, with only a modest modification on CO_2 loading capacity and reactivity (Chowdhury et al., 2009 and 2011). Some undisclosed solvents, which can allegedly cut the regeneration energy by ~30% compared to MEA, were investigated by several researchers (Goto et al., 2009 and 2011; Kim et al., 2011; Knudsen, 2007; Notz et al., 2007; Puxty et al., 2009), but the desorption still needs to be carried out with steam stripping at over 120 °C. Blended amine solvents such as MEA+MDEA and MEA+AMP can be an approach to achieve better performance parameters in both absorption and regeneration. Recently, the CESAR project (Mangalapally and Hasse, 2011) undisclosed their absorbents such as piperazine (PZ) activated AMP and EDA (1,2-Ethanediamine) and Rochelle et al. (2011a) also recommended the use of PZ-activated K_2CO_3 or MDEA, however, the desorption temperature required for PZ is higher than 150 °C. In addition, Alstom proposed a chilled ammonia process to reduce the regeneration cost (Telikapalli et al., 2011), but the low temperature and high pressure required for limiting ammonia vaporisation was still a big challenge.

Singh et al. (2007, 2008, 2009 and 2011) screened various amines for identifying new alternative absorbents and demonstrated that alkyl and amine groups were found to be the most suitable substituted functional groups for enhancing CO_2 loading capacity and solvent regeneration. However, their study was limited to single phase solutions.

1.2.2   Conventional processes and modifications

An absorption column and stream stripping column with associated heat exchangers comprise the most important units for a chemical CO_2 scrubbing process. As seen in Figure 1, the cooled lean solvent from regenerator is fed to the top of absorber for scrubbing the cooled flue gas contacted counter-currently; the treated gas is then washed by water to scrub the vaporised solvent and vented to the atmosphere; the rich solvent attained at the bottom of absorber is warmed up through a cross-flow heat exchanger by the regenerated lean solvent and sent to the stripper; where absorbed CO_2 is liberated form solvent by thermal treatment in stripper and sent to compression; the regenerated solvent is recycled to the absorber after cooling. Heat supplied to the reboiler at the bottom of stripper contributes the major energy penalty of the whole process. The high temperature applied for steam stripping leads to thermal solvent degradation and oxygen contained in flue gas causes oxidative solvent degradation. A reclaimer is thus required to remove the heat stable salts (HSSs) formed in the system.
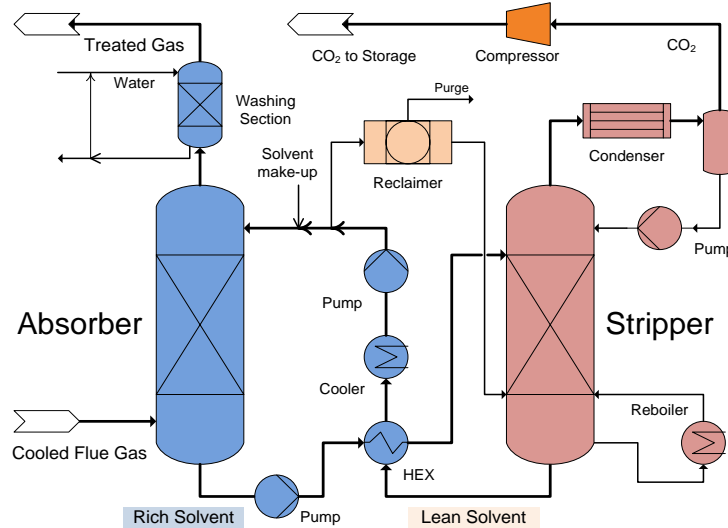
Figure 1. Basic process flow scheme for PCC

To improve the absorption characteristics or to reduce the energy consumption, process flow sheet modifications such as inter-stage cooling in absorption, split flow, lean split and rich split in desorption were proposed (Cousins et al., 2011). Absorption

1. Introduction

of CO_2 into amine solutions is an exothermic reaction resulting in a temperature increase in absorber, which limits the driving force for absorption and reduces CO_2 loading capacity of amine solvent, although the kinetics becomes more favourable at higher temperatures. An overall consideration recommends an operating temperature for absorption at 40-60 °C to achieve the highest mass transfer rates (Aroonwilas, 2004). A process flow scheme with temperature controlling with in absorption column can potentially improve the vapour-liquid equilibrium. _Inter-stage cooling_ for absorber was previously devised by Woertz (1966). It can be located at each available position along the column, where the liquid flow is withdrawn from the column and cooled to suitable temperature, typically at 40 °C, and then recycled to the column at the same location. Such process modification proved able to enhance the CO_2 loading capacity but the reboiler duty was subsequently slightly increased.

(A) Inter-stage cooling   (B) Split flow
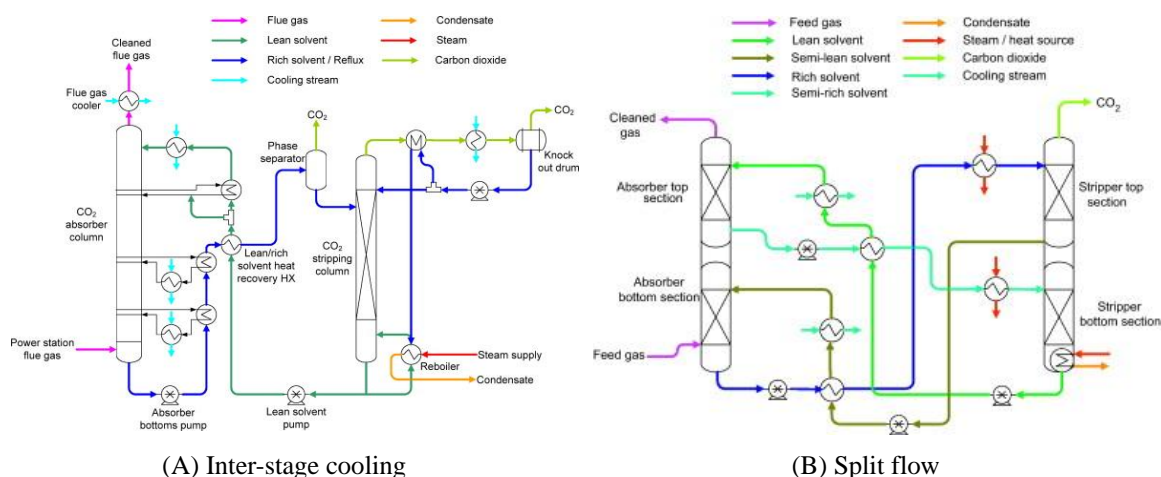
Figure 2. Modified process flow diagrams with inter-stage cooling and split flow
(Aroonwilas, 2004; Cousins et al., 2011; Shoeld, 1934)

The high thermal energy required for desorption is the major challenge for development of amine-based absorption technology. Shoeld (1934) hence suggested a _split flow_ _process_, where the rich solution from the bottom of the absorber is divided into two streams, one being fed to the top of the desorber and the other to the midpoint. The top stream flows downwards counter-current to the stream of rising vapours and is withdrawn at a point above the midpoint which is the inlet of the second portion of the rich solution. The liquid withdrawn from the upper portion of the desorber is not completely stripped and is recycled back to the absorber column at the midpoint to absorb the CO_2 in the lower portion of the absorber column where the CO_2 concentration is still high. This semi-lean-process is thus called _partial regeneration_.

5

The portion of solution, which is introduced near the midpoint of the desorber, flows towards the bottom and is very thoroughly stripped of absorbed CO_2. This solution is returned to the top of the absorber column where it serves to reduce CO_2 content of the product gas to the desired low level. In this system, the quantity of vapours rising through the desorber is less than that in a conventional plant (Kohl et al., 1997). The whole process is hence called *partial deep regeneration*. The split-stream cycle can also be simplified by dividing the lean (or rich) solution before its entrance into the absorber (or desorber) into two unequal streams so called *lean split* (or *rich split*) process (Estep et al., 1962; Eisenberg et al., 1979), which may be more economical than the basic flowsheet, since the splitted major stream can be warmed to a higher temperature before it enters to stripper and the reboiler duty is thus reduced.

1.2.3 New generation CO_2 capture technologies

Due to drawbacks of conventional MEA-based CO_2 capture process, which is regarded 1st generation technology (G1), new generation technologies were proposed to overcome such shortcomings, especially in energy consumption and degradability. Development of alternative solvents or modification of process flow scheme such as using inter-cooling in absorber, split-flow and heat exchange integration in stripper are so called 2nd generation technology (G2). A scope for further improvement of capture technology in the overall process efficiency using novel absorbent and process leads to more economic 3rd and 4th generation technologies (G3 & G4), for instance CO_2 absorption systems with polyamine solvents, non-aqueous solvents and phase change solvents. A comparison of the four technology generations in thermal regeneration energy consumption is shown in Table 3 (Feron, 2009).

Table 3. Energy requirement for various generation capture technologies

Generation	Absorbent		Process	
	Reaction enthalpy	**Flow rate**	**Thermal energy**	**Reflux ratio**
	kJ/mol_{-CO2}	m^3/ton_{-CO2}	GJ/ton_{-CO2}	ton_{-H2O}/ton_{-CO2}
G1	80	20	4.5	0.7
G2	70	10	3.3	0.6
G3	55	8	2.3	0.4
G4	30	4	<1	0.1

1.2.4 Gaps in knowledge of PCC

Amine solvents have been used to remove acid gas from natural and synthesis gases since the 1930s and the amine-based gas scrubbing technology has been commercialised for H_2S and CO_2 absorption for over 80 years (Kohl et al., 1997). However, such sour gases contain low concentrations of CO_2 and minor amount of O_2 and are operated at high pressure. Such circumstances are quite different from fossil fuel-fired flue gases, which comprise more CO_2 and O_2 and are only at atmospheric pressure. In order to continue use of fossil fuel and limitation of CO_2 emission, CCS must be applied and amine scrubbing process is probably the most promising technology for PCC from existing fossil fuel power plant (Rochelle, 2009).

Several PCC pilot and demonstration plants have been operated worldwide. Nevertheless, economic issue is one of the principal barriers for the application of PCC technology, since the efficiency of power generation will be reduced by ~9% for coal-fired or ~6% for gas-fired power plant. The energy requirement for CO_2-Amine thermal separation typically contributes more than half of the total PCC energy penalty. Reduction of energy consumption, especially for solvent regeneration, is thus critical to be developed. Thermal and oxidative degradation cannot be avoided for amine-based solvents, when thermal regeneration is required and O_2 is present in flue gas. Such degradations are irreversible. It not only consumes the absorbents but also gives rise to another one of the main concerning - environmental impact. Since amines are volatile to some extent and most absorbents can be degraded to a certain degree, it is detrimental if the volatile components exit through the exhaust gas, a washing unit must be applied to absorb all the soluble substances, while the non-volatile degradation products which are harmful to human health and environment also must be removed. Since PCC is being used to solve the issue of global warming, we must avoid creating a new environmental problem (Svendsen et al., 2011). Although the demonstrations have shown the potential of using amine scrubbing for CO_2 capture from flue gas, but it is still a challenge to scale-up the absorption and desorption columns for large power plants. It is uncertain that how large of the columns are required and the technical feasibility must be further proved.

1.3 CO₂ capture using liquid-liquid phase change systems

1.3.1 DMX^TM process from IFP

A research group at the French Institute of Petroleum (IFP) Energy Nouvelles has filed several patents on PCC process with demixing solvents since 2006. Dipropylamine (DPA) is the first solvent proposed for fractionated regeneration in the deacidification process (Cadours et al., 2007). However, low boiling point and precipitation are its disadvantages (Zhang, J. et al., 2011b). N,N,N´,N´-tetramethyl-1,3-isobutane-diamine (TMiBDA) is followed, exhibiting high loading capacity and stability, but it is miscible with water below 90°C, which indicates a poor performance of the liquid-liquid phase separation (LLPS) and requires a high regeneration temperature.
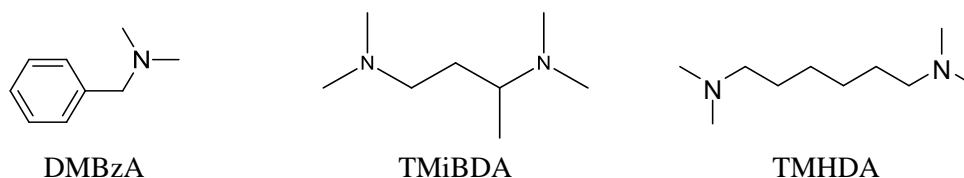
Figure 3. Structure of amines used for DMX^TM process

Recently, IFP has disclosed N,N-dimethylbenzylamine (DMBzA) and N,N,N´,N´-tetramethyl-1,6-hexane-diamine (TMHDA) as new solvents for the DMX^TM process (Aleixo et al., 2011; Jacquin, 2010), but their absorption rates are not so satisfactory, only being comparable to that for MDEA or even slower (Qiao, 2011).
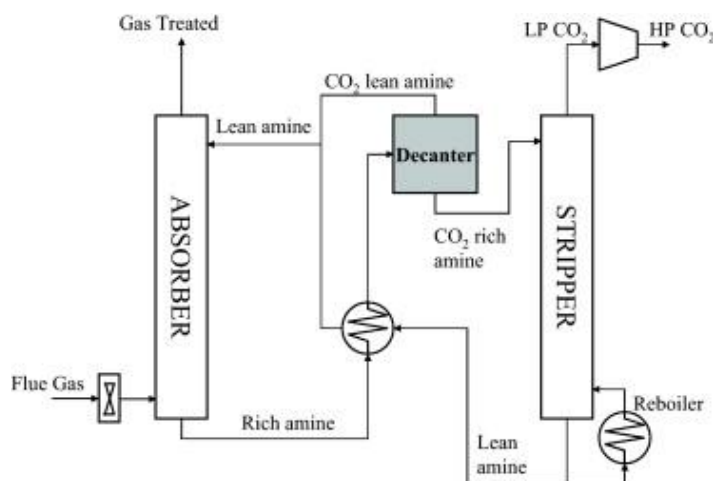
Figure 4. Flow scheme of DMX™ process
(Raynal et al., 2011b)

Besides the solvent improvement, IFP has also developed the absorption and desorption processes. A basic flow scheme is shown in Figure 4. A homogeneous absorbent is employed for absorption and a decanter with LLPS of the loaded solution at

90 °C is used prior to thermal regeneration: the lean organic phase is recycled to the absorber and the CO_2 rich aqueous phase is sent to a steam stripping column. The demixing process has advantages such as high CO_2 capacity, low reaction enthalpy, regeneration with a fraction of solvents, an "abnormally" high CO_2 loading in rich phase, considerable energy savings and low degradation. Additionally, modified process flow schemes, such as integration of multiple-stage cooling system into absorption column for CO_2 loading enhancement and multiple-stage decanter into stripping column for regeneration intensification, were also developed by Bouillon et al. (2010a and 2010b).

1.3.2 "Self-concentrating" process from 3H

This process initially used partially miscible organic solvents such as alamine as activated component and alcohol, e.g. isooctanol, as extractive agent (Hu, 2005). As shown in Figure 5, the initially homogeneous absorbent splits into two phases after absorption: CO_2 rich aqueous phase and CO_2 lean organic phase (Hu, 2009b). By separating the two phases in decanter, the rich phase is sent to the thermal stripper. After desorption, the regenerated solvent from the stripper, combining with the lean organic phase from decanter, forms a lean absorbent to complete the cycle.
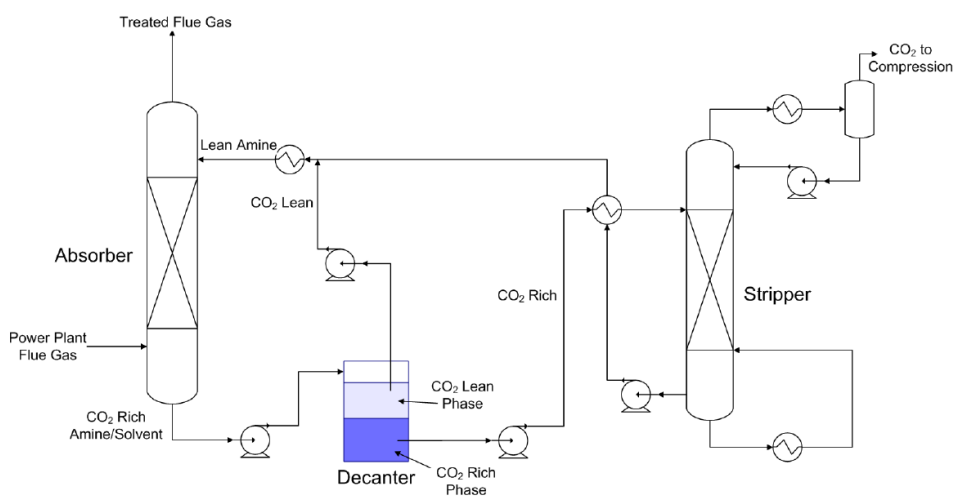
Figure 5. Flow scheme of a "Self-concentrating" process
(Hu, 2009a)

Recently, lipophilic amines, for example dibutylamine (DBA), were employed in such process and claimed to save energy consumption by 80% (Hu, 2010a and 2010b). However, those alamines are large molecular tertiary amines, and the concentration of activating groups is thus significantly limited, which cannot exceed 2 M; moreover, precipitation of protonated DBA salts also causes the problem of fouling in the absorber

9

(Zhang, J., 2008). According to the amine screening test in this work (see Section 3.3.2.1), slow absorption rate is another shortcoming for DBA. Since DBA is insoluble in water, the extractant isooctanol plays a role of solubiliser to attain a homogenous absorbent before absorption.

Molecular structure of
a typical Alamine

$(C_8H_{17})_3N$
Trioctylamine
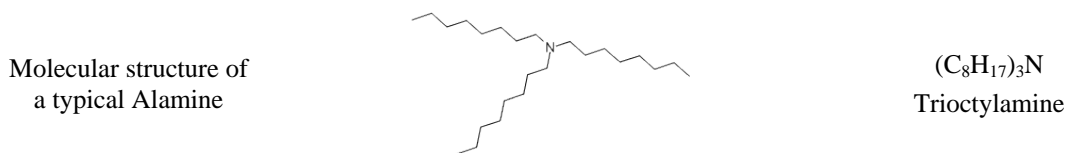
Figure 6. An example of Alamine

The "Self-concentrating" process has several advantages, such as high CO_2 loading, faster reaction, low regeneration temperature ≈90 °C and reduced energy required for desorption. However, the estimated value was only based on the activating component, the additional inert solvent with more than 50 vol.% will increase the total operational cost, which shouldn't be neglected. Furthermore, solvent volatile loss and high solvent circulation rate due to large amount of inert solvent addition will be its main disadvantages.

1.3.3 iCap phase change process

Concerning the preponderance of phase change solvent, the innovative CO_2 capture (iCap) project also focuses to develop absorbent systems with LLPS that forms two liquid phases after CO_2 loading, where one of the phases is CO_2 lean, can directly be recycled to the absorber, and another has a very high CO_2 concentration, thereby having a potential for low circulation rate and more energy efficient CO_2 desorption. The process flow scheme is illustrated in Figure 8. It is different from the IFP's demixing process by the LLPS occurring in the aqueous blended N,N-diethylethanolamine (DEEA) and 3-(methylamino)propylamine (MAPA) solution at low temperature ≈20 °C (Bruder et al., 2011).

DEEA

MAPA

Figure 7. Molecular structure of amines used for iCap process

This process has advantages such as high cyclic capacity, improved equilibrium curves, high pressure desorption, low liquid flow in desorber and retaining good liquid load in

the absorber; however, the disadvantages, for instance increased complexity, possibly higher heat of reaction and heat dissolution, must be taken into account.
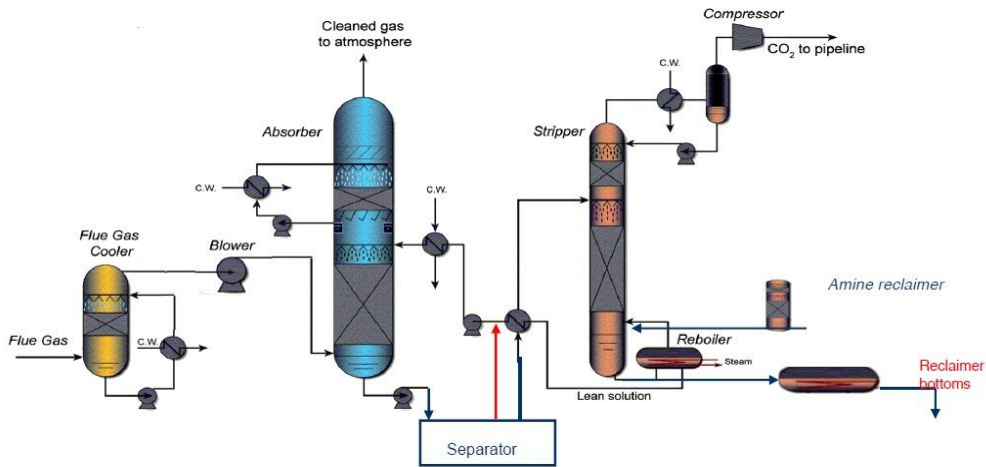
Figure 8. Flow scheme of iCap phase change process
(Monteiro et al., 2011)

1.3.4 Thermomorphic biphasic solvent system

Thermomorphic biphasic solvent (TBS) was initially proposed by Agar et al. (2008a) to reduce the regeneration temperature down to 80 °C or even lower, enabling the utilisation of low temperature or even waste heat for regeneration purposes. As illustrated in Figure 9, the concept was first introduced by Zhang, X. (2007): due to the limited aqueous solubility of these "lipophilic" amines, a thermal-induced miscibility gap arises upon modest heating of the loaded solvent in the temperature range of 60-80 °C. The organic phase thus formed acts as an extractive agent, removing the amine from the aqueous phase and thus favourably displacing the regeneration equilibrium and driving the reaction towards dissociation of the carbamate and bicarbonate species in the loaded aqueous phase according to Le Chatelier's principle (Tan, 2010). In general, a comparison on the features, advantages and disadvantages of the liquid-liquid phase change CO_2 capture processes are listed in Table 4.
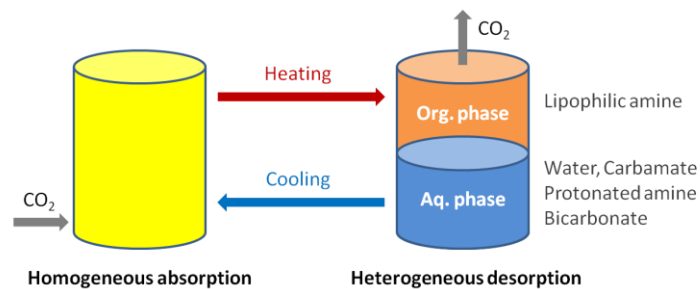
Figure 9. Principle concept of CO_2 absorption using TBS system

11

Table 4. Comparison of liquid-liquid phase change systems

Process	Solvent	Apparatus	Pros	Cons	Reference
DMX	Alkylamine	Absorber, decanter, stripper	High net CO_2 capacity Low liquid flow for desorber to reduce the regeneration energy	Volatile loss High viscosity	Raynal et al., 2011a
3H	Alamine + isooctanol	Similar to DMX	High CO_2 loading Low regeneration Temperature: 90 °C Reduced desorption energy consumption	Significant solvent volatile loss High solvent circulation rate	Hu, 2010b
iCap	DEEA + MAPA	Similar to DMX	High net CO_2 capacity Low liquid flow for desorber to reduce the regeneration energy High pressure desorption to save the compression cost	High viscosity High reaction enthalpy	Bruder et al., 2011
TBS	Lipophilic amine	Absorber, phase separator	High net CO_2 capacity Low desorption temperature: 80-90 °C Use of waste heat for regeneration	Volatile loss High viscosity	This work

1.4 Research background

Improvement of CO_2 loading capacity, reaction kinetics, mass transfer, regenerability and solvent stability as well as reduction of the energy consumption are the most significant challenges facing the post-combustion carbon capture process. The TBS absorbent, comprising lipophilic amines as activating component, exhibits a thermomorphic phase transition upon heating, giving rise to extractive behaviour, which enhances desorption at temperatures well below the boiling point of the solution (Agar et al., 2008a). In comparison to conventional alkanolamines, the vapour liquid equilibrium (VLE) data for lipophilic amines indicate their considerable potential for the CO_2 absorption process, in particular the high cyclic loading capacity approaching 0.9 $mol_{CO_2}/mol_{absorbent}$ and the low regeneration temperature, which enables the use of low value heat utilities for desorption purposes. The absorption enthalpies of selected amine solvents were determined by an indirect method and the solvent degradation with respect to that of alkanolamines was also investigated.

1.4.1 Previous studies

The lipophilic amine solvents, for example N,N-dimethylcyclohexylamine (DMCA) and dipropylamine (DPA) in blends or individually, have been studied extensively in previous work with respect to their CO_2 loading capacities, kinetics, regeneration rates, residual loadings and so forth (Zhang, X., 2007). The tertiary amine DMCA acts as the main absorbent, because of its high CO_2 loading capacity in absorption and low residual loading upon regeneration. DPA is regarded as an activator, due to its rapid CO_2 absorption kinetics (Tan, 2010). Blending DMCA and DPA in aqueous solution combines the advantages of both.

Screening studies to identify new lipophilic amine solvents were conducted both theoretically and experimentally (Zhang, J., 2008). A novel absorbent system comprising aliphatic amines di-*sec*-butylamine (DsBA) with remarkable regeneration characteristics and MCA exhibiting a significantly faster absorption rate, were selected from a comparison of over thirty different lipophilic amines. The outstanding performance parameters of the new blended DsBA+MCA and DMCA+MCA solvents make them the promising candidates for assessing the technical viability in future development work. However, there are still several challenges, solvent vaporisation loss, two phase problem in absorption, degradation, non-stripping regeneration techniques and packing wettability of the TBS system, therefore, further study must be carried out to determine their behaviour and solve those issues if they arise.

1.4.2 Research objectives and outline

This project has focused on development of new generation CO_2 capture technologies to overcome the challenges, for instance high energy consumption in stripping and elevated temperature required for solvent regeneration as well as amine degradation in the absorber and desorber, that occurred in the conventional alkanolamine. Using novel lipophilic amine solvent systems has proved advantages such as remarkable CO_2 loading capacity, rapid absorption rate, high regenerability, low regeneration temperature and moderate reaction enthalpy, but there are still some unsolved issues: its lower critical solution temperature (LCST) was not satisfied, vaporisation was found to be a significant challenge, degradation was not measured, feasible techniques for regeneration at 80-90 °C was not devised and a suitable process scheme was not developed. Therefore, the objective of this work is not only to improve the solvent recipe but also to ameliorate those existing and potential issues.

In ***Chapter 2***, basic knowledge and theoretical studies of aqueous solubility, novel concept of biphasic system and fundamentals of gas scrubbing have been summarised. According to the structural influence of amine molecule for CO_2 absorption and desorption, new lipophilic amines were continuously explored by screening tests and the LLPS behaviour was also observed, which are presented in ***Chapter 3***. After classification and selection of suitable amines, blended lipophilic amine solvents were formulated by varying concentrations and proportions for optimising absorbent system. To control the phase change behaviour, solubilisation with partial protonation and foreign solvent addition was also investigated for regulating the LCST. Those results are given in ***Chapter 4***. Volatility and degradability of lipophilic amines solvents were studied and countermeasures for reduction of solvent losses were also proposed, which are discussed in ***Chapter 5***. Further research was conducted to intensify the solvent regeneration without steam stripping at temperatures lower than 85 °C, thus permitting the use of waste heat for desorption. ***Chapters 6-7*** disclose novel techniques, such as nucleation, agitation, ultrasound and extraction, devised to enhance CO_2 regeneration. After the solvent and process amelioration, the bench-scale unit with a 1 m height packed absorption column was employed for packing wettability tests and the energy consumption was also estimated, which is described in ***Chapters 8-9***.
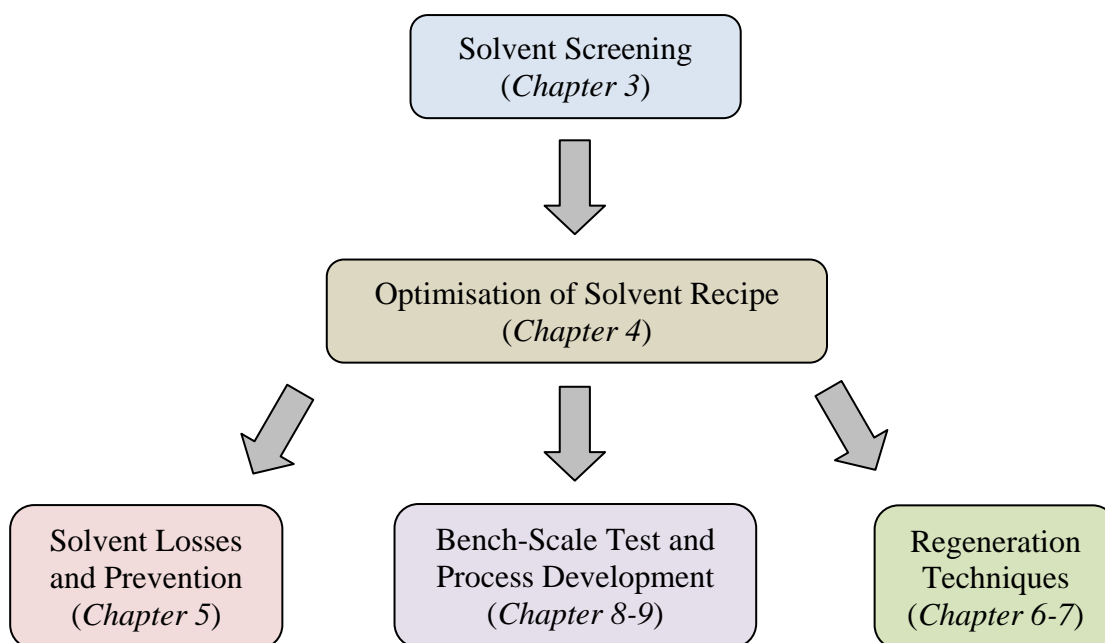
Figure 10. Structural overview of this dissertation

2 Theoretical background

2.1 Aqueous solubility

The solubility of one substance dissolving in another is determined by the balance of intermolecular forces between the solvent and solute. In addition, solvation behaviour is always accompanied with change of entropy. The solubility can be modified by altering the parameters, such as temperature and pressure, to shift the balance. All the absorption experiments in this work were conducted at ambient pressure and hence temperature became the major influence factor for the miscibility study between amine and water. Most aliphatic amines exhibit a weak miscibility with water, along with forming hydrogen bonds, and the aqueous solubility decreases with an increase in the number of carbon atoms in the molecule. When the carbon atom number is greater than 7, most corresponding alkylamines are insoluble in water.

2.1.1 Amine-water system: Solubilisation

Lipophilic amines are constituted of hydrophilic (amino) and hydrophobic (alkyl) groups (see Figure 11). To some extent, the solubility depends on the structure of alkyl groups. Upon experience a popular aphorism used for predicting solubility is "Like dissolves like", which indicates a solute will dissolve best in a solvent that has a similar polarity to itself. It is a rather simplistic view, since it ignores many solvent-solute interactions, but it is a useful rule of thumb. For example, alcohol-water mixtures both have a similar structure "-OH" group. But the validity of this rule is limited by many exceptions, such as methanol and benzene which are chemically dissimilar compounds.
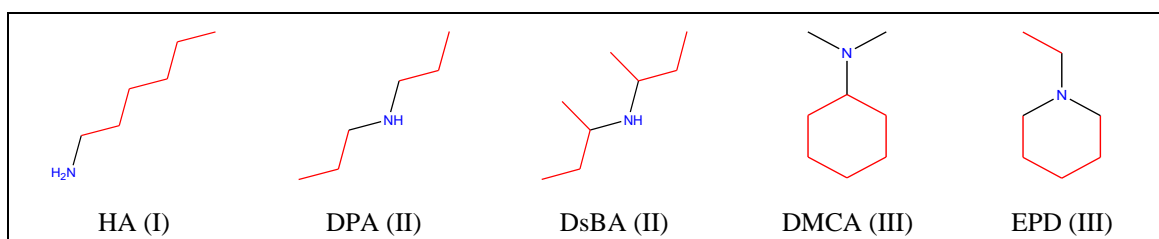
Figure 11. Examples of lipophilic amines
Red: hydrophobic alkyl group(s); blue: hydrophilic amino group

However, rather than the rule of "like dissolves like", the mutual solubility is determined by the intermolecular interaction between solvent and solute molecules. The solute (A) dissolves in the solvent (B) only when their respective intermolecular attraction forces K_{AA} and K_{BB} can be overcome by the interaction force K_{AB} in solution.

Jiafei Zhang   *Chemische Verfahrenstechnik*

The sum of the interaction forces between the solute and solvent molecules can be described by the term "polarity" (Reichardt, 2003). The compounds with large respectively interactions are regarded as polar, and those with small interaction as nonpolar. A qualitative prediction of solubility is indicated in Table 5 (Pimentel, 1963). In cases 2 and 3, the solubility might be low because it is difficult to break up the strong interaction A-A or B-B.

Table 5. Relationship of solubility and polarity

Case	Solute	Solvent	Interaction			Solubility
	A	B	A-A	B-B	A-B	A in B
1	nonpolar	nonpolar	weak	weak	weak	can be high
2	nonpolar	polar	weak	strong	weak	probably low
3	polar	nonpolar	strong	weak	weak	probably low
4	polar	polar	strong	strong	strong	can be high

In aqueous lipophilic amine systems, water is a strong self-associate component, and lipophilic amine is contributed by hydrophilic and hydrophobic groups. The hydrophilic group plays a major role in primary amine, so it is typically water soluble while the tertiary amine has low aqueous solubility due to its hydrophobic groups. Several examples are given in Table 6. With an increase of carbon number in the alkyl group, the aqueous solubility decreases, because the influence of the hydrophobic group is enhanced. Additionally, amines with branched or cyclic structures have higher solubility than those which have the same carbon number with only linear chains. Because the alkyl chains are shortened by branched and cyclic structures, the influence of hydrophobic groups is weakened.

Table 6. Solubility of amines in water at room temperature

(unit: g/L)

Primary amine	Solub.	Secondary amine	Solub.	Tertiary amine	Solub.
Propylamine	c.s.*	Dipropylamine	49	Trimethylamine	c.s.
Isopropylamine	c.s.	Diisopropylamine	110	Triethylamine	170
Hexylamine	14	Dihexylamine	0.3	Tripropylamine	2.6
Cyclohexylamine	c.s.	Dicyclohexylamine	1	Tributylamine	0.4

* c.s.: completely soluble

2.1.2 Amine-alkane-water system: Extraction

Liquid-liquid extraction is a separation technology based on the relative solubility of the component in two different immiscible liquids to be distributed between the two phases. This depends on the mass transfer of the component to be extracted from one of the liquid phases to another. In this work, an extraction system involving alkanes as extractant was studied for amine regeneration to reduce the required desorption temperature (Agar et al., 2008b), and thus to enhance the feasibility of using waste heat for solvent regeneration to cut the exergy demand.

Hamborg et al. (2011) have described a method for enhancing the regeneration of MDEA by adding water-soluble organic solvents, such as methanol and ethanol, which reduces the dielectric constant of the mixed solution, leading to the conversion of a protonated alkanolamine to a non-ionised molecule. Extractive regeneration using additional inert hydrophobic solvents reduces the dielectric constant still further, resulting in a displacement of the equilibrium in the loaded solution and giving rise to CO_2 release with simultaneous extraction of the amine into the inert solvent at very low temperatures of ≈50 °C or even less (Zhang, J. et al., 2011c).

2.2 Novel concepts

2.2.1 Switchable-polarity solvents

A switchable polarity solvent is a liquid whose polarity can be changed between two forms by a trigger (Phan et al., 2007). With addition of CO_2 as the switching agent, the lipophilic amines can be switched to a higher polarity solvent and be turned back to a lower polarity solvent by removal of CO_2 with thermal or N_2 stripping (see Figure 12). Therefore, it can be used as an extraction agent for mixtures comprising polar and nonpolar solvents due to such switchable-polarity characteristics. In the blended amine solutions, the easily regenerated amines such as DMCA and DsBA can be regarded as switchable polarity solvents, switching from polar to nonpolar during regeneration to extract the less regenerable amines, for example MCA and DPA, from the polar aqueous solution to enhance the overall depth of desorption.
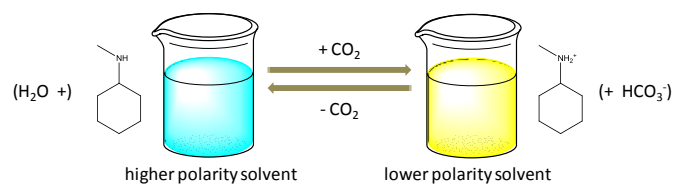
Figure 12. Switch of solvent polarity

2.2.2 Lower critical solution temperature

Since lipophilic amines possess both the hydrophilic and hydrophobic functional groups, most of them are partially miscible in water and exhibit lower critical solution temperature (LCST) behaviour. As illustrated in Figure 13(C), LCST is the critical temperature below which the components of a mixture are miscible (Yalkowsky, 1999). It differs from the regular binary mixture system depicted in Figure 13(A) since the miscibility of most binary liquid systems increases with the temperature rising, for examples phenol-water and n-butanol-water both exhibit upper critical solution temperatures (UCST).
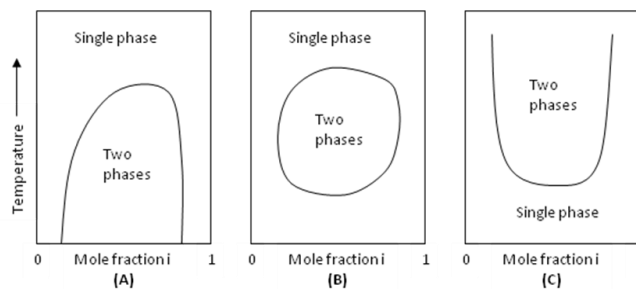
Figure 13. Partial miscibility curves for binary liquid-liquid mixtures
(A) UCST; (B) Both UCST and LCST; (C) LCST

The lipophilic amine and water system, on the other hand, is miscible at low temperatures and separates into two immiscible phases with temperature increase. The miscibility gap of the binary system is explained by a specific solute-solvent interaction: the LCST is initiated by the breakdown of strong cohesive interactions between the solute and solvent. A typical example is the triethylamine-water system (Counsell et al., 1961). The triethylamine does not self-associate at low temperatures, due to the absence of hydrogen bonding, and it is completely soluble in water. However, the cohesive interaction can be reduced by increasing the temperature resulting in phase separation by self-association of the hydrophobic groups (Yalkowsky, 1999). The phase transition behaviour can be resolved into the following stages:

- At temperatures below LCST, the lipophilic amine is completely dissolved in water and the molecular system is in an orientational configuration.
- With increasing temperature, the extent of hydrogen bonds diminishes: the amine-water hydrogen bonding (9 kJ/mol) is first destroyed and the breakage of the amine-amine intra-molecular hydrogen bonding (13 kJ/mol) follows, while the water-water hydrogen bonding remains strong (21 kJ/mol).

18

- When LCST temperature is achieved, the amine molecules are driven out of the aqueous phase and an organic phase is formed by the molecular self-association behaviour. Two separate phases thus arise with the water-water hydrogen bonding decreasing at still higher temperatures.

However, most binary liquid-liquid systems with a miscibility gap usually exhibit UCST, because they do not have the interactions observed in solutions with LCST.

2.2.3 Liquid-liquid phase separation

Due to the benefits of using LCST characteristics to reduce the regeneration temperature required, lipophilic amines have been employed as novel absorbents for circumventing the energy demands for CO_2 capture through the thermomorphic liquid-liquid phase separation (LLPS). Initial development work focussed on the miscibility of organic and aqueous phases and their temperature dependent phase transition behaviour. The concept of the phase transition CO_2 capture process is primarily determined by two processes:

- The homogeneous loaded lipophilic amine solution separates into two phases upon heating at temperature of around 80 °C during regeneration; the organic phase formed mainly contains the regenerated lipophilic amine, while the aqueous phase comprises water, carbamate, bicarbonate and protonated amine species.

- The regenerated lean biphasic solvent reverts to a single phase upon cooling to the critical solution temperature of ca. 40 °C, i.e., the absorbent becomes homogeneous again at the operating temperature of the absorber.

Such a biphasic system potentially offers considerable advantages (Svendsen et al., 2011). Since the absorbent is resolved into one phase highly concentrated in CO_2 and another phase low in CO_2, only the concentrated phase needs be sent to the stripper. This is equivalent to a system operated with an extremely high CO_2 capacity. In addition, the concentrated phase can be loaded up to a very high level, enabling desorber operation at elevated pressure, reduced temperature or both. Furthermore, there is no deterioration of wetting in the absorber operation, even when a very concentrated solution is circulated to the absorber. This could facilitate the use of an absorber with a greater cross-sectional area and thus a lower pressure drop.

Recognising the advantages of integrating LLPS in the post-combustion capture (PCC), a new CO_2 capture technology - the DMX™ process - has been developed by IFP to reduce energy consumption with a demixing unit prior to thermal regeneration:

the lean organic phase is returned to the absorber while the CO_2 rich aqueous phase is sent to a steam stripping column (Raynal et al., 2011a and 2011b). The activating solvent used in such a process has a LCST of 50 °C, however, the LLPS temperature is higher than 90 °C, being elevated by the solubilisation effect of the ionised CO_2. In the TBS process illustrated in Figure 14, on the other hand, the LLPS unit is designed to achieve "deep" solvent regeneration (>90%) with simultaneous CO_2 release (Zhang, X., 2007). By removing the regenerated CO_2 from the LLPS unit, the required LLPS temperature of the partially protonated amine solution is reduced and equilibrium is driven in the direction of desorption.
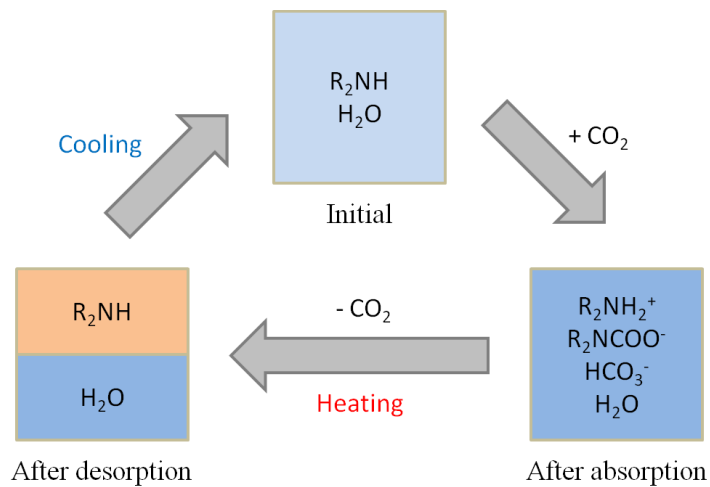
Figure 14. Basic concept of TBS system

According to the screening tests, several of the selected alternative lipophilic amine absorbents studied, such as hexylamine (HA), dipropylamine (DPA) and N-methylcyclohexylamine (MCA), exhibit critical solution behaviour around 40 °C, but the required LLPS temperature is too high (≈90 °C) to permit utilisation of waste heat in regeneration. However, for other less soluble lipophilic amines, such as N,N-dimethylcyclohexylamine (DMCA) and di-*sec*-butylamine (DsBA), the LLPS can be reduced to temperatures of lower than 80 °C, but the critical solution temperature is even lower - below 20 °C, which makes it possible to exploit low value heat for regeneration but renders a homogeneous solution for absorption unfeasible. Blended lipophilic amine solutions were therefore used in the TBS system to enable a compromise overcoming these drawbacks.

2.3 Chemistry of reactions between CO_2 and amine

The chemical reaction of CO_2 and amines in aqueous solution is extraordinary complex and the mechanism is significantly difficult to describe. Referring to the previous researches on alkanolamines, such as MEA, diethanolamine (DEA), 2-amino-2-methyl-1-propanol (AMP) and methyldiethanolamine (MDEA), some stable carbamates and bicarbonates were found in their absorbed solutions (Dang et al., 2003; Hagewiesche et al., 1995; Horng et al., 2002; Jou et al., 1995; Mandal et al., 2001 and 2003).

(1) Primary and secondary amines

Primary and secondary amines, for instance MEA and DEA, have been extensively studied on their reaction kinetics and the following main reactions are considered:

$$CF \qquad CO_2 + 2RNH_2 \leftrightarrow RNH_3^+ + RNHCOO^- \qquad \text{(R. 2.1)}$$

$$BF \qquad CO_2 + RNH_2 + H_2O \leftrightarrow RNH_3^+ + HCO_3^- \qquad \text{(R. 2.2)}$$

$$CR \qquad CO_2 + RNHCOO^- + 2H_2O \leftrightarrow RNH_3^+ + 2HCO_3^- \qquad \text{(R. 2.3)}$$
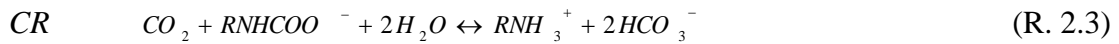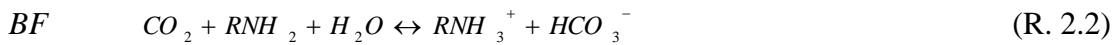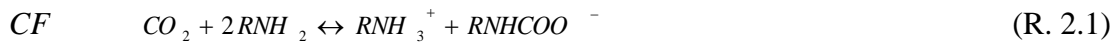
During absorption process, carbamate formation (CF) takes place in the condition of amine excess; bicarbonate formation (BF) occurs in the condition of CO_2 excess; and carbamate reversion (CR) happens while the mole ratio of CO_2 to amine is above 0.5. In order to reach high recover ratio of CO_2, excess absorbent is used for the reactions; R. 2.1 is thus the leading reaction (Astarita, 1983), which can be established to a mechanism with formation of zwitterions in two steps:

$$CO_2 + RNH_2 \xleftrightarrow{Slow} R\overset{+}{N}H_2COO^- \qquad \text{(R. 2.4)}$$

$$R\overset{+}{N}H_2COO^- + RNH_2 \xrightarrow{Fast} RNH_3^+ + RNHCOO^- \qquad \text{(R. 2.5)}$$
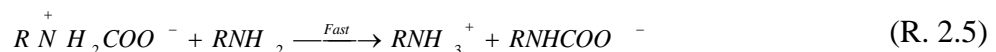
During the first step, CO_2 reacts with amine and forms zwitterion intermediate, $R\overset{+}{N}H_2COO^-$ or $R_2\overset{+}{N}H\ COO^-$; the zwitterions then donate the protons to bases such as RNH_2 or R_2NH and forms carbamate.

Bicarbonate formation is the only overall reaction to take place. A possible mechanism with formation of zwitterion intermediate is given by R. 2.4 and 2.6.

$$R\overset{+}{N}H_2COO^- + H_2O \rightarrow RNH_3^+ + HCO_3^- \qquad \text{(R. 2.6)}$$
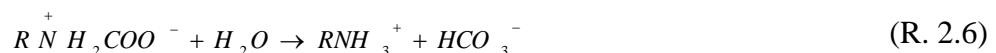
The mechanism of carbamate reversion to bicarbonate is a little complicated. The sequence of elementary steps is shown below:

$$RNHCOO^- + RNH_3^+ \leftrightarrow R\overset{+}{N}H_2COO^- + RNH_2 \qquad \text{(R. 2.7)}$$

$$R\overset{+}{N}H_2COO^- \leftrightarrow RNH_2 + CO_2 \qquad \text{(R. 2.8)}$$

$$H_2O \leftrightarrow OH^- + H^+ \tag{R. 2.9}$$

$$CO_2 + OH^- \xrightarrow{slow} HCO_3^- \tag{R. 2.10}$$

$$RNH_2 + H^+ \rightarrow RNH_3^+ \tag{R. 2.11}$$
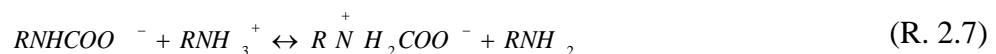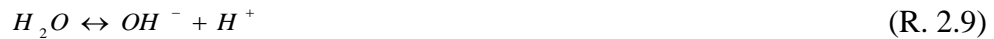
(2) Tertiary amines

Theoretically, tertiary amines, e.g. MDEA, could form zwitterions $R_3\overset{+}{N}COO^-$, but they cannot form the neutral carbamic acid. Therefore, the main reaction is:

$$BF \qquad CO_2 + R_3N + H_2O \leftrightarrow R_3NH^+ + HCO_3^- \tag{R. 2.12}$$

It is comparable to R. 2.2, and its mechanism can be conjectured as:

$$CO_2 + R_3N \xleftrightarrow{Slow} R_3\overset{+}{N}COO^- \tag{R. 2.13}$$

$$R_3\overset{+}{N}COO^- + H_2O \rightarrow R_3N^+ + HCO_3^- \tag{R. 2.14}$$

(3) Sterically hindered amines

Sterically hindered amines such as AMP have attracted attention because of their potential high CO_2 capacities and their low regeneration energies, but there is no universal agreement on the relevant kinetic expressions (Gabrielsen et al., 2007). It has experimentally been confirmed by Nuclear magnetic resonance (NMR) spectroscopy that bicarbonate anion predominantly exists at equilibrium when CO_2 is absorbed in aqueous AMP solutions (Chakraborty et al., 1986). Theoretical investigations on the AMP-H_2O-CO_2 system are very limited. Ismael et al. (2009) studied the carbamate formation mechanism (R. 2.15) for CO_2 and AMP in both gas and aqueous phases.

$$HOCH_2C(CH_3)_2NH_2 + H_2O + CO_2 \leftrightarrow HOCH_2C(CH_3)_2NHCOOH + H_2O \tag{R. 2.15}$$

It was also confirmed by the intrinsic reaction coordinate (IRC) calculation that the zwitterion formation exists in aqueous solution:

$$HOCH_2C(CH_3)_2NH_2 + CO_2 \leftrightarrow HOCH_2C(CH_3)_2\overset{+}{N}H_2COO^- \tag{R. 2.16}$$
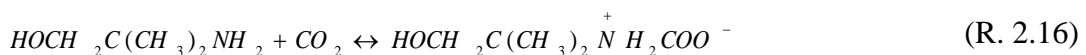
According to the IRC calculation with comparison of the activation energies for various reactions and conformations (Yamada et al., 2011), carbamate forms easily and decomposes reversibly in nonequilibrium states (see R. 2.15), bicarbonate forms from AMP, H_2O and CO_2 by a single-step termolecular mechanism (see R. 2.2), while the carbamate hardly undergoes hydrolysis to form the bicarbonate (see R. 2.17).

$$HOCH_2C(CH_3)_2NHCOO^- + H_2O \xleftarrow{\times} HOCH_2C(CH_3)_2NH_2 + HCO_3^- \tag{R. 2.17}$$

2.4 Fundamentals of packed column for gas-liquid system

2.4.1 Column packing

The column packing plays an important role in the mass transfer between the gas and liquid phases. It provides wide surface area for enhancing liquid and gas contact. Its open structure also attains uniform liquid distribution and gas vapour flow across the column. There are two type of packings commonly used in absorption columns: random and structured packings. For the convenience of operation to test the wettability of various packing materials, random packing was studied in this work. The geometric parameters of packings were calculated by the following equations (Maćkowiak, 2003; Walzel, 2006).

I. Porosity (ε):

$$\varepsilon = \frac{V_{voids}}{V_C} = \frac{V_C - V_P}{V_C} \qquad\qquad \text{Eq. 2.1}$$

where V_C is the volume of the column, V_P is the total volume of the packings.

II. Particle diameter (d_P):

$$d_P = 6 \cdot \frac{V_P}{A_P} \qquad\qquad \text{Eq. 2.2}$$

where A_P is the surface area of the packings.

III. Specific surface (a):

$$a = \frac{A_P}{V_C} = 6 \cdot (1 - \varepsilon) \cdot \frac{1}{d_P} \qquad\qquad \text{Eq. 2.3}$$

where A_P is the total surface area of packings.

2.4.2 Fluid dynamics

To understand the motion of fluid flow in the absorption column, several parameters, e.g. Reynolds number, liquid hold-up and pressure drop, were studied in this section and calculated by the equations below (Billet, 1995; Górak, 2006).

I. Hydraulic diameter (d_h):

$$d_h = 4 \cdot \frac{V_C - V_P}{A_P - A_w} = \frac{2}{3} \cdot \frac{\varepsilon}{1 - \varepsilon} \cdot d_p \cdot K \qquad\qquad \text{Eq. 2.4}$$

where A_w is the wall area.

II. Wall factor (K):

$$\frac{1}{K} = 1 + \frac{2}{3} \cdot \frac{\varepsilon}{1 - \varepsilon} \cdot \frac{d_P}{d_C} \qquad\qquad \text{Eq. 2.5}$$

where d_C is column diameter.

III. Reynolds number

The Reynolds number (*Re*) is an important parameter used in fluid mechanics to help predict similar flow patterns in different fluid flow situations. In the column model (Maćkowiak, 2003), the Reynolds number of the gas phase is defined as following:

$$Re_G = \frac{3}{2} \cdot \frac{\bar{u}_G \cdot d_h}{v_G} = \frac{3}{2} \cdot \frac{\bar{u}_G}{\varepsilon} \cdot \frac{\rho_G}{\eta_G} \cdot d_h \qquad \text{Eq. 2.6}$$

where $\bar{u}_G$ is the effective gas velocity, v_G is the kinematic viscosity, and η_G is the dynamic viscosity. By inserting Eq. 2.4 into Eq. 2.6, the Re_G can be calculated as

$$Re_G = \frac{u_G \cdot d_p}{(1-\varepsilon) \cdot v_G} \cdot K = \frac{u_G}{(1-\varepsilon)} \cdot \frac{\rho_G}{\eta_G} \cdot d_p \cdot K \qquad \text{Eq. 2.7}$$

The Reynolds number of liquid phase is defined as below:

$$Re_L = \frac{u_L}{a \cdot v_L} = \frac{u_L \cdot \rho_L}{a \cdot \eta_L} \qquad \text{Eq. 2.8}$$

IV. Gas load factor:

$$F_G = u_G \sqrt{\frac{\rho_G}{\rho_L - \rho_G}} \qquad \text{Eq. 2.9}$$

or $\qquad F_G = u_G \sqrt{\rho_G} \qquad (\text{if } \rho_L \gg \rho_G) \qquad \text{Eq. 2.10}$

where u_G is the gas velocity, ρ_L the density of the gas and ρ_G is the density of the liquid.

V. Pressure drop

The pressure drop is a major criterion for selecting packings in absorption columns. It is usually expressed as a function of the gas load factor:

$$\frac{\Delta p}{H} = f(F_G) \quad (\text{at a constant liquid-gas ratio}) \qquad \text{Eq. 2.11}$$

VI. Liquid hold-up

The liquid hold-up (h_L) in packed column consists of two parts: the static hold-up (h_{st}) and the dynamic hold-up (h_{dyn}). The static remains within the bed and the dynamic flows downwards; the latter, depending upon the hydrodynamics of the flow, provides the more valuable information on the column operation.

$$h_L = \frac{V_L}{V_C} = h_{st} + h_{dyn} \qquad \text{Eq. 2.12}$$
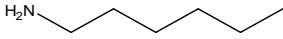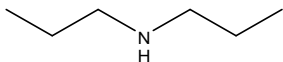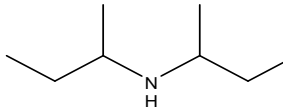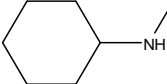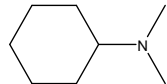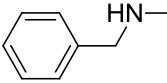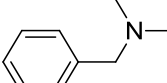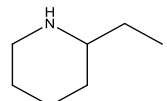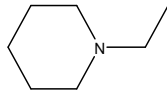
where V_L is the volume of the retained liquid.

3 Selection of new lipophilic amines

3.1 Chemicals: Lipophilic amines

More than thirty lipophilic amines with varying molecular structures have been studied in the screening experiment; some of them are representatively listed in Table 7. The full list is presented in Appendix A. All the amines studied in this work were purchased from chemical suppliers with high purity ($\geq$97%).

Table 7. List of advanced tested lipophilic amines

Chemical	Abbr.	CAS	Structure	M_r (g/mol)	Supplier
Hexylamine	HA	111-26-2		101.19	Merck
Di-n-propylamine	DPA	142-84-7		101.19	Fluka
Di-sec-butylamine	DsBA (B1)	626-23-3		129.25	Aldrich
N-Methylcyclo hexylamine	MCA (A1)	100-60-7		113.20	Acros
N,N-Dimethylcyclo hexylamine	DMCA	98-94-2		127.23	Merck
N-Methylbenzyl amine	MBzA	103-67-3		121.18	Merck
N,N-Dimethyl benzylamine	DMBzA	103-83-3		135.21	Merck
2-Ethylpiperidine	2EPD	1484-80-6		113.20	Aldrich
N-Ethyl piperidine	EPD	766-09-6		113.20	Fluka

3.2 Experiment: Test tube amine screening

The screening experiment was initially carried out in Schott GL-18 test tubes at 25 °C with 20 mL/min of CO_2 gas flow for absorption and then stepwise increased the temperature from 40 to 90 °C for desorption. Both the barium chloride (Jou et al., 1995) and weight methods were used to determine the mass of CO_2 loaded into the amine solution. The detailed setup is illustrated in Appendix B.1.

3.3   Preliminary amine screening

3.3.1   Performance of screened amines

The preliminary amine screening was conducted in the test tube experiment for determination of suitable amines as alternative CO_2 absorbents (Zhang, J., 2008; Zhang, J. et al., 2012a). A comparison of their performance is presented in Table 8. MCA was identified as an excellent solvent with high CO_2 loading and rapid reaction kinetics; additionally, DsBA was also selected due to its remarkable net CO_2 capacity and regenerability during the screening test over 40 amines.

Further researches on exploring more potential lipophilic amines were carried out over more than 20 other lipophilic amines, e.g. cyclic amines, derivatives of benzylamine (BzA), N-methylmorpholine (MMP) and diamines in this work. 2-ethylpiperidine (2EPD) and N-methylbenzylamine (MBzA) were selected as alternative absorbents from structure study and also experimentally proved in the test according to their outstanding performance in absorption. Figure 15 indicates the performance parameters of 2EPD are as good as MCA with respect to reactivity and capacity in absorption. MBzA also exhibits fast reaction rate, but the loading is a little lower. Precipitation (Pr) was found in both BzA and N-ethylbenzylamine (EBzA), which is similar to cyclohexylamine (CHA) and N-ethylcyclohexylamine (ECA). As a diamine, N,N,N´,N´-Tetramethyl-1,6-hexane-diamine (TMHDA) exhibits high CO_2 loading but low absorption rate; both DMBzA and MMP were unsatisfactory due to their slow reaction and undesirable solubility behaviour. In combination with previous screening results, lipophilic amines with an α-carbon branch (⌇HN─<), e.g. MCA and 2EPD, are greatly interested, owing to the remarkable absorption kinetics and CO_2 capacities.

(A) Aromatic amines   (B) Other amines
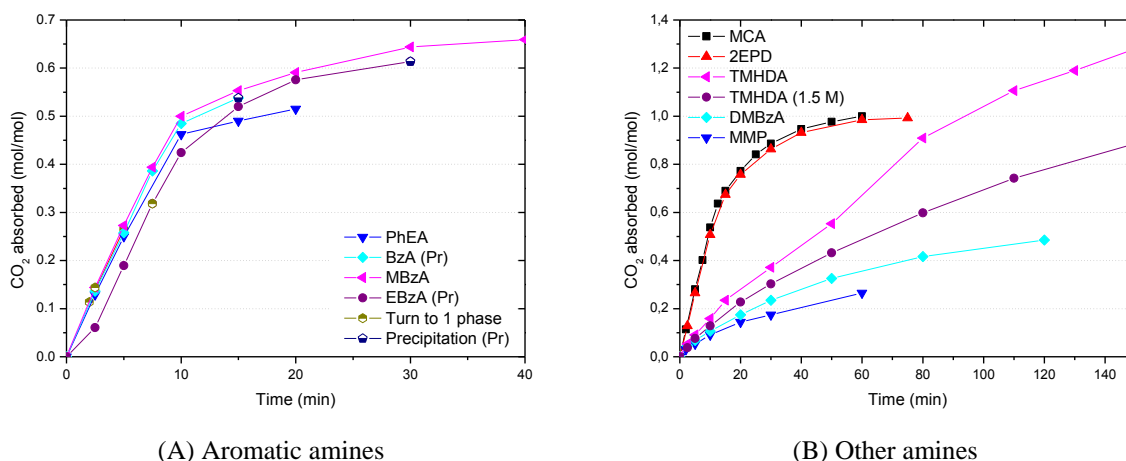
Figure 15. Absorption characteristics of 3M lipophilic amines

Table 8. Performance and evaluation of preliminary screened lipophilic amines

No.	Solvent	Abbr.	Type[a]	Sub.[b]	Phe.[c]	α[d]	Reg.[d]
1	Hexylamine	HA	I	L	/	2	3
2	Heptylamine	HpA	I	L	Gl	5	\
3	Octylamine	OtA	I	L	Gl	5	\
4	Di-*n*-propylamine	DPA	II	L	Pr	1	2
5	Diisopropylamine	DIPA	II	B	Sa	2	5
6	N-Ethylbutylamine	EBA	II	L	Pr	1	4
7	Di-*n*-butylamine	DBA	II	L	Pr	2	1
8	Diisobutylamine	DIBA	II	B	Sa	3	1
9	Di-*sec*-butylamine	DsBA	II	B	/	2	1
10	N-*sec*-Butyl-*n*-propylamine	SBPA	II	B	Sa	2	\
11	Triethylamine	TEA	III	L	/	3	\
12	Tripropylamine	TPA	III	L	/	5	\
13	Tributylamine	TBA	III	L	/	5	\
14	N,N-Diisopropyl methylamine	DIMA	III	B	/	3	3
15	N,N-Diisopropyl ethylamine	DIEA	III	B	/	4	\
16	N,N-Dimethyl butylamine	DMBA	III	L	/	2	2
17	N,N-Dimethyl octylamine	DMOA	III	L	/	2	1
18	Cyclohexylamine	CHA	I	O	Sa	2	3
19	Cycloheptylamine	CHpA	I	O	Pr	2	2
20	Cyclooctylamine	COA	I	O	Pr	3	\
23	2-Methylcyclohexyl amine	2MCA	I	O	Pr	4	\
21	N-Methylcyclohexyl amine	MCA	II	O	/	1	3
22	N-Ethylcyclohexyl amine	ECA	II	O	Sa	2	4
24	N-Isopropyl cyclohexylamine	IPCA	II	O,B	Sa	2	\
25	Dicyclohexylamine	DCHA	II	O	Sa	3	\
26	N,N-Dimethyl Cyclohexyl amine	DMCA	III	O	/	2	1
27	N,N-Diethyl Cyclohexyl amine	DECA	III	O	/	3	\
28	2,6-Dimethyl piperidine	2,6-DMPD	II	P	Sa	1	4
29	3,5-Dimethyl piperidine	3,5-DMPD	II	P	Pr	3	\
30	2,2,6,6-Tetramethyl piperidine	TMPD	II	P	Gl	\	\
31	2-Methyl piperidine	2MPD	II	P	/	2	3
32	2-Ethyl piperidine	2EPD	II	P	/	1	3
33	N-Methyl piperidine	MPD	III	P	/	2	1
34	N-Ethyl piperidine	EPD	III	P	/	2	2
35	Benzylamine	BzA	I	Z	/	2	\
36	N-Methyl benzylamine	MBzA	II	Z	/	2	3
37	N-Ethyl benzylamine	EBzA	II	Z	Pr	2	\
38	N,N-Dimethyl benzylamine	DMBzA	III	Z	/	4	1
39	Phenylethylamine	PhEA	II	Z	/	2	\
40	N-Methylmorpholine	MMP	III		/	4	\
	Benchmarks						
41	Monoethanolamine	MEA	I	L	/	3	5
42	N-Methyldiethanolamine	MDEA	III	L	/	4	3
43	2-Amino-2-methyl-1-propanol	AMP	I	B	/	2	3
44	Piperazine	PZ	II		/	1	5

[a] Type: I - primary amine, II - secondary amine, III - tertiary amine;

[b] Substitute (Sub.): L - liner chain, B - branched chain, O - cycloalkane, P - piperidine, Z - benzyl group;

[c] Phenomenon (Phe.): Gl - gel formation, Pr - precipitation, Sa - salts formation, / - none;

[d] CO_2 loading (α) & Regenerability (Reg.): 1 - excellent, 2 - good, 3 - moderate, 4 - unsatisfactory, 5 - poor, \ - untested (no value for further experiment).

3.3.2 Main screening criteria

The overall screening among those amines is based on the comprehensive performance in absorption and regeneration, which mainly include absorption capacity, reaction rate, and cyclic capacity as well as absence of precipitation, salts or gel formation and presence of thermomorphic phase transition. The phase change behaviour is the most significant phenomenon observed in the lipophilic amine solutions and it will be discussed in detail in Section 3.5, while other performance parameters are studied in the this section.
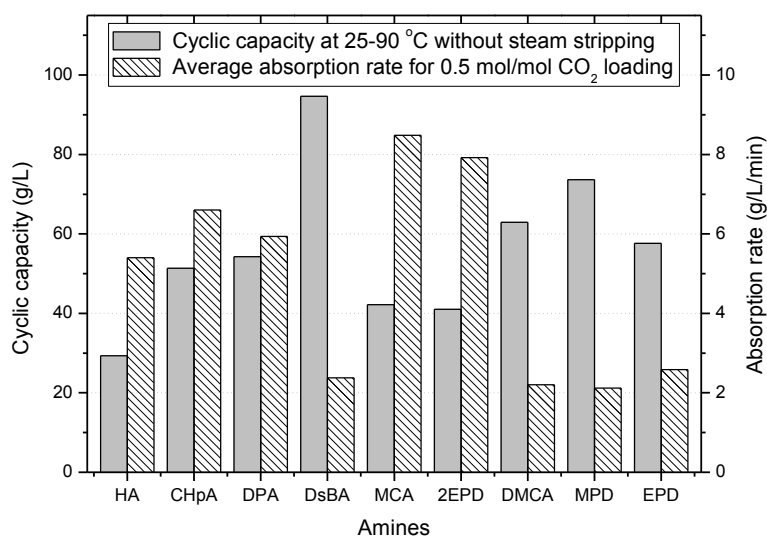
Figure 16. Cyclic CO_2 capacity and absorption rate of selected amine solutions
(Test tube solvent screening experiment, c_{amine}=2.7M)

3.3.2.1 Reaction rate

The reaction rate in absorption is mainly influenced by aqueous solubility, steric structure and basicity of amine. According to the experimental investigation, aqueous solubility is the key factor on reaction rate for TBS since the fast reactions were found in amine solutions, such as MCA and 2EPD, which were completely or partially aqueous miscible whereas the slow reactions were detected in those, DMCA and DsBA for instance, that were slightly aqueous miscible or immiscible (see Figure 16). This is principally due to the biphasic behaviour obstructing the mass transfer between the aqueous and gas phases. Large hydrocarbon substituents can also hinder the reaction between CO_2 and amino group and thus slows the absorption kinetics. Basicity is a minor influence factor for reaction rate, the more basic solvent can stabilise the reaction products and leads to a fast absorption rate.

3. Selection of new lipophilic amines

The most interesting case is MCA, which is partially miscible with water but achieves the highest absorption rate in the experiment. In addition, very fast initial reaction rate is also found in most partially aqueous soluble amines, when the solution is still heterogeneous. This phenomenon can be explained by the shuttle mechanism, (Astarita, 1983; Versteeg et al., 1990; Hagewiesche et al., 1995).
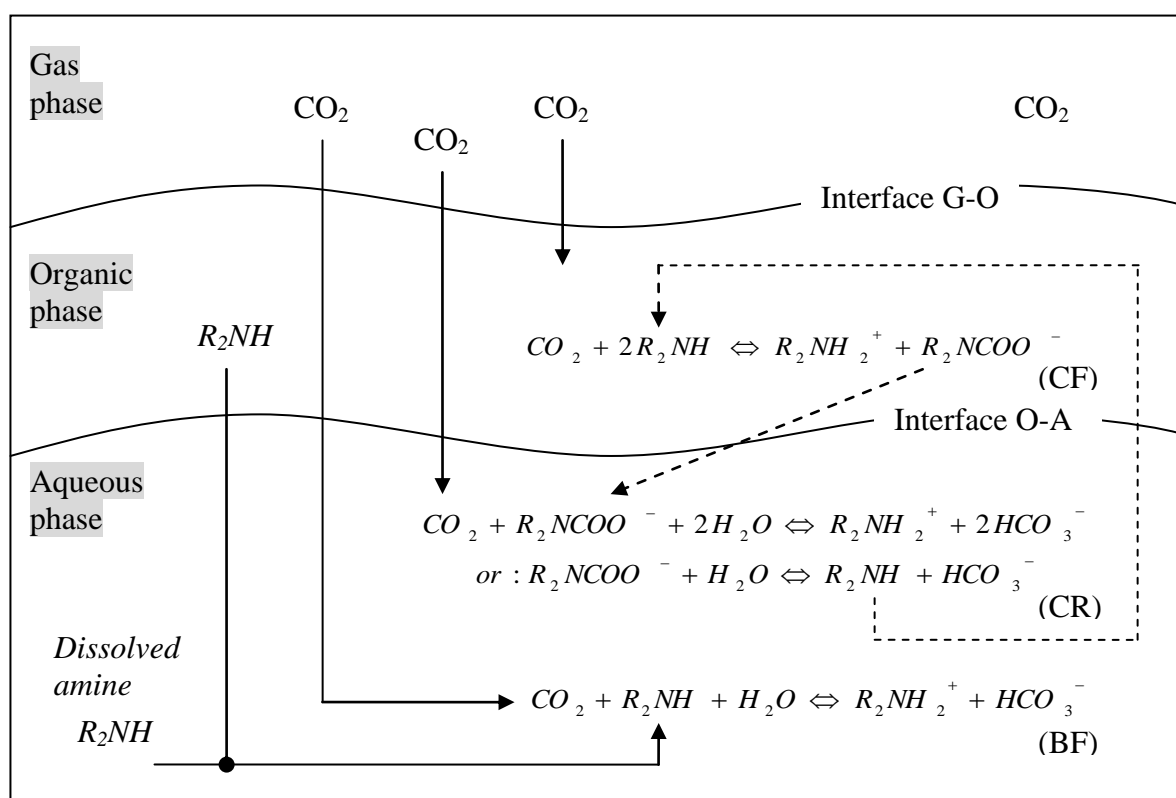
Figure 17. Illustration of shuttle mechanism in biphasic amine solution

As illustrated in Figure 17, the reaction system is in three phases: gas, amine and water. Reactions take place when CO_2 is supplied into the solvent:

(i)   In organic phase and at the interface of gas and organic phases (G-O), carbamate formation (CF) takes place;

(ii)   At the interface of organic and aqueous phases (O-A), the hydrophilic ions $R_2NH_2^+$ and R_2NCOO^- which are produced in organic phase transmit to aqueous phase;

(iii)   In aqueous phase and at the interface of organic and aqueous phases, carbamate reversion (CR) and bicarbonate formation (BF) occur;

(iv)   Due to limitation of solubility, the aqueous phase is a saturated amine solution; as more and more dissolved amine is consumed by reaction BF, more and more free amine is supplied from organic phase;

29

(v)   When amine is consumed by reactions CF and BF, the organic phase is reduced continuously until all the amine molecules are "dissolved" into aqueous phase.

Initially, CF is the main reaction, since it takes place immediately. While more and more carbamate is accumulated in liquid phase, CR takes place sequentially. In the partially miscible amine solutions, BF also occurs in the aqueous phase because CO_2 has opportunity to contact both amine and water simultaneously; the reaction rate is thus accelerated. Conversely, BF is considered in the slight soluble or insoluble amine solutions, since there is little amine in aqueous phase and it is hard for CO_2 to contact both amine and water simultaneously; the reaction rate is therefore unable to be kept fast after the achievement of the half reaction ($\alpha = 0.5$ mol$_{-CO2}$/mol$_{-amine}$).

3.3.2.2   Absorption capacity

The capacity of CO_2 absorption theoretically depends on the reaction mechanism, such as typically tertiary amine is able to achieve higher capacity than primary and secondary amines. However, according to the experimental results, it is very complicated in practice; because sterically hindrance is also an important influence on the capacity.

Based on the reaction mechanism introduced in section 2.3, tertiary amine can react with equivalent moles of carbon dioxide and water, the direct formation of bicarbonate is the only main reaction that needs be considered; the formation of carbamate, as well as the formation of bicarbonate and reversion of carbamate all should be considered in primary and secondary amine solutions. If precipitation or salt formation takes place, the produced carbamate is unable to reverse to bicarbonate and the capacity is thus reduced. However, if the reactions are carried out in aqueous environment, additional water will promote both the carbamate reversion and bicarbonate formation, hence, the capacity is comparable to tertiary amine. As shown in Figure 15(B), the CO_2 loading in secondary amines MCA and 2EPD can approach 1 mol$_{-CO2}$/mol$_{-amine}$, due to the shuttle mechanism illustrated in Figure 17.

3.3.2.3   Precipitation and salts formation

Both precipitation and salts formation are undesired phenomena in absorption (see Figure 18). They reduce the CO_2 loading capacity by impediment of carbamate reversion to bicarbonate and they also can damage the equipment by fouling; however, they have positive influence on reaction rate. Due to different reaction mechanisms,

precipitation and salts formation do not take place in tertiary amine solutions. However, the phenomena in primary and secondary amine solutions are irregular or unpredictable. In this experiment, those discovered potential amines without precipitation or salts formation are DsBA, MCA, HA, CHpA and all the tertiary amines.

According to experimental observation, salt formation usually takes place very early, between 5-15 min, because it is caused by carbamate formation in the organic phase. The solid salts are self-associated and adhering on the glass wall and carbamate reversion cannot be carried out since no carbamate is dissolved into aqueous phase; therefore, the capacity is reduced. In contrast, precipitation typically occurs near the end of reaction, because carbamate formation is much faster than carbamate reversion, then more and more carbamate is accumulated in the aqueous phase; after it is saturated, the pairs of ions salt out. In some cases, the precipitate suspends in the saturated solution and the liquid becomes a non-Newtonian fluid, which results in high viscosity and even leads to gel formation.

Precipitation of DPA solution:
$R_2NH_2^+ + HCO_3^-$

Salts formation of DIPA solution:
$R_2NH_2^+ + R_2NCOO^-$

Both precipitation and salts formation of ECA solution

Figure 18. Precipitation and salts formation of CO_2 into lipophilic amine solutions

3.3.2.4 Regenerability

Thermomorphic phase transition is the most expected phenomenon in regeneration experiments and the amount or fraction of desorbed CO_2 is a quantitative presentation of an amine's regeneration property. The thermomorphic phase transition was found in most tertiary amines (III), some secondary amines (II) and a few primary amines (I) in experiment. Those amines are listed below:

- Amines with thermomorphic phase transition at all the concentrations:

DBA (II), DIBA (II), DSBA (II), DMCA (II), DMOA (III), DECA (III);

- Amines with thermomorphic phase transition at high concentration, ≥2.7M:

HA (I), DPA (II), SBPA (II), ECA (II), DIEA (III), DMBA (III), MPD (III), EPD (III).

As shown in Figure 19, secondary amine DsBA and tertiary amines DMCA, MPD and EPD have exhibited the relative higher regenerability compared to others. They are the most potential solvents for further study on the phase change based desorption behaviour.
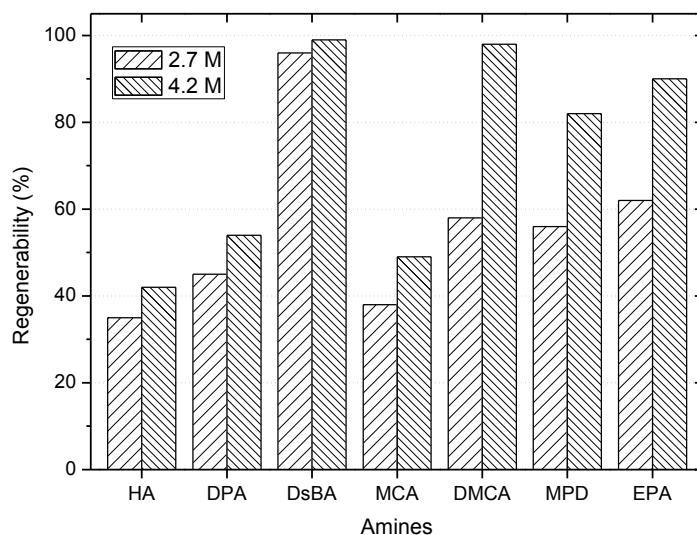
Figure 19. Regenerability of CO_2 loaded lipophilic amine solutions

3.4   Structural influence of amine molecule

According to the selection criteria: (a) reactivity, (b) CO_2 capacity, (c) regenerability, (d) physical and chemical stability, (e) biological degradability, (f) toxicity, etc., screening investigation to identify new lipophilic amines was conducted both theoretically and experimentally. Several phenomena, such as liquid-liquid phase transition, gel formation, insoluble carbamate salts formation and precipitation of bicarbonate, were observed in the absorption process during the absorbent screening, but only the miscibility gap was of interest in this work, and the remaining features were detrimental to performance. Aliphatic amines with varying structures, such as primary, secondary and tertiary amines, linear, branched and cyclic chains, have thus been studied. The influence of amine molecules structure on the physical and chemical properties is evident. Due to either low boiling point or high viscosity, most ***primary amines*** are unfavourable; because of their high basicity, ***secondary amines*** are preferred; on account of their extensive loading capacity, outstanding regenerability and remarkable chemical stability, ***tertiary amines*** are thus also recommended.

3.4.1   Primary and secondary amines

Most primary and secondary amines have fast absorption rate, but precipitation is a major problem in many of their aqueous solutions. **Linear chain** primary and secondary amines are not suitable as alternative absorbents, because of the following disadvantages with varying carbon numbers:

- *Linear chain primary amine*

  C5:   Significant volatile loss (bp. 104 °C)

  C6:   High volatile loss (bp. 131 °C)

  C7 & C8:   Gel formation

- *Linear chain secondary amine*

  C3+C3:   Precipitation, high volatile loss (bp. 105 °C)

  C2+C4:   Precipitation, high volatile loss (bp. 108 °C)

  C4+C4:   Precipitation, very slow reaction

The **branched** or **cyclic chain** primary and secondary amines have various performances in absorption. According to the branch position, they are classified by:

- α-carbon branch(es)
- β-carbon branch(es)
- α and β carbon branches

Branch at the *α-carbon* has the remarkable advantage of enhancing the absorption kinetics; for instance, rapid reaction rate has been observed in MCA, 2MPD and 2EPD solutions. However, it also has potential to induce insoluble carbamate salts formation, examples are given in Appendix C. Branch at the *β-carbon* can also result in insoluble salts formation; for example, it was found in 3,5-DMPD and DiBA solutions, but MBzA is an exception, since it is quite comparable to MCA and no detrimental phenomenon was observed. Lipophilic amines with branches at *both the α- and β-carbons* such as 2MCA were not suggested to be used as alternative absorbents since insoluble carbamate salts formation was detected as well.

3.4.2   Tertiary amine

Due to different reaction mechanisms, neither insoluble carbamate salts formation nor bicarbonate precipitation was found in tertiary amine solutions. But slow absorption rate is it weakness, mainly caused by the sterically hindered structure-induced poor aqueous solubility. Therefore, the carbon numbers must be limited for obtaining a desired molecule as an alternative solvent.

3.4.3 Sterically hindered amine

According to the definition by Sartori et al (1987), a sterically hindered amine has a bulky alkyl group attached to the amino group. It is more specifically defined as belonging to either of these classes:

- a primary amine in which the amino group is attached to a tertiary carbon;
- a secondary amine in which the amino group is attached to at least one secondary or tertiary carbon.

Generally, secondary amine presents high activities compared to tertiary amine. However, DsBA is exception, since it is highly sterically hindered - a secondary amine in which the amino group is attached to two secondary carbons. Since the amine functional group is surrounded by a crowded steric environment, the performance of sterically hindered amines is very similar to that for tertiary amines. Therefore, highly sterically hindered secondary amines, for instance DsBA, can achieve high regenerability in the experiment.

3.4.4 Overall comparison

As shown in Table 9, compared to alkanolamine, lipophilic amine is a less polar solvent with a lower dielectric constant (ε_r) due to absence of the hydroxyl group (-OH), it thus has a weaker interaction with water, which is a polar solvent (Reichardt, 2003). This facilitates the separation of organic phase from the aqueous solution and hence enhances CO_2 release and solvent regeneration.

Table 9. Comparison of dielectric constant for amines and water

	HA	DPA	DiBA	MCA	DMCA	MPD	MEA	DEA	AMP	Water
ε_r *	4.1	2.9	2.7	3.6	2.9	2.6	37.7	25.8	20.6	80.4
T (°C)	25	21	22	20	20	20	25	20	20	20

* Provided by the suppliers in the material safety data sheet.

According to the influence of molecular structures observed during the amine selection tests, an increase in the length of chain leads to gel formation for primary amines and results in a slower reaction rate but an improved regenerability for all other amines, e.g. DPA and DMBA exhibit a faster absorption rate but lower regenerability compared to DBA and DMOA. Branched chain shows a positive influence on reaction rate but also has potential to cause insoluble carbamate salts formation of primary and secondary amines, such as DIPA, DIBA and IPCA. Cyclic structure is recommended to
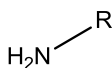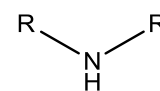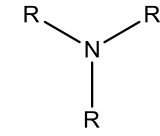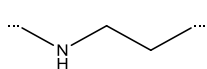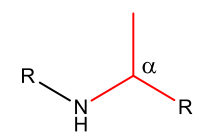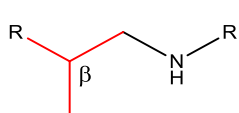
increase the aqueous solubility and reaction kinetics, precipitation is however still its unpredictable weakness in some primary and secondary amines.

Tertiary amine is the most favourable solvent to act as regeneration promoter due to the low dielectric constant and aqueous immiscibility. Secondary amine is the most likely one to achieve rapid reaction kinetics because of its high basicity and partially miscibility. Both cycloalkylamine and cyclic amine exhibit better performances than chain amine and aromatic amine, owing to less detrimental phenomena observed in experiment. The major structural influence on ab-/desorption performances is presented in Table 10. Since none of single amine solvents was found to meet all the screening criteria, blended solvents were studied to improve the drawbacks of the single amine solutions in the next Chapter.

Table 10. Summary of structural effects

Type	Functional group	Examples	Pros	Cons
According to the number of organic substituents				
Primary (I)		HA	Fast reaction rate	High volatility High viscosity (R=C7+) Low regenerability
Secondary (II)		DPA, MCA	Fast reaction rate	High volatility
Tertiary (III)		DMBA, DMCA	Good regenerability No precipitation	Slow reaction rate
According to the substructure of organic substituent for primary and secondary amines				
Linear		HA, DPA	Fast reaction rate	High volatility Gel formation (R=C8+) Precipitation (II)
Branched or Cyclic				
α-carbon		DsBA MCA	Rapid reaction rate High CO$_2$ loading	Potential of precipitation
β-carbon		DiBA 35DMPD	Rapid reaction rate	High potential of precipitation

35

3.4.5 Ideal molecular structure

According to the screen results and the investigation of structure influence, the most potential molecules of lipophilic amines are proposed to comprise the following desired substitutes (R^i):

Secondary amine (II): R^1=H,

R^2=C1,

R^3=C5-C8 with a branch at α carbon;

Example: MCA

Tertiary amine (III): R^1=C1,

R^2=C1-C2,

R^3=C5-C6 with branch(es);

Example: DMCA

For secondary amines, the reaction kinetics can be significantly decreased if the substitute R^2 contains more carbons, such as DsBA; precipitation is very likely to occur if the substitute R^3 is linear or with a branch at β carbon; gel formation will take place if the substitute R^3 contains more carbons or becomes high volatile if less carbons. For tertiary amines, the reaction kinetics can also be decreased if the substitute R^1 or R^2 contains more carbons; high volatile loss will be caused by less carbon in the substitute R^3; branches can shorten the chain and reduce the solvent viscosity.

3.5 Phase change behaviour

3.5.1 Experimental determination of phase change temperatures

The critical solution temperature measurement was carried out in test tubes (Schott GL-18) with 5 mL aqueous amine solutions at various concentrations from 0.02 to 0.95 wt.%. The temperatures were regulated by thermostats (Julabo F33 / HAAKE F3) with water or oil bath. The phase transition behaviour was observed by varying temperatures in preloaded selected amine solutions at different CO_2 loadings between 0.2 and 0.6 mol$_{CO2}$/mol$_{amine}$. Once the phase transition occurred, the exact temperature was determined by adjusting heating or cooling system stepwise with internal of 1 °C.

3.5.2 LCST for amine-water system

The lipophilic amine and water are not completely miscible in all proportions at certain temperatures, since lipophilic amine has a hybrid molecule with hydrophilic and hydrophobic functional groups. Due to the restricted miscibility, the characteristics of

lower critical solution temperature (LCST) behaviour were found in mixtures, e.g. DPA and water (Davison, 1986; Zhang, X., 2007). The aqueous solubility of lipophilic amine decreases with increasing temperature and thus exhibits a phase separation upon heating. Figure 20 illustrates the LCST of the selected aqueous fresh amine solutions is at concentrations of 30-60 wt.% and between -10 and 30 °C, while in the regenerated lean solutions it rises to 10-60 °C, since the aqueous soluble species, such as protonated amines, carbamates and bicarbonates, play the role of solubilisers in dissolving all the non-protonated amine in water, which significantly improves the technical feasibility by providing more degree of freedom for regulating the phase transition behaviour in the absorption process.
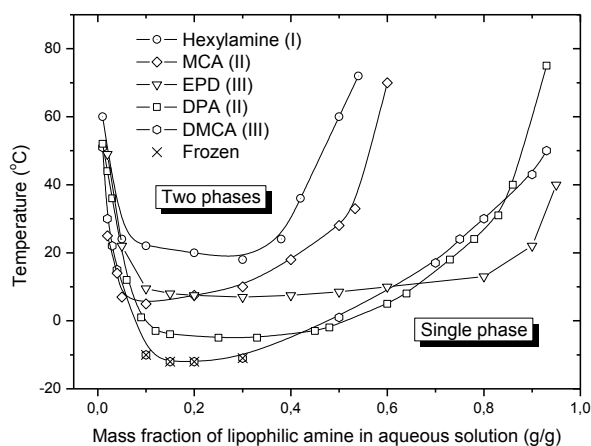
Figure 20. LCST of lipophilic amines solutions

3.5.3   LLPS in regeneration

The temperature-induced liquid-liquid phase separation (LLPS) is a distinctive and very beneficial phenomenon in the regeneration process using lipophilic amine absorbents (see Figure 21). It was observed in the aqueous solutions of some primary (I) and secondary (II) amines as well as most tertiary (III) amines at 60-90 °C (see Table 11). In the DMX™ process proposed by IFP, the CO_2 lean phase is split off from the rich phase by using LLPS and the lean phase recycled directly to the absorber to save energy in the stripping step (Raynal et al., 2011b). However, in the TBS process, the regeneration technology has been developed still further to the point where steam stripping becomes superfluous. Due to the excellent performance characteristics of the lipophilic amines selected, deep regeneration was achieved without steam stripping, i.e. only by LLPS and the extractive regeneration behaviour of blended lipophilic amine systems.

37
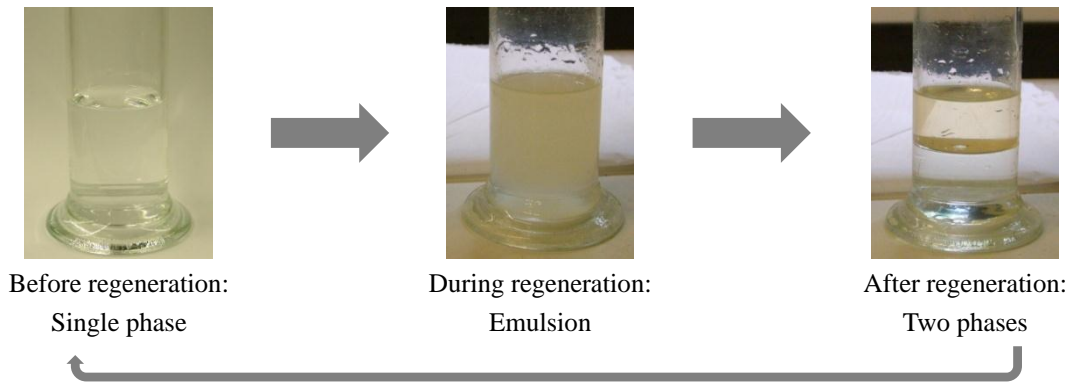
Figure 21. LLPS behaviour observed in experiment

As seen from Table 11, the temperature difference between the LCST and LLPS is at least 70 °C, which means that steam stripping is still required for absorption activators to attain deep regeneration, and regeneration promoters remain as two phase systems in the absorber feed at 40 °C. Therefore, an important objective of solvent formulation is to reconcile these differences.

Table 11. LCST and LLPS temperatures of lipophilic amine solutions

	Amine	Type	LCST	LLPS Temp. of 3 M solution	Regenerability at 80°C
			°C	°C	%
Activator	HA	I	20	90	~40%
	DPA	II	-5	90	~50%
	MCA	II	10	90	~50%
	2EPD	II	10	90	~50%
Promoter	DsBA	II	-20	60	>95%
	DMCA	III	-15	70	>90%
	EPD	III	10	80	>80%

3.5.4 Explanation of biphasic concept with the van't Hoff equation

Low temperature swing between absorption (at 30-40 °C) and desorption (at 80-90 °C) is a remarkable advantage for the TBS system in comparison to conventional alkanolamines with $\Delta T > 80$ °C. According to the van't Hoff equation:

$$\ln\left(\frac{K_2}{K_1}\right) = -\frac{\Delta H^{\ominus}}{R}\left(\frac{1}{T_2} - \frac{1}{T_1}\right)$$ Eq. 3.1

To attain the same depth of CO_2 desorption from the loaded amine solution, a lower temperature swing (ΔT) will lead to a higher ab-/desorption enthalpy. However, the heat of desorption (ΔH_{des}) for lipophilic amines comprises not only the reaction enthalpy

($\Delta_r H$) but also additional heat (ΔH_{mix}) when phase separation occurs (Eq. 3.2), since an exothermic mixing of lipophilic amine and water was observed.

$$\Delta H_{des} = \Delta_r H + \Delta H_{mix}$$ Eq. 3.2

The desorption enthalpy of lipophilic amines measured in experiment is comparable to that for alkanolamines. In tertiary amines, the absorption enthalpy is 48.7 kJ/mol$_{CO2}$ for 30 wt.% MDEA (Carson et al., 2000), while it is ≈69 kJ/mol$_{CO2}$ for DMCA (Tan, 2010); in secondary amines, it is 70.3 kJ/mol$_{CO2}$ for DEA, while ≈84 for kJ/mol$_{CO2}$ for DPA (see Table 12). In this case, to achieve the same reaction equilibrium of MDEA (40-120 °C), the required temperature swing for DMCA is only (40-75 °C); while compared to DEA at the same condition the required temperature swing for DPA is (40-90 °C), based on van't Hoff equation. Therefore, the TBS system cannot save the energy cost in terms of absorption enthalpy, but rather in the sensible heat and stripping energy. The most remarkable advantage is it enables the use of waste heat for solvent regeneration purpose due to the low required desorption temperature together with high CO$_2$ loading capacity and excellent regenerability.

Table 12. Heat of reaction of CO$_2$ with 3M amine solutions

(kJ/mol$_{CO2}$)

Absorbent	MEA (5M)	MDEA	DPA [b]	DMCA [b]	DMCA+DPA (3:1) [b]	DsBA	DsBA+MCA (3:1)
Experiment [a]	79	48	84	69	74	56	61
Literature [c]	82	49	-	-	-	-	-

[a] measured by the thermodynamic method at rich CO$_2$ conditions; [b] from Tan, 2010; [c] from Carson et al., 2000.

3.5.5   Challenges for thermodynamic modelling

Some thermodynamic modelling works using the COSMO-RS program were carried out with support from the Chair of Separation Science & Technology at Friedrich-Alexander-Universität Erlangen-Nürnberg (FAUEN). COSMO-RS is a novel predictive method for thermodynamic properties of pure and mixed fluids. It calculates the thermodynamic data from molecular surface polarity distributions, which result from quantum chemical calculations of the individual compounds in the mixture. It has recently proved to be one of the most reliable and efficient tools for the prediction of vapour-liquid equilibrium (VLE) among those presently available (Klamt et al. 2010). It is expected to simulate the phase change behaviour and resolve the enthalpy-temperature paradox, as well as to predict solvent basicity and reaction kinetics.

During the collaboration with FAUEN, various thermodynamic data, such as pK_a, vapour-liquid equilibrium (VLE) and liquid-liquid equilibrium (LLE) for amine-water systems as well as the partition coefficients for amine-water-alkane systems, were calculated with COSMOthermX software. The model was initially validated with the MEA-water system, however, the results for lipophilic amine-water systems were unsatisfactory because of large deviations between the experimental and simulated values. In the previous study, Tan (2010) also conducted an empirically modified Kent-Eisenberg thermodynamic model to predict the concentration of ionic species but it did not fit the biphasic system so well, since a discontinuity of the concentrations of ionic species was observed at the phase change point.

Additionally, flowsheet simulations using AspenPlus^{TM} with an electrolyte NRTL model was also conducted and worked well with conventional alkanolamines but poorly with lipophilic amines (Hussain, 2012). This was primarily due to the LCST behaviour of lipophilic amine-water systems, which cannot be recognised by those models.

3.6 Summary

According to the preliminary screening results and amine molecular structure study, primary amines HA and CHpA as well as secondary amines DPA, MCA and 2EPD were selected due to their rapid reaction kinetics; tertiary amines DMBzA, DMCA and EPD together with secondary amine DsBA, were recommended because of their remarkable desorption performance. The ideal molecular structure of alkylamines has been proposed: the major substituent (R^3) should contain 5-7 carbons and the other minor two (R^1 and R^2) should comprise no more than 3 carbons; secondary amine has the highest potential to achieve rapid absorption rate, and tertiary amine are competent to attain good regenerability; cyclic and branched structures at α-carbon position are favoured to not only reduce the solvent viscosity but also to increase the absorption rate. Phase change behaviours are also determined in the selected amines, but the LCST for most of them is lower than 40 °C, which is the typical operation temperature in the absorber; further improvement is therefore required.

4　Optimisation of solvent recipe

4.1　Experiment: Bubble column solvent screening

The absorption experiments were conducted in a 100 mL glass bubble column containing 40 mL of the aqueous amine solution at 40 °C. Selected amines with varying amine concentrations and CO_2 partial pressures were tested. Desorption was initially carried out by N_2 stripping and afterwards by magnetic agitation at 70-80 °C. The gas phase was monitored online by gas chromatography (GC) and the CO_2 loading in the liquid phase was ascertained by the barium chloride method, total amine concentration was determined by acid-base titration and the blended amine compositions were determined by GC analysis. The detailed method is described in Appendix B.2.

4.2　Absorbents classification

After the screening experiments of more than 60 lipophilic amines, solvents such as cycloheptylamine (CHpA), methylbenzylamine (MBzA), methylcyclohexylamine (MCA), N,N-dimethylcyclohexylamine (DMCA), 2-ethylpiperidine (2EPD) and di-*sec*-butylamine (DsBA) have been selected as alternative absorbents. Tertiary amine is the most favourable solvent for promoting regeneration by its low dielectric constant and thermal-induced liquid-liquid phase separation (LLPS). Secondary amine has the most potential for achieving rapid reaction kinetics due to its high basicity and partially miscibility with water. Increasing the length of chain improves solvent regenerability but leads to slower absorption rate. Branched chain has positive influence on reaction rate but enhances the detrimental insoluble carbamate salts formation of protonated primary and secondary amines. Cyclic structure is recommended to increase the aqueous solubility and reaction kinetics, because it relatively reduces the chain length. Since none of the single amine solvents was found to be a perfect solvent to meet all the screening criteria, blended solvents have been considered and studied to improve the drawbacks of the individual amines and combine the advantages of each.

According to the performance parameters in absorption and desorption, lipophilic amines are classified into two categories: absorption activator (*ACV*), for instance, CHpA, MBzA and MCA, with rapid reaction kinetics, as well as regeneration promoter (*PRM*), such as DsBA, DMBzA and DMCA, exhibiting outstanding regenerabilities. Based on the reaction mechanism and results from screening experiments, primary and some secondary amines can be considered as activator, but most of them were excluded

in this study due to the detrimental phenomena and low CO_2 loadings. Tertiary and a few secondary amines can be regarded as promoter; the reactivity was however limited.

Figure 22 shows fast absorption rate and high CO_2 loading have been achieved in MCA solution, but its regenerability is not so satisfactory as it requires higher temperatures >90°C for deep regeneration; however, it still performs much better than conventional MEA. Additionally, the rapid desorption and lower regeneration temperature can be obtained in DsBA or DMCA solution, but slow absorption is its weakness; nevertheless, it is superior to alkanolamine MDEA.

Amine	Reg.
1. MCA	85.6%
2. DMCA	98.5%
3. MEA	46.4%
4. DsBA	98.8%
5. MDEA	88.2%
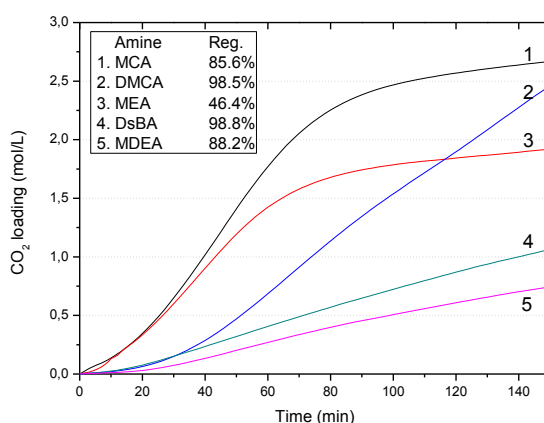
Figure 22. Absorption of CO_2 into 3M single amine solutions in bubble column test (Treated with 30 vol.% CO_2 at 40°C)

Due to the difficult circumstance of obtaining a single lipophilic amine as a perfect solvent to meet all the screening criteria, i.e. both of high reactivity and good regenerability, blended solvent (*BLD*), activator + promoter, has been recommended to improve the drawbacks of the individual amines and combine the advantages of both. Several formulations, e.g. MCA+DMCA and MCA+DsBA, have been studied and present good performance with respect to the loading capacity, reaction kinetics, desorption temperature and regenerability. Some examples are given in Table 13 and more details are discussed in the following section.

4.3 Blended solvents

Since no single amine can achieve all the desired selection criteria in both absorption and desorption, blended solvents were considered to optimise the absorbent formulations. In the MCA-based solvents, regeneration promoters were added to improve the performance in desorption, while in DMCA-based solvents absorption activators were added to accelerate the reactions in absorption.

Table 13. Performance of some selected amines and their blends

Type	Absorbents (3:1 in blend)	CO$_2$ loading [a]	Absorption rate [b]	Residual loading [c]	Cyclic capacity	Note
Units		mol/L	$\times 10^5$ mol/(L·s)	mol/L	mol/L	
ACV	3M MCA	2.95	45.5	0.81	2.14	this work
	5M MCA	3.87	42.6	0.59	3.28	this work
	5M MEA	3.12	35.7	1.62	1.50	benchmark
PRM	3M DMCA	2.71	27.8	0.18	2.53	this work
	3M DsBA	1.27	11.8	0.15	1.25	this work
	3M MDEA	0.87	8.3	0.10	0.77	benchmark
BLD [d]	3M DMCA+MCA	2.76	44.9	0.25	2.51	this work
	4M MCA+DMCA	3.56	43.1	0.36	3.20	this work
	4M MCA+DsBA	3.47	42.9	0.29	3.18	this work
	3M DMCA+DPA	2.34	42.3	0.23	2.11	Tan, 2010
	3M MDEA+MEA	2.01	33.4	0.31	1.70	benchmark

[a] Absorption with CO$_2$ partial pressure 14.6 kPa at 40 °C;

[b] Measured at CO$_2$ loading of 0.6 mol/L;

[c] Desorption with 200 mL/min N$_2$ gas stripping at 75 °C;

[d] Solvents are blended in proportion of 3:1.

The optimisation experiments were carried out at various temperatures between 25-90 °C and amine concentrations as well as for different proportions of the main absorbent and activator. The best amine concentrations and ratios were observed at 3-4M total amine concentration with a 3:1 ratio (mol$_{-PRM}$/mol$_{-ACV}$). An increase in amine concentration generally reduces the solution circulation rate required and hence cuts the capital and operational expenses (Kohl and Nielsen, 1997). However, no significant loading capacity increase was found when the concentration was raised to a high level >4M, since water is also a reactant in the absorption process. Increasing the proportion of promoter to activator slows down the reaction kinetics, but improves solvent regeneration. The most suitable absorption temperature was found to be 40 °C. Although the exothermic reaction means that low temperatures favour high CO$_2$ loadings, reaction kinetics are enhanced by higher temperatures. When the temperature exceeds 50 °C, the thermomorphic phase transition may take place and the loading capacity can be significantly reduced. The optimal regeneration temperature is believed to lie in the range of 70-80 °C, since a deep desorption can be achieved by using waste heat for regeneration.

4.3.1 Activator as principal component

In order to improve the regenerability of MCA-based solvent, additional regeneration promoters such as DMCA, N,N-dimethylbenzylamine (DMBzA) and di-*sec*-butylamine (DsBA) have been used in the blended solvent. Most promoters could significantly increase the desorption rate of loaded solutions with minor influence of absorption rate and CO_2 capacity when the proportion of promoter and MCA was limited to no more than 1:2. Addition of DMBzA can ameliorate the desorption but negative influence was found in absorption due to its slow reaction kinetics. As a regeneration promoter, DsBA performs a little better than DMCA, but more significant volatile loss becomes the major weakness for DsBA. Therefore, DMCA is considered as the most suitable promoter to improve the performance of MCA-based solvent in further studies.
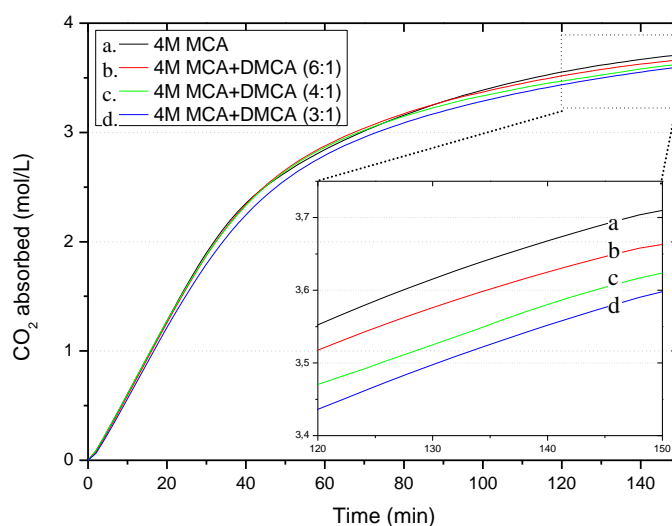

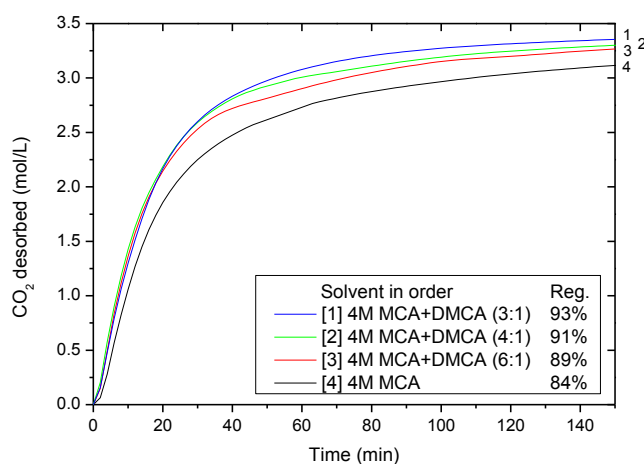**Figure 23.** CO_2 absorption into solutions using MCA as principal component

Figure 24. CO_2 desorption from rich solutions using MCA as principal component

44

Figure 23 and Figure 24 present the ab-/desorption characteristics in MCA-based solvents blended with DMCA, which proved the positive effect in regeneration but limited influences on absorption rate and loading capacity. Figure 25 illustrates the net CO_2 capacity ($\Delta\alpha = \alpha_{rich} - \alpha_{lean}$) of MCA-based solvent is much higher than conventional MEA and also better than DMX-1 solvent in the vapour-liquid equilibrium (VLE) test with CO_2 partial pressures from 50 to 500 mbar.
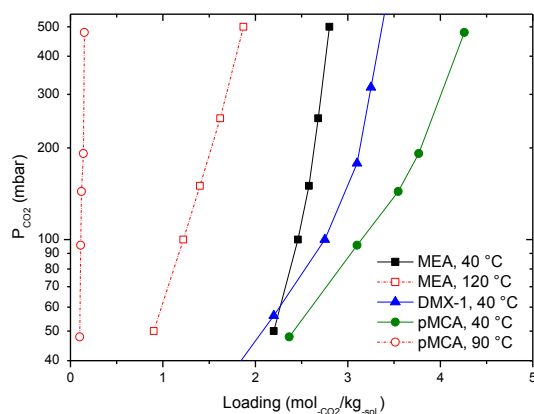
Figure 25. VLE of MCA-based solvent

(MEA: 30wt%; DMX-1: data from Raynal et al., 2011a; pMCA: MCA+DMCA, 4+1M)

4.3.2 Promoter as principal component

DMCA, DsBA, DMBzA and N-ethylpiperidine (EPD) with their high loading capacity and outstanding regenerability were identified as alternative solvents for CO_2 absorption, but activators are required to improve their reaction rates. Due to unfavourable degradation of EPD and low reactivity of DMBzA, neither of them was recommended as principal components.
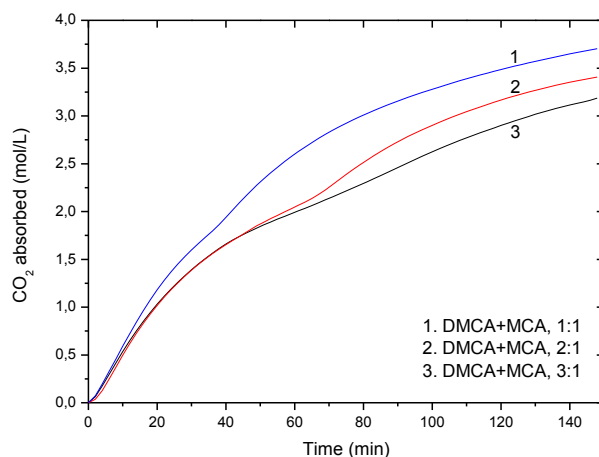
Figure 26. CO_2 absorption into 4M solutions using DMCA as principal component

45
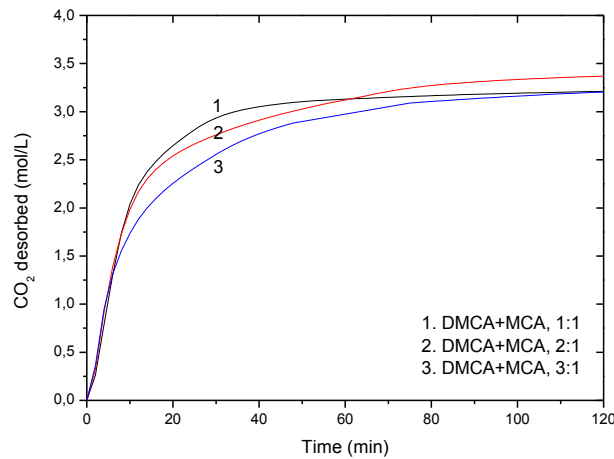
Figure 27. CO_2 desorption from 4M solutions using DMCA as principal component

To investigate the influence of activators on the ab-/desorption characteristics of DMCA-based solvents, experiments with varying amine proportions were conducted in bubble column test. Figure 26 and Figure 27 demonstrate addition of MCA has a positive influence on absorption kinetics and CO_2 loadings but minor effect on regenerability. Figure 28 proves the net loading capacities of DMCA-based solutions are much higher than that for conventional MEA (30wt% ≈ 5M) at CO_2 partial pressures from 0.04 to 0.15 bar, which is the typical range for flue gas from fossil fuel combustion. Deep regeneration at 75-80 °C is the most remarkable superiority to conventional amines.
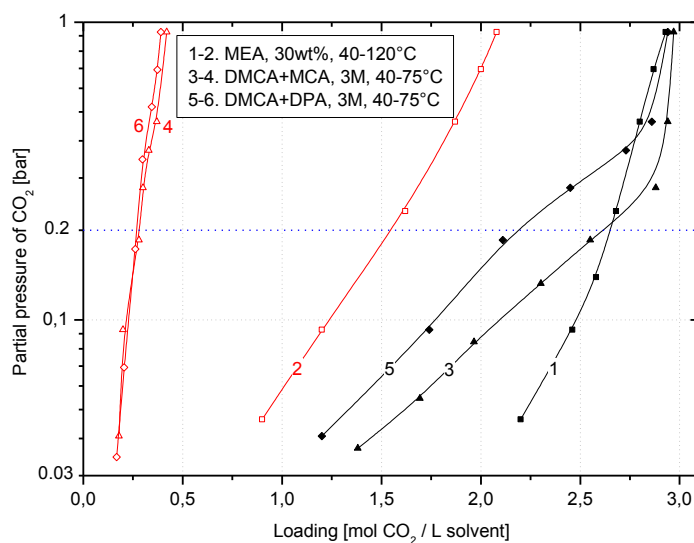
Figure 28. VLE of DMCA-based solvents

46

4.4 Solubilisation

Since most of the preliminarily formulated absorbents still exhibit a biphasic behaviour, which is undesired for absorption, several countermeasures such as varying of concentration, decrease of temperature and addition of solubiliser were used to convert the heterogeneous solvent to single phase under absorption conditions.

4.4.1 Influence of molecular structure and concentration

Most lipophilic amines present a lower critical solution temperature (LCST) at mass fraction 0.1-0.3 in aqueous solutions. When increasing the concentration to >30 wt.%, the corresponding phase transition temperature will also be elevated. For example, the LCST of MCA is 7 °C at 10 wt.%, while it increases to 30 °C at 50 wt.% and to 40 °C at 55 wt.%, which can meet the requirement for absorption. The absorption process typically prefers a high amine concentration to reduce the solvent circulation flow rates, but it is limited to no more than 5M for TBS.

In the aliphatic amine solutions, the LCST is influenced by the hydrophobic group(s), which means more carbons in the substituent, lower LSCT and also in the order of primary amine > secondary amine > tertiary amine, for chain structured amines (see Figure 20). Since the cyclic structure reduced the length of amine molecule, the derivatives of piperidine present higher LCST in comparison to aliphatic amines. Proportion of blended compositions also has an influence on the phase change temperature. As illustrated in Figure 29, both the LCST and phase separation temperature (PST) are enhanced by decreasing the proportion of DMCA and MCA.
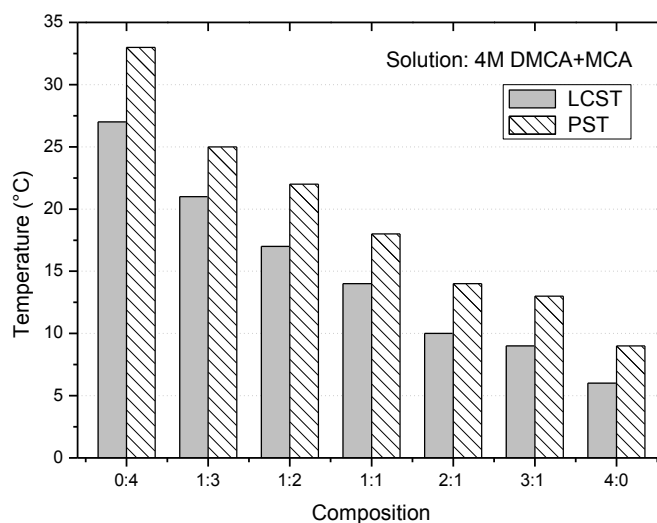

Figure 29. LCST and LPST of blended DMCA+MCA solutions

4.4.2 Solubilisation by partially protonated lipophilic amine

Influences of CO_2 loadings on the phase separation behaviour and temperature on solvent regenerability were also observed in this work. The LCST of the most aliphatic amines is elevated by protonation, but the derivatives of piperidine and N,N,N´,N´-Tetramethyl-1,6-hexane-diamine (TMDAH) are exceptions (see Figure 30A and Figure 31A), where both the LCST and PST are reduced by increasing the CO_2 dissolution into the N-methylpiperidine (MPD) or EPD solutions at loadings <0.25 mol_{CO_2}/mol_{amine}. A similar phenomenon was also found in high concentration DMCA solutions at low CO_2 loadings (see Figure 30B).

(A) MCA and TMDAH   (B) DMCA
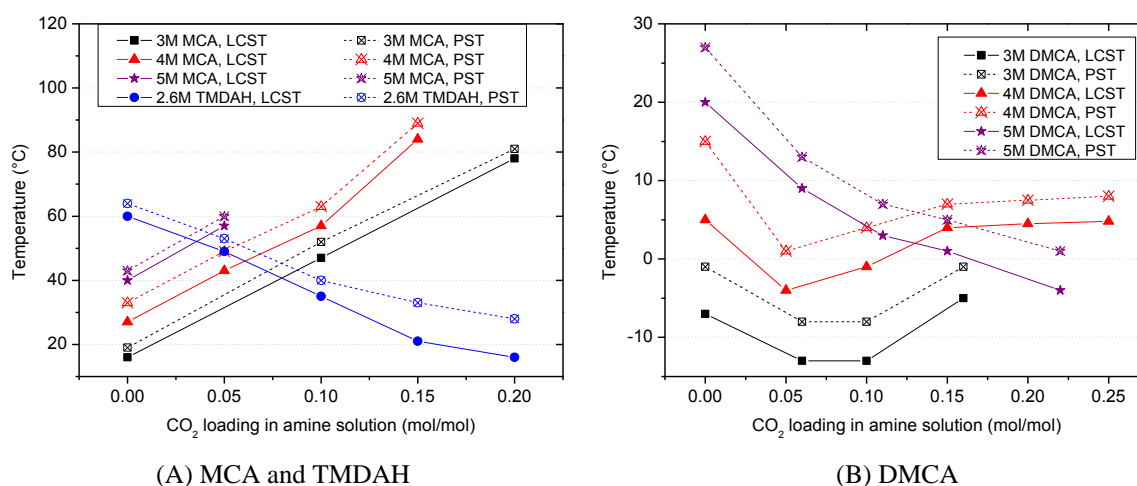
Figure 30. Influence of CO_2 loading on LCST in single amine solvents

In the MCA-based blended solvents, the protonated lipophilic amines were found competent to play the role of solubiliser for elevating the critical solution temperature, As illustrated in Figure 31B, the LCST of unloaded 5M MCA+DsBA (4:1) solution is 15 °C, while in the lean loaded (0.05 mol/mol) solution it increases to 40 °C, which demonstrates the technical feasibility for implementing absorption. Therefore, most of the solutions, comprising only activators or activators as primary solvent, can directly be used for CO_2 absorption since they are homogeneous at 40°C with lean CO_2 loadings <0.1 mol/mol. However, in solutions using promoters as principal solvent, the LCST is still lower than 30°C, even with 0.2 mol/mol CO_2 loading (see Figure 31A), it is thus inconvenient for absorption and solubiliser addition should be considered for elevating the LCST.

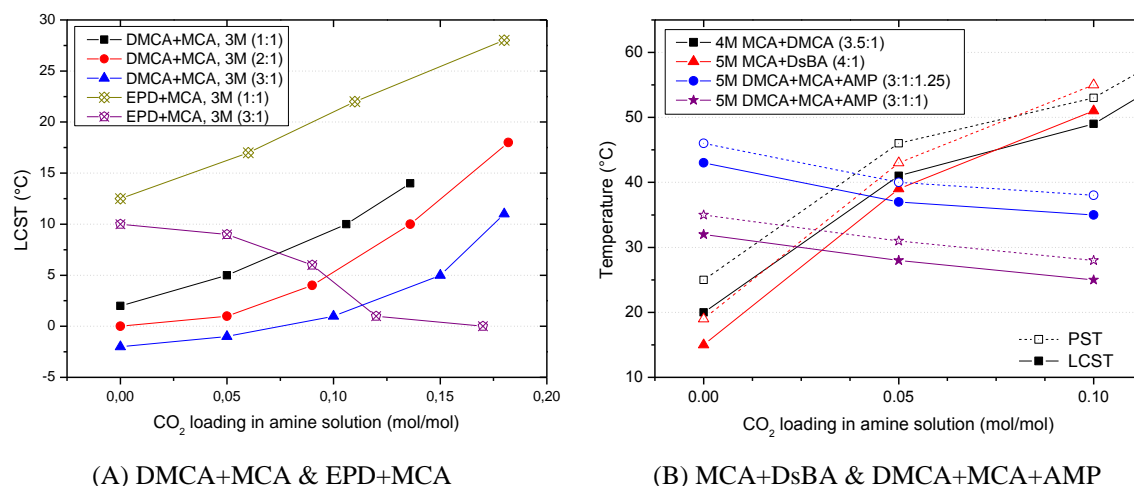(A) DMCA+MCA & EPD+MCA   (B) MCA+DsBA & DMCA+MCA+AMP

Figure 31. Influence of CO_2 loading on LCST in blended solvents

4.4.3 Solubilisation by foreign solvent

Thermal-induced phase transition is a distinctive property for TBS systems. The homogeneous solution converts to heterogeneous upon heating after achieving the LCST; contrarily, the regenerated biphasic solution reverses to single phase by cooling. Most of the aliphatic amines exhibit the phase transition behaviour in aqueous solutions, but very few of them can be employed as absorbent, because of the high volatile loss of lower alkylamines (C5-C7) due to low boiling point and low LCST of fatty alkylamines (C8-C10) whose LCST is lower that the freezing point of water. To improve the solubility property of those lipophilic amines, aqueous solubiliser was employed for regulating the phase transition behaviour. Varying organic solvents, e.g. alkanols, alkanolamines and diamines (see Table 14), were hence studied in screening tests. The ideal solubiliser should meet the following criteria:
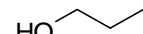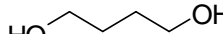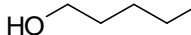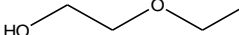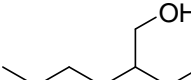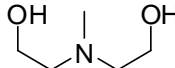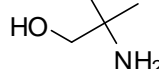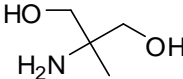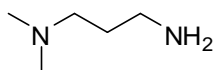
- Effectively elevate LCST of lipophilic amine solutions with only a small amount,
- No negative influence on absorption or desorption,
- High chemical stability, no significant degradation,
- Low volatility.

Figure 32 demonstrates 2-Amino-2-methyl-1-propanol (AMP) has a more effective performance on the regulation of LCST than other tested solubilisers, such as MDEA and ethylene glycol (EG). An increase in mass fraction of AMP exhibits a positive influence on the LCST of DMCA+MCA solutions (see Figure 33). But the percentage

of AMP is limited, since the regenerability is significantly depressed when 20 wt% of AMP is added in TBS systems.

Table 14. List of studied solubilisers

Chemical	CAS	Structure	M_r (g/mol)	bp. (°C)	Supplier
Alkanol					
1-Propanol	71-23-8		60.09	97	Merck
1,4-Butandiol	110-63-4		90.12	236	Merck
1-Pentanol	71-41-0		88.15	137	Merck
Ethylglycol (EG)	110-80-5		62.07	197	Merck
2-Ethylhexanol	104-76-7		130.23	180	Merck
Alkanolamine					
N-Methyl-diethanolamine (MDEA)	105-59-9		119.16	247	Merck
2-Amino-2-methyl-1-propanol (AMP)	124-68-5		89.14	165	Merck
2-Amino-2-methyl-1,3-Propandiol (AHMP)	115-69-5		105.14	151	Sigma
Diamine					
Piperazine (PZ)	110-85-0		86.14	146	Merck
N,N-dimethyl-1,3-propyl-diamine (DMPDA)	109-55-7		102.18	135	Fluka
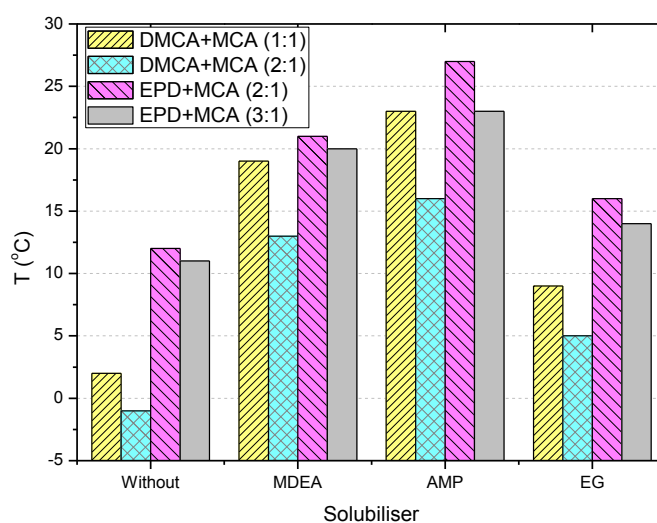
Figure 32. Influence of various solubilisers on LCST

(c_{amine}=3M, addition of solubiliser: 9 wt.%)
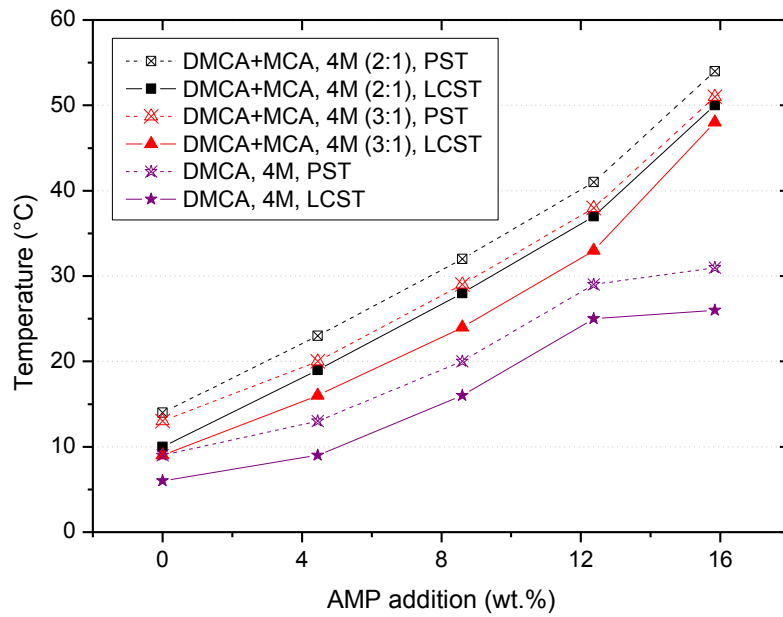
Figure 33. Influence of solubiliser AMP on LCST of DMCA-based solutions

As illustrated in Figure 34, the critical solution temperature (CST) is enhanced by MDEA addition and CO_2 dissolving. Figure 35 shows addition of 9 wt.% AMP increases the CST of DMCA solution by 15 or 20 °C at varying amine concentrations with minor influence on CO_2 capacity of the original TBS system. Figure 36 proves AMP also successfully elevates the CST of DMCA+MCA solutions at different proportions. Only limited influence was found on the absorption and desorption performances for lipophilic amine solutions with small amount of AMP addition (see Figure 37), since AMP is also an active component for CO_2 capture.
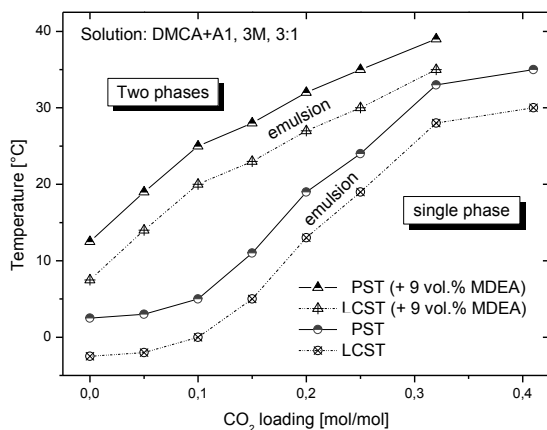
Figure 34. Influence of MDEA and CO_2 loading on LCST of DMCA+MCA solution
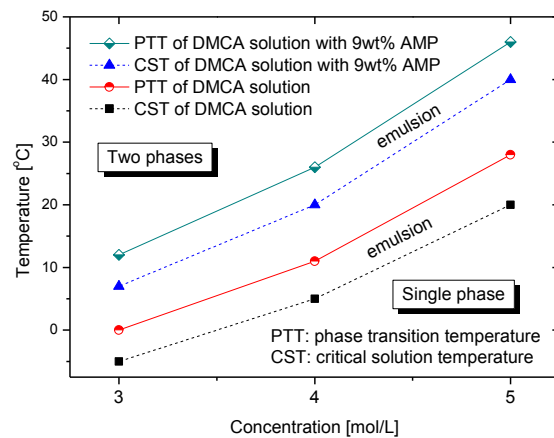
Figure 35. Influence of concentration and AMP addition on CST of DMCA
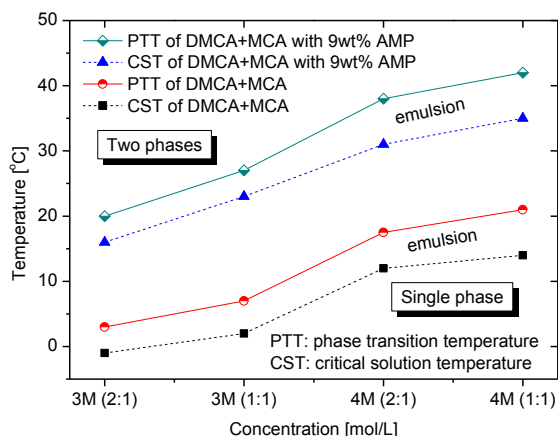
Figure 36. Influence of concentration, proportion and AMP addition on CST
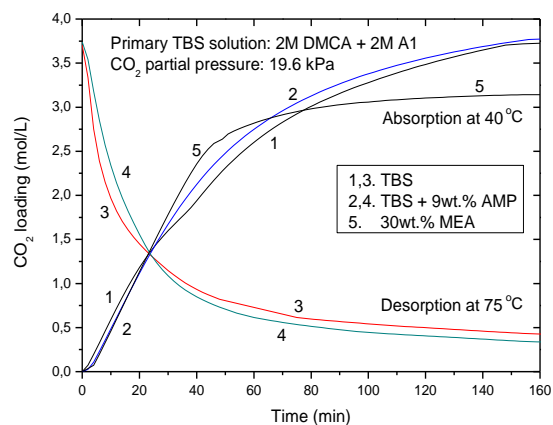
Figure 37. Influence of AMP on the ab-/desorption characteristics

The experimental results above prove an effective solubiliser such as AMP can competently elevate the CST of lipophilic amine solvents without any negative influence on the ab-/desorption performance parameters compared to the original TBS solutions. It offers a great facility for selecting more lipophilic amines with low CST to formulate new TBS absorbents.

4.4.4 Influence of foreign solubiliser on ab-/desorption

The introduction of foreign solubilisers has successfully increased the LCST of corresponding amine solutions, but their influence on CO_2 absorption and desorption must be controlled within a reasonable range. Experimental study on various solubilisers with suitable weight percentages of additions was conducted in the bubble column screening unit. It showed that amine solubilisers performed better than alkanols and no significant influence on ab-/desorption was found in solvents with less than 10 wt.% additives. Therefore, the optimised solvent formulations typically consist of additional 8-10 wt.% of solubiliser in the original TBS solutions.

Alkanols such as 1-propanol, 1,4-butanediol, 1-pentanol and 2-ethyl-1-hexanol were initially considered as foreign solubilisers for biphasic solvents. As presented in Figure 38, negative effects were observed in absorption since CO_2 loading capacity was reduced. It is expected to have a positive influence on desorption, according to the study from Hamborg et al. (2011), by the low polarity of those alkanols. However, the regenerability was depressed by 1,4-butanediol, because LLPS was postponed.

(A) Absorption   (B) Desorption
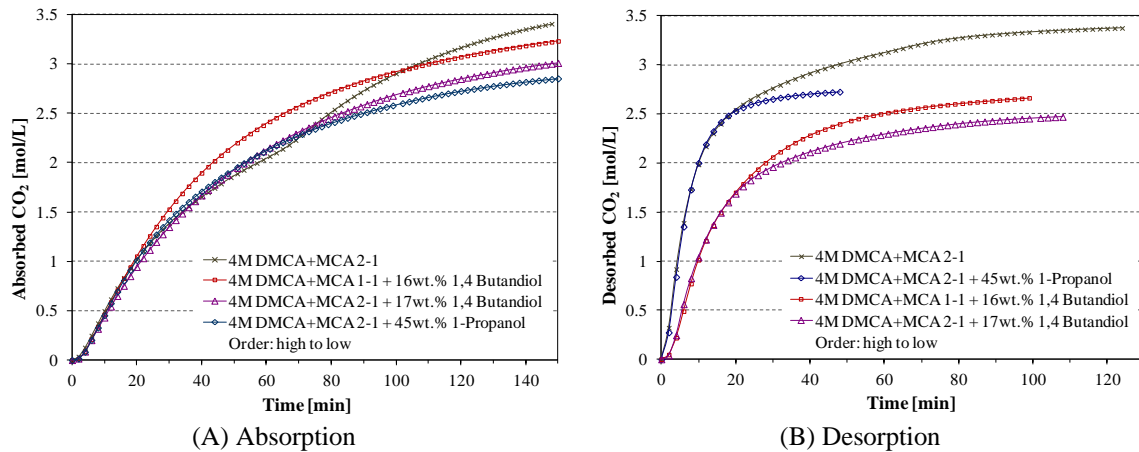
Figure 38. Influence of alkanol addition on CO_2 ab-/desorption characteristics

Sterically hindered amine AMP and diamine N,N-dimethyl-1,3-propyldiamine (DMPDA) were selected as effective amine-based foreign solubilisers. As illustrated in Figure 39, they both exhibited positive influences on CO_2 absorption owing to the increase of total amine concentration. However, the regenerability was decreased with addition of DMPDA, since the required phase separation temperature was increased by an additional hydrophilic amino group on the DMPDA molecule; but with AMP addition, no negative effect was observed.

(A) Absorption   (B) Desorption
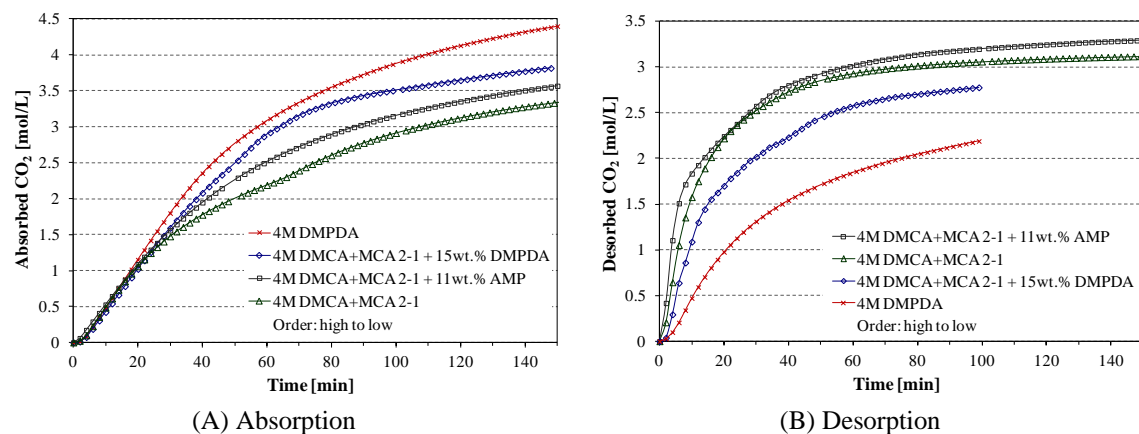
Figure 39. Influence of AMP and DMPDA addition on CO_2 ab-/desorption

4.5   Summary

Blended solvents comprising an absorption activator and a regeneration promoter are recommended to formulate an advanced solvent recipe for CO_2 absorption, since single amine solutions cannot meet all the selection criteria, but blending is able to combine the advantages of both. Solvents using activator as principal component with addition of promoter such as DMCA+MCA (1:3) achieve both rapid absorption kinetics and good

regenerability, however, oxidative degradation becomes a challenge and regeneration temperature requires over 90 °C; contrarily, solvents containing promoter as principal component with addition of activator e.g. DMCA+MCA (2:1) exhibit remarkable absorption and desorption characteristics, but their LCST is lower than 40 °C and present an biphasic behaviour before absorption. Solubiliser is thus introduced to improve such problems. The solubilised solvent, for example DMCA+MCA+AMP (3:1:1), dramatically increased the LCST to 40 °C or above without any negative influence on absorption and regeneration performances.

5 Solvent losses and countermeasures

5.1 Foaming

5.1.1 Literature review on foaming

Foaming is one of the most severe operational problems encountered in both absorber and regenerator at amine scrubbing plants. It can be caused by high gas velocity and chemical contaminants entering the process, for example fine particulates from feed gas, condensed liquid hydrocarbon, water-soluble surfactants, amine degradation products and additives (Stewart and Lanning, 1994; Thitakamol and Veawab, 2008). To investigate the cause of foaming, the effect of amine concentration, degradation products, ferrous/ferric ions, liquid hydrocarbon, corrosion/oxidation inhibitors and antifoam agent was measured by Chen et al. (2011) and a foaming model with parameters such as bubble radius, difference in density of gas and liquid, surface tension of liquid, viscosity of liquid and superficial gas velocity was established by Thitakamol and Veawab (2009) for the MEA-based CO_2 absorption process.

5.1.2 Foaming in TBS system

Solvent foaming was found to be serious for some biphasic systems, i.e. regeneration promoter-based solvents. It is mainly influenced by gas velocity, amine concentration, CO_2 loading, temperature and contaminants. Due to the low surface tension of the lipophilic amine formed as a supernatant phase on top of the aqueous solvent, foaming becomes significant with accumulation of organic phase. Low CO_2 loading, high amine concentration, solvent volume and temperature, promoting the formation of two liquid phases, will thus enhance the foaming. It was frequently observed in the lipophilic amines N,N-dimethylcyclohexylamine (DMCA) and di-*sec*-butylamine (DsBA) and also alkanolamine dimethylethanolamine (DMMEA) solutions in the bubble column experiment, and DMCA is the most serious. Figure 40 indicates that foaming can be initially enhanced by increasing gas velocity and temperature, but suppressed afterwards with higher gas flow rates under low temperature operating conditions due to turbulence. It was intensified by increasing the concentration of DMCA or the proportion of DMCA in blended solution and by the contaminants accumulated by recycling the solvent. Foaming wasn't found in activator N-methylcyclohexylamine (MCA), blended DMCA+MCA+AMP or benchmark MEA solutions in the same experimental conditions.
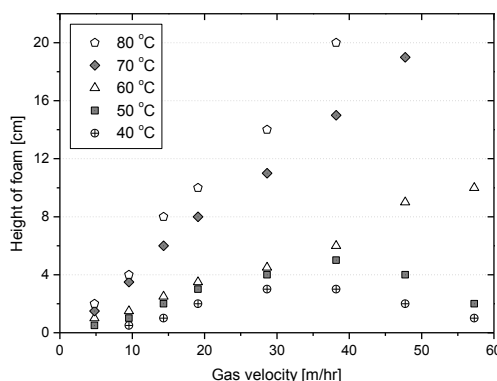
Figure 40. Influence of gas flow rate and temperature on foaming
Solvent: 3 M DMCA+MCA (3:1) solution

5.2 Volatility

5.2.1 Literature review on volatility

Vaporisation loss was found in CO_2 absorption process using volatile amine solvent, which is transferred to the flue gas and vented into atmosphere (Rochelle et al., 2011a). It significantly influences process economics and environmental impact. There are a few publications on vapour pressure of amines in aqueous systems but only very limited measurements on volatility. Nguyen et al. (2010 and 2011) have studied the volatility of several amine solvents and the heats of vaporisation loss with the influence of temperature, amine concentration and CO_2 loading. The volatility of their studied amines is in the following order: AMP > 1-MPZ (1-methylpiperazine) > MEA > EDA (ethylenediamine) > MAPA (3-methylaminopropylamine) > 2-MPZ (2-methylpiperazine) > PZ (piperazine) > DGA (2-aminoethoxyethanol) > MDEA.

5.2.2 Vapour pressure and volatility measurement

Vapour pressure measurement was carried out in a 500 mL three-neck glass flask. A condenser was connected to one of the necks for minimising the vaporisation loss. The system was initially degassed by vacuum pump and the solvent was then heated by oil bath with thermostat (HAAKE F3) and was maintained at boiling conditions during the measurement. The temperature and corresponding total vapour pressure were determined stepwise from 25 to 130 °C.

5.2.3 Vapour pressure and volatile loss

Solvent losses, including vaporisation and degradation, were observed during the experiments. The vaporisation of the amine solution is a function of temperature and

amine concentration, reflecting volatility and vapour pressure, which must thus be determined for the design of absorption and desorption columns preventing solvent loss. Figure 41 depicts the vapour pressures of the lipophilic amines DMCA and MCA, whose values lie between those of alkanolamine MEA and water. The higher volatility with respect to alkanolamine leads to greater vaporisation losses during operation. The experimental data were fitted using an empirically modified Clausius-Clapeyron relation (Eq. 5.1). The results indicated a good agreement for vapour pressures below 500 mbar. In the aqueous lipophilic amine solution, the total vapour pressures of which are a little higher than those of water (see Figure 42), may exhibit azeotrope formation. However, this was not observed at atmospheric pressure until 90 °C and thus does not arise for low temperature operation below 80 °C.

$$\ln\left(\frac{P_1}{P_2}\right) = \frac{\Delta_v H}{R} \cdot \left(\frac{1}{T_2} - \frac{1}{T_1}\right) \qquad\qquad \text{Eq. 5.1}$$
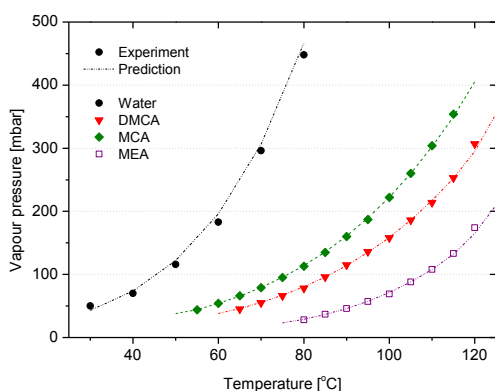
Figure 41. Vapour pressure of various amines (fitted by Clausius-Clapeyron equation)
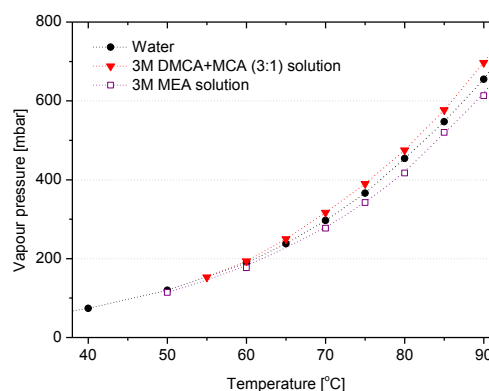
Figure 42. Vapour pressure of aqueous amine solutions

Solvent loss through vaporisation is measured by the difference in amine concentrations before and after the reaction. The concentration reduction of DMCA-MCA solution is a much higher value for the alkanolamine MEA and it approaches 10 %/day in a 100 mL bubble column with 300 mL/min gas flow rate at 40 °C (see Table 15). The vaporised amine should, therefore, be recovered in subsequent experimentation. According to the Gas chromatography (GC) analysis results, the volatility loss of the activator MCA is minor, even though its vapour pressure is higher, since not only the aqueous solubility of MCA is much higher than for DMCA, but also the reaction rate of MCA is extremely rapid and the ionised MCA dissolved in aqueous phase hinders its vaporisation.

5.2.4   Reduction of volatile loss

Since volatile loss is the main challenge in the biphasic lipophilic amine system, which contributes more than 90% of total solvent loss during the DMCA+MCA-based absorption process, countermeasures for reducing solvent vaporisation have hence been studied. Operating temperature is one of the major influence factors, the vaporisation loss can thus be effectively reduced by more than 60% by decreasing the temperature from 40 °C to 30 °C in the absorber (see Table 15). Compared to alkanolamine, the volatile loss for lipophilic amine is also caused by the separate supernatant organic phase, a significant solvent loss reduction of 70% can be achieved by regulating phase transition, i.e. converting the two phases to single phase by means of cooling or foreign solubiliser addition.

Table 15. Vaporisation loss of 3M amine solutions

Amine	Temperature	Loss
	°C	*%/day*
MCA	30	<0.5
	40	1.8
DMCA	30	4.8
	40	12
DMCA+MCA (3:1)	30	4.1
	40	10
	50	14
MEA	40	0.7
AMP	40	1.6

In alkanolamine systems, water scrubbers have been successfully employed for solvent recovery and to cut vaporisation losses. Due to the lower aqueous solubility of lipophilic amines, the efficacy of such a water scrubber is much lower than that in alkanolamine system. Only 15-20% of the vaporised amines from solution DMCA+MCA were captured in a single water absorption stage at room temperature, but 50-55% of them were scrubbed by thermally stable hydrophobic solvent in the same condition. The process is still technically feasible when multistage counter-current operation is considered, since more than 80% of amine vapour has been recovered by hydrophobic solvent scrubbing in a three-stage equilibrium. Condensation with chilled water at 5 °C rather than 20 °C was also evaluated and a vaporisation loss reduction of over 50% was achieved. Moreover, foaming was observed to be a serious problem

during absorption when contaminants were present in the solution. However, after removal of the contaminants, the formation of foam was clearly reduced. A water scrubber was able to achieve efficient defoaming and recover 80% of the foaming losses.

5.3 Thermal degradation

5.3.1 Literature review on thermal degradation

Thermal degradation of amine solvent was primarily observed in the stripping column at temperatures above 100 °C. It is quantified as a function of amine concentration, CO_2 loading, pressure and temperature at stripper conditions (Davis and Rochelle, 2009, Rochelle 2012). The mechanisms for thermal degradation of MEA and DEA were described by Kennard (1980 and 1985), Meisen (1982) and Polderman et al. (1955).

Davis (2009), Freeman et al. (2011b) and Rochelle et al. (2011b) have reported the thermal degradation of aqueous amines with varying solvent concentrations, CO_2 loadings and temperatures. Significant degradation of MEA was detected at high concentrations, high CO_2 loadings, elevated pressures and temperatures over 120 °C, while minor degradations were found in MDEA, AMP and PZ solutions. The chemical stability of amines against thermal degradation is in the following order: cyclic amines with no side chains < long chain alkanolamines < alkanolamines with steric hindrance < tertiary amines < MEA < straight chain di- and triamines.

CO_2 plays the roles of not only reactant but also catalyst for degradation in most commercial amines. It reacts with MEA to form a substituted imidalidone and also catalyses polymerisation of DEA (Polderman et al., 1955; Meisen et al, 1982). Therefore, CO_2 loading significantly enhances the thermal degradation of the corresponding amine solvent (Lepaumier et al., 2011). A comparison study of CO_2-induced thermal degradation among 12 amines was conducted by Lepaumier et al. (2009a) in a 100 mL batch reactor at 140 °C and 2 MPa CO_2 pressure for 15 days. The amount of amines and degradation products were determined by GC and GC-MS. Cyclic, tertiary and sterically hindered amines were identified as stable structures while secondary amines were the most unstable. Oxazolidinones/imidazolidinones formation and demethylation/methylation were observed as main reactions.

5.3.2 Experimental method

The thermal degradation tests were conducted in 20 ml glass test tubes with 10 ml CO_2 saturated amine solution for each immersed in an oil bath at 120 °C for 5 weeks. Before analysis, the solution was treated with 15% CO_2, so that the results could be compared with those in the VLE test. The collected samples were degassed and then analysed by Shell Method Series (SMS, 2006) for determination of the heat stable salts (HSSs) and by GC-MS (HP 5973) for identification of volatile oxidation products.

5.3.3 Amine losses and HHSs formation

Due to high temperature, typically 120-140 °C for alkanolamines, applied in the desorber, thermal degradation occurs during solvent regeneration. For lipophilic amines, the desorption takes place at ≈80 °C, thermal degradation is therefore negligible (Nwani, 2009, Zhang, J. et al., 2011b and 2012b). To explore the thermal degradation of such biphasic solvents, the investigation was carried out at an elevated temperature of 120 °C. It is much higher than the regeneration temperature required for lipophilic amines, but the thermal degradation products can thus been determined in a relative short term. Figure 43 presents the total amine losses, including degradation and vaporisation losses, after a 6-week thermal degradation test. It proves CO_2 has a significant influence in inducing thermal degradation, MCA is unstable at high temperatures and DMCA performs better than the benchmark solvent MEA. Therefore, it is recommended to use DMCA as the principal component in the optimised biphasic solvents.
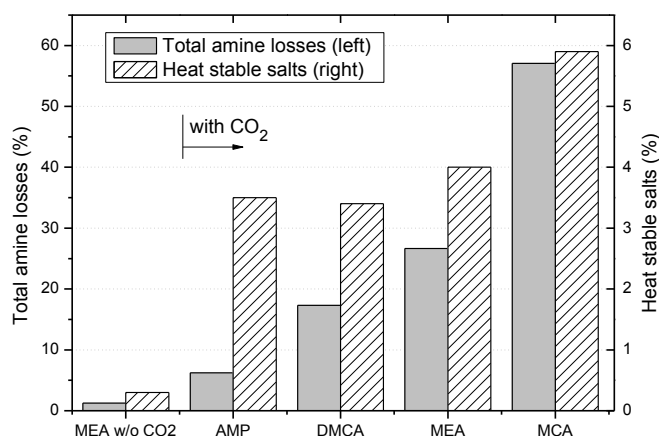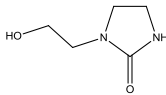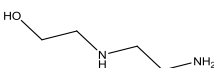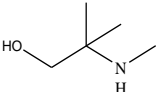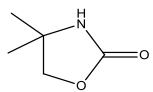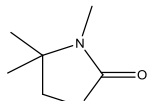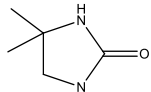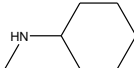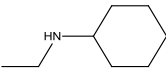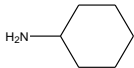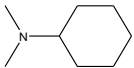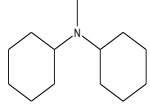
Figure 43. Thermal degradation of amine solvents in presence of CO_2

5.3.4 Thermal degradation products and mechanisms

According the analysis of degradation products, the CO_2 involving oxazolidinone formation (R. 5.1 and 5.2) is the major degradation reaction for alkanolamines MEA and AMP, while demethylation and methylation (R. 5.3) are the main reactions for lipophilic amines MCA and DMCA. Thermal degradation reforms a lipophilic amine to other amines which are still active to react with CO_2 and also have capability to be regenerated and recycled for absorption. Table 16 shows the main degradation components formed in a thermal condition with presence of CO_2 at 2 bar.

Table 16. Main thermal degradation products

Amine	Degradation compounds
MEA	1-(2-hydroxyethyl)-2-imidazolidone N-(2-hydroxyethyl)-ethylenediamine
AMP	2-Methylamino-2-methyl-1-propanol 4,4-dimethyl-2-Oxazolidinone 3,4,4-trimethyl-2-Oxazolidinone 4,4-dimethyl-2-imidazolidinone
DMCA	MCA ECA
MCA	CA DMCA N-Methyl dicyclohexylamine

Oxazolidinones Formation

R. 5.1

R. 5.2
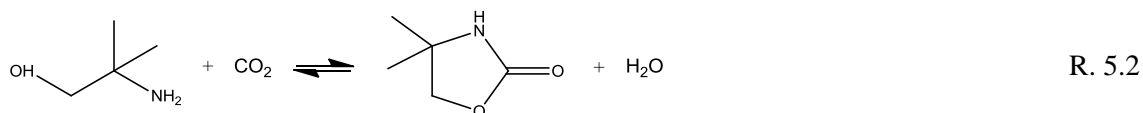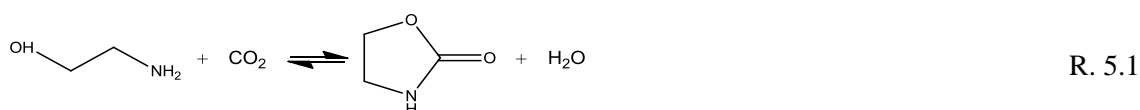
Demethylation / Methylation Reactions

$X^{\ominus} = C_6H_{11}N(CH_3)COO^-$ or HCO_3^-

R. 5.3
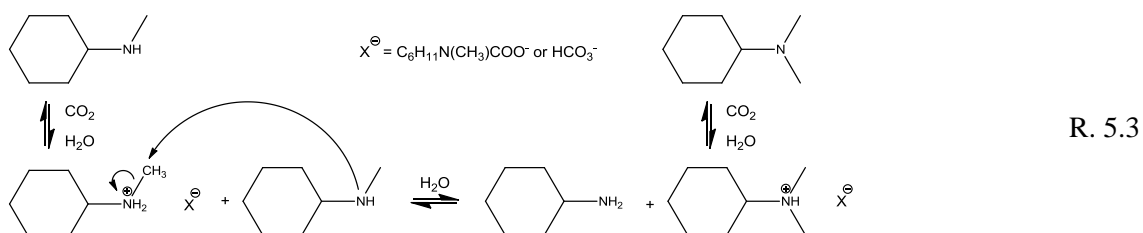
5.4 Oxidative degradation

Oxygen is typically presented in flue gas with 4-10 vol.% after fossil fuel combustion, hence, oxidative degradation must be taken into account in the post-combustion capture (PCC) process. It is a lengthy effect and is influenced by temperature, pressure, amine concentration and CO_2 loading. To reduce the experimental time, intensive conditions such as high oxygen concentration at 98 vol.% and elevated temperature at 50 °C were applied to accelerate solvent oxidation. Both the total amine losses and HHSs were analysed in this study.

5.4.1 Literature review on oxidative degradation

Oxidation of amines to organic salts was determined in the presence of O_2 during absorption. This reaction can be catalysed by iron which is present in steel column and packings and by copper that is added as a corrosion inhibitor (Sexton and Rochelle, 2009). Oxidative degradation of MEA was extensively studied and the main products were volatile components, other amines, aldehydes and carboxylic acids (Bello et al., 2006; Chi, 2000; Goff, 2004; Strazisar et al., 2003). High temperature and O_2 partial pressure can increase degradation rates without any influence on reaction mechanisms.

Generally, tertiary and sterically hindered amines are more stable than primary and secondary amines. Demethylation, methylation, dealkylation and carboxylic acids formation are the major reaction in oxidative degradation of most ethanolamines and ethylenediamines (Lepaumier et al., 2009b). Ring closure reaction also takes place if the amine molecule can easily form a five- or six-membered ring (Lepaumier et al., 2010). Piperazine, as a cyclic amine, oxidises only at high temperatures over 160 °C (Rochelle et al., 2011b; Sexton, 2008).

5.4.2 Experimental method

The oxidative degradation experiment was carried out in a 300 ml glass bubble column containing 200 mL amine solution at 50 °C with 2 mL/min CO_2 and 98 mL/min O_2. An intensified condition, such as high O_2 partial pressure, was applied to reduce the reaction time. A condenser with chilled water at 10 °C was used to minimise the solvent vaporisation and a control experiment with N_2 in place of O_2 was performed for the purposes of comparison and to distinguish oxidative degradation from other losses. Fe (II/III) ions (0.2 mM) were also added in solvents to catalyse the oxidation.

The samples were taken at an interval of 2 days and analysed by acid-base titration to determine total amine losses. After completion of two weeks oxidation, the solution was degassed and HSSs and volatile oxidation products were subsequently analysed by the same method presented in Section 5.3.2.

5.4.3   Amine losses and HHSs formation

Lipophilic amines, for instance MCA and DMCA, exhibit more significant amine losses in comparison to MEA and AMP (see Figure 44). This is mainly caused by volatility loss since the test was conducted in an open system. As discussed in section 5.2.3, controlled experiments demonstrated that vaporisation of activating components during absorption is the major loss for lipophilic amines. HHSs are the most harmful products formed in oxidative degradation and must be measured. Figure 45 illustrates that the blended lipophilic amine solvent (DMCA+MCA+AMP, 3+1+1M) and DMCA presented good chemical stabilities against oxidation while MCA significantly degrades to form HHSs in presence of O_2; therefore, as an activator it must be controlled at low concentrations in blends (Wang, 2012; Zhang, J. et al., 2013). Further studies in solvents with presence of Fe^{2+} / Fe^{3+} found oxidative degradations were catalysed by such ions. Additionally, as demonstrated in Figure 48, oxidation was also slightly enhanced by increasing amine concentrations.
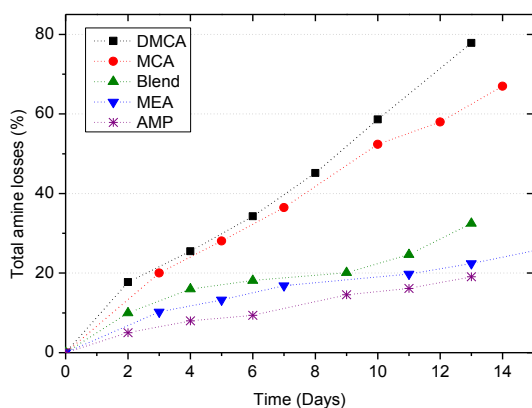
Figure 44. Total amine losses in oxidative degradation
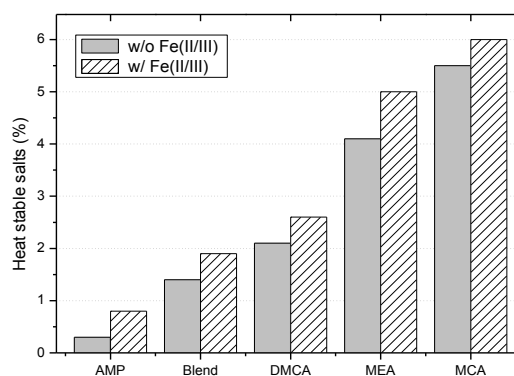
Figure 45. HSSs formed by oxidative degradation
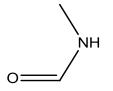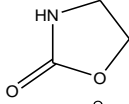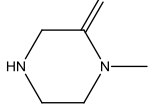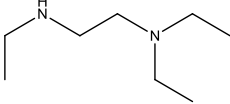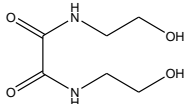
5.4.4   Oxidative degradation products and mechanisms

The mechanisms of MEA oxidative degradation have already been elucidated by Chi, (2000) and Goff and Rochelle (2004). Sexton and Rochelle (2006) analysed the MEA solution after oxidative degradation, which includes formate, formamide and trace of

acetate, oxalate, oxamide, nitrite and nitrate in the form of HHSs in liquid, as well as trace of acetate formaldehyde and acetaldehyde in vapour. As seen in Table 17, N-methylformamide and 4-methylpiperazin-2-one are the most abundant degradation products from MEA observed in this study. Those components are inactive for CO_2 absorption, thus must be removed from the recycle stream and lean MEA needs to be made up for the feed stream.

Table 17. Main oxidative degradation products of MEA

No.	Component	M_r (g/mol)	Structure	Abundance
1	N-Methylformamide	59.07		major
2	Oxazolidin-2-one	87.08		moderate
3	4-Methylpiperazin-2-one	114.15		major
4	N,N,N'-Triethylethylenediamine	114.26		moderate
5	N,N'-bis-(2-Hydroxyethyl)-oxamide	176.17		minor

(A) MEA   (B) AMP
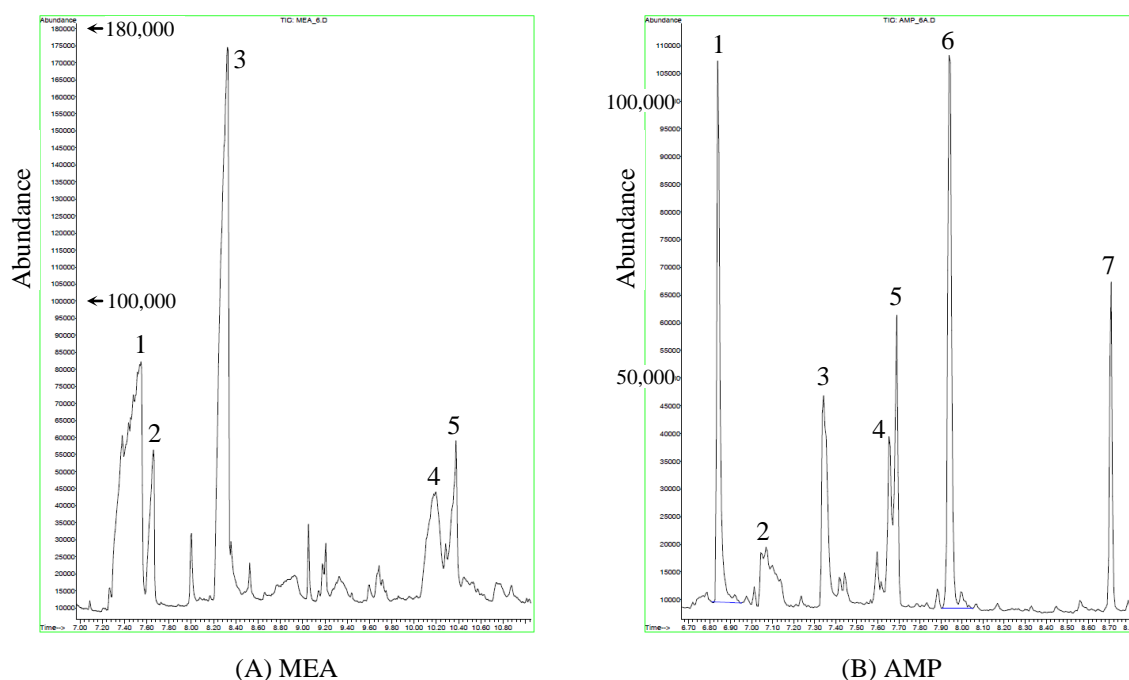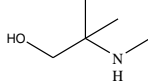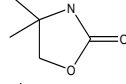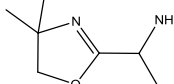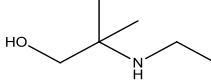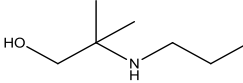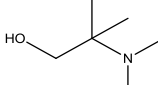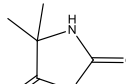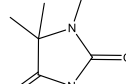
Figure 46. GC-MS chromatograms for degradation products of alkanolamines

Oxidative degradation products of MEA and AMP as benchmarks were initially determined in this work. Figure 46 shows the chromatograms for degradation products of MEA and AMP and their mass spectra are presented in Appendix D. Those components listed in Table 17 and Table 18 were identified using the National Institute of Standards and Technology (NIST) Standard Reference Database - Chemistry Webbook. The oxidative degradation of MEA is much more significant compared to AMP. The major degradation products of MEA are its oxidative components while those for AMP are formed by oxidation and methylation. They are in good agreement with the study from Lepaumier et al. (2009b).

Table 18. Main oxidative degradation products of AMP

No.	Component	M_r (g/mol)	Structure	Abundance
0	2-(Methylamino)-2-methyl-1-propanol	103.16		moderate
1	4,4-Dimethyl-2-Oxazolidinone	115.13		moderate
2	1-(4,4-Dimethyl-2-oxazoline)-Ethylamine	142.20		minor
3	2-(Ethylamino)-2-methyl-1-propanol	117.19		minor
4	2-(Propylamino)-2-methyl-1-propanol	131.22		minor
5	2-(Dimethylamino)-2-methyl-1-propanol	117.19		minor
6	1,5,5-Tetramethylimidazolidine-2,4-dione	142.16		moderate
7	1,3,5,5-Tetramethylimidazolidine-2,4-dione	156.18		minor

Due to different molecular structures, the degradation products of lipophilic amines are quite distinctive from alkanolamines. Figure 47 presents the chromatograms for degradation products of MCA and DMCA. Cyclohexanone and cyclohexanone oxime were determined as the most considerable oxidised components for MCA (see Table 19) via ketonisation (R. 5.4) and oximation (R. 5.5) while other trace components were

restructured alkylamines via dealkylation and alkylation by shifting -CH_3 or -C_6H_{11} groups described by R. 5.3.

Ketonisation

R. 5.4

Oximation

R. 5.5

(A) MCA   (B) DMCA
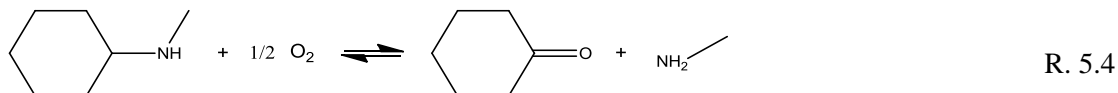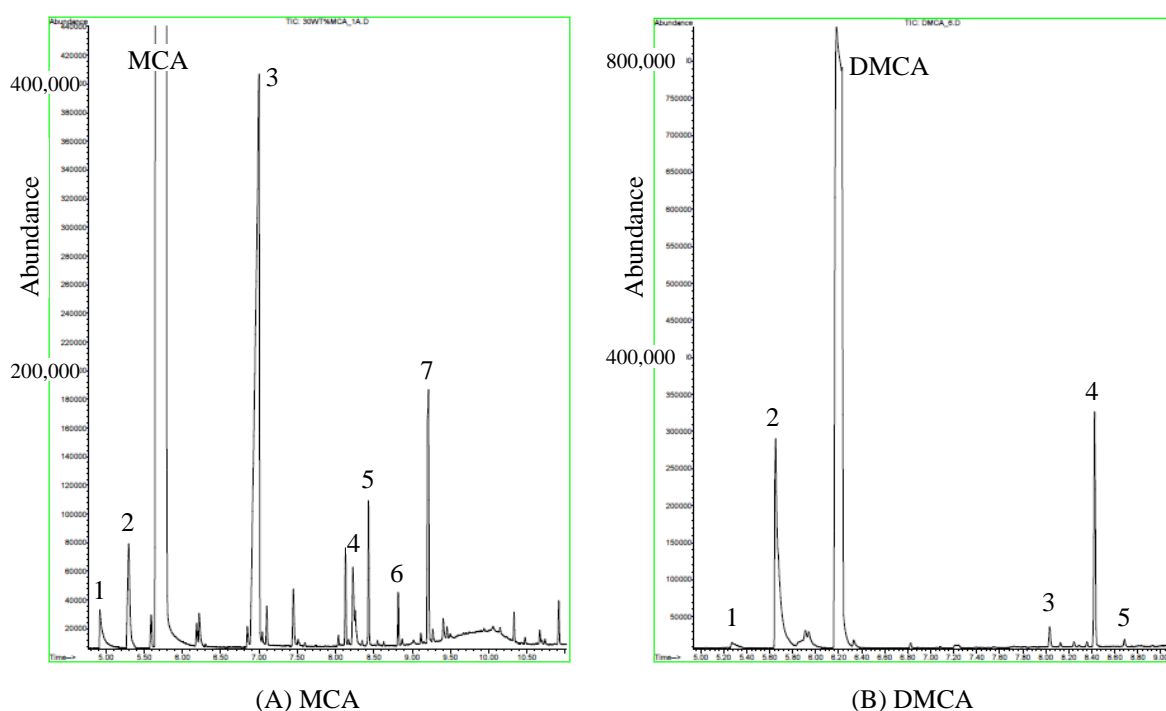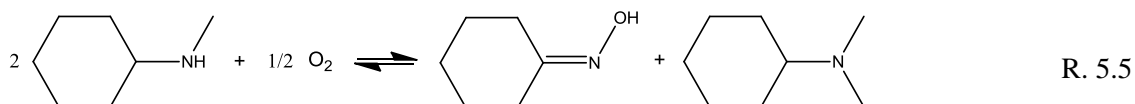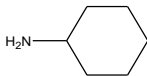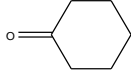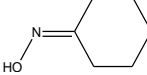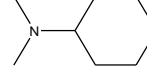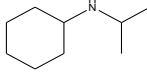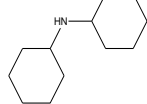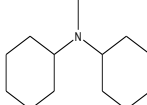
Figure 47. GC-MS chromatograms for degradation products of lipophilic amines

Compared to MCA, the oxidative degradation of DMCA is very low, which is a typical preponderance for tertiary amines. No oxidised product was observed in DMCA solutions. Dealkylation and alkylation are the major reactions and the main degradation products are the reformed alkylamines (see Table 20), which are still active for CO_2 absorption. DMCA is thus proved to be a chemically stable solvent for capturing CO_2 from flue gases. However, the less stable MCA can only be used as an activator with limited concentrations or low proportions in the blend solutions to reduce the degradation rate.
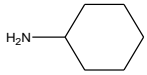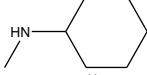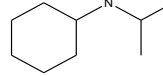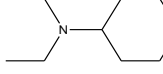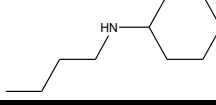
Table 19. Main oxidative degradation products of MCA

No.	Component	M_r (g/mol)	Structure	Abundance
1	CHA	99.17		minor
2	Cyclohexanone	98.14		minor
3	Cyclohexanone oxime	113.16		major
4	DMCA	127.23		minor
5	IPCA	141.25		minor
6	DCA	181.32		minor
7	N-Methyldicyclo hexylamine	195.34		moderate

Table 20. Main oxidative degradation products of DMCA

No.	Component	M_r (g/mol)	Structure	Abundance
1	CHA	99.17		minor
2	MCA	113.20		moderate
3	IPCA	141.25		minor
4	DECA	155.28		moderate
5	N-Butyl-cyclohexanamine	155.28		minor

5.4.5 Inhibition

To minimise the oxidation of amine solvents in CO_2 absorption, inhibition is considered for preventing amine degradation. Several inhibitors were proposed by Goff (2005), Sexton (2008), Sexton and Rochelle (2009) and Supap et al. (2011), but their effectiveness for lipophilic amines should be measured due to different oxidation mechanisms and some of the specified inhibitors are only valid for specific solvents. As an effective inhibitor, it must scavenge O_2 at ambient temperature with more favourable

kinetics than the partial oxidation reactions involved in the degradation (Veldman, 2000). Rochelle et al. (2011b) suggested the inhibitor selection should be followed by the criteria of thermal stability, water solubility, low volatility and non-corrosion.

In this study, inhibitors such as ascorbic acid (IHB-1, 0.01 M), sodium sulfite (IHB-2, Na_2SO_3, 0.05 M) and potassium sodium tartrate tetrahydrate (IHB-3, $KNaC_4H_4O_6 \cdot 4H_2O$, 0.01 M) were applied to prevent the oxidation of lipophilic amine, i.e. MCA, which exhibits a high degradability at 120 °C. Figure 49 demonstrates all the inhibitors can depress the degradation rate of MCA, and $KNaC_4H_4O_6 \cdot 4H_2O$ is the most effective.
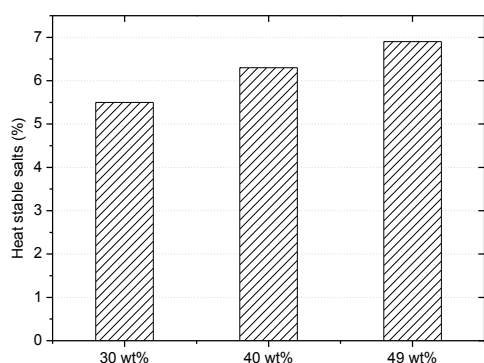
Figure 48. HHSs from oxidative degradation of MCA with varying concentrations
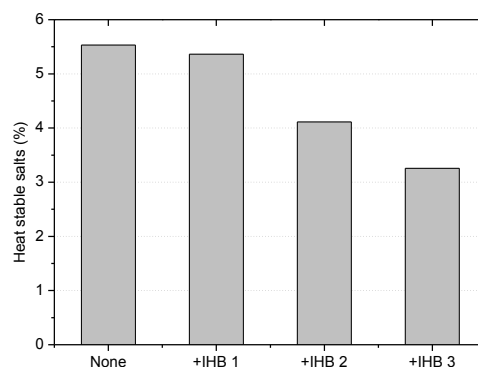
Figure 49. HHSs from oxidative degradation of 49 wt.% MCA with inhibitors

5.5 Summary

Due to lower operating temperature for lipophilic amines (≈90°C) compared to that for conventional alkanolamines (120-140 °C) in solvent regeneration, TBS system exhibits a lower thermal degradation. The less reactive regeneration promoters are quite stable in the presence of O_2 and the degradation components are still active amines reformed by alkylation and dealkylation; however, the oxidative degradation of absorption activators is significant, since oxime was found as one of the major oxidation products. The optimised ternary blended amine solvent (DMCA+MCA+AMP) presents a good chemical stability. However, vaporisation loss becomes the major weakness of the TBS system. It can be reduced by an additional inter-stage cooling system and recovered by a water wash or hydrophobic solvent scrubbing process, since it is much easier to eliminate such physical loss compared to those irreversible chemical losses via thermal and oxidative degradations.

6 Intensification of solvent regeneration

Lipophilic amine solvent regeneration with thermomorphic liquid-liquid phase separation (LLPS) has been proved to be an effective means for cutting the exergy demands and reducing the quality of heat source required for solvent regeneration. However, the slow desorption rate becomes a challenge if steam stripping is not used. To accelerate CO_2 release from loaded solutions, measures for intensifying solvent regeneration without gas stripping were hence studied.

6.1 Experimental methods

CO_2 loaded amine solutions for intensified regeneration methods such as extraction, agitation, nucleation, ultrasound, etc., were first prepared in a 500 mL glass bubble column at 30 °C. Regeneration was initially conducted by nitrogen gas stripping as benchmark and then using other intensive means in a 100 mL cylindrical glass reactor with 50 mL loaded solution at 70-85 °C. Agitation was carried out with a magnetic stirrer to agitate the rich solution for accelerating CO_2 desorption. Nucleation was performed with different materials and various porous sizes, for instance, silica beads, aluminium oxide spheres, active carbon spheres, zeolite chips, PTFE boiling stones, molecular sieves, cotton and wood fibres, etc., placed in the glass column.

Ultrasonic desorption was initially carried out in the test tube screening unit immerse into an Economic Ultrasonic Bath and the electronic energy consumption was measured by an ammeter. A bench-scale ultrasonic-assisted desorption rig with batch systems and continuous flow devices was also employed for further investigations in the Brandenburg Technical University of Cottbus. The detailed experimental setups are described in Appendix B.3.

6.2 Nucleation

Nucleation was studied as an intensification method for accelerating CO_2 regeneration in loaded solutions. It usually arises at nucleation sites on surfaces contacting liquids or gases. Nucleation sites in this study are generally provided by suspended particles or minute bubbles, so-called heterogeneous nucleation, which occurs much more common than homogeneous nucleation that takes place without preferential nucleation sites. Bubble formation at nucleation sites depends on the surface roughness, fluid properties and operating conditions (Maruyama et al., 2000; Thome, 2010).

6. Intensification of solvent regeneration

Various porous materials were used to enhance nucleate bubble formations in the desorption experiments. Since they provide extensive nucleation sites, CO_2 regeneration can hence be intensified. Significantly rapid CO_2 desorption was observed by using particles such as zeolite chips, Al_2O_3 spheres and PTFE boiling stones. Those porous materials with cavities on the surface, which are poorly wetted by the liquid, have the greatest tendency to entrap gases and show a positive influence on bubble nucleation according to classical nucleation theory (Cole, 1974). The effective surface energy is lowered at such preferential sites, thus diminishing the free energy barrier and facilitating bubble nucleation. However, acceleration of amine degradation was found with ceramic materials and Sylobeads, decolourisation was detected with active carbons and gel formation was observed with fibres and silica beads, those materials were hence not employed in further investigations.
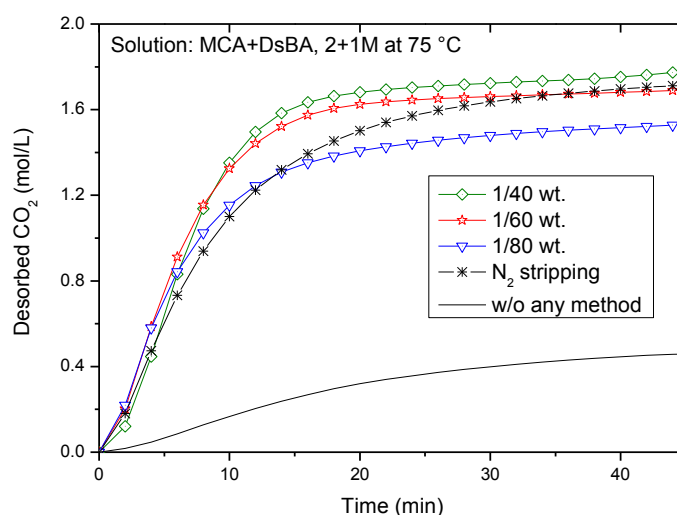
Figure 50. Solvent regeneration by nucleation with Al_2O_3 spheres

Before desorption, the CO_2 concentration of the loaded solution prepared from absorption is quite high. By raising the temperature, the equilibrium of dissolved CO_2 in the aqueous phase is displaced toward the dissociation of the carbamate and bicarbonate species, and the solution attains a supersaturated state. The additional porous particles thus provide active nucleation sites for reducing the free energy barrier of bubble nucleation and initiating the formation of "excess" CO_2 bubbles. Thus, nucleation promotes CO_2 releasing from loaded solutions. However, the particles only influence the desorption rate but not the reaction equilibrium, since they are inert in terms of the absorption. Figure 50 shows the good experimental results achieved by using porous

70

particles, Al_2O_3 spheres, at levels of only 1.25-2.5 wt.% in amine solvents, to accelerate CO_2 evolution from the loaded solution.

6.3 Agitation

Bubble formation was observed in stirred vessels and is typically influence by speed of agitation and surface tension of solvent. The low surface tension promotes the bubble breakage and reformation, leading to more bubbles regenerated with smaller sizes (Laakkonen et al, 2005). Agitation also breaks the surface tension of the solution to increase the cavitation level, bubbles are thus more likely to be formed.

Agitated regeneration was hence applied in a continuous stirred tank reactor (CSTR) as a substitute for steam stripping. Figure 51 illustrates that the desorption rate with agitation is comparable to that with gas stripping in blended MCA+DsBA solutions. Agitation speed also has a positive influence on CO_2 desorption, with more CO_2 being desorbed at higher agitation rates. Because cavitation is formed by agitation and it is enhanced by increase of agitation speed. By immediate implosion of cavities in the liquid solution, CO_2 is consequently liberated from liquid phase to gas phase, reaction is therefore driven towards CO_2 desorption. The higher speed of agitation creates more cavitation bubbles and thus intensifies CO_2 releasing. In addition, agitation also promotes the mass transfer in the reactor and accelerates the reaction towards CO_2 releasing.
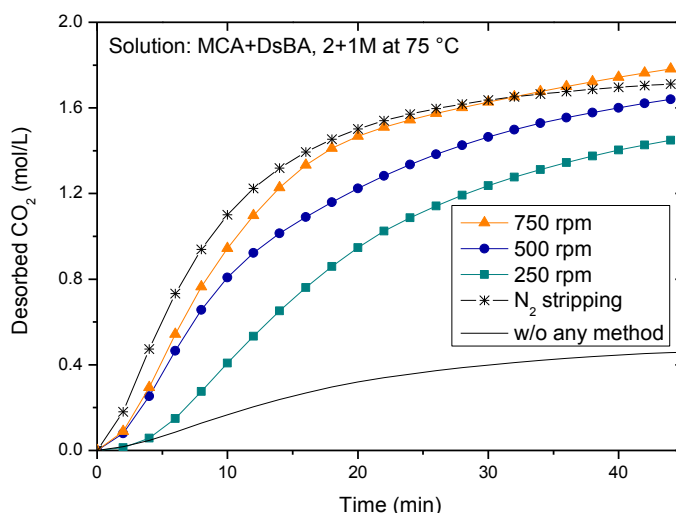
Figure 51. Influence of agitation speed on CO_2 evolution

Figure 52 illustrates that the regeneration rate of the loaded DMCA+MCA solution is very slow without any enhancement technique, releasing only 30 g/L/hr of CO_2 in the

initial 20 min, but that it becomes much faster upon 250 rpm agitation (180 g/L/hr) and even more rapid at 1000 rpm agitation (240 g/L/hr). The corresponding desorption rate with 200 mL/min N_2 stripping is 220 g/L/hr as reference. This indicates the tremendous potential of exploiting agitation to reduce solvent loss and operating costs in the regeneration step still further. Therefore, a CSTR was employed for desorption in the further experiment and this achieved very deep regeneration, for instance, 95% amine recovery from 3 M loaded DMCA+MCA solution at 75 °C.
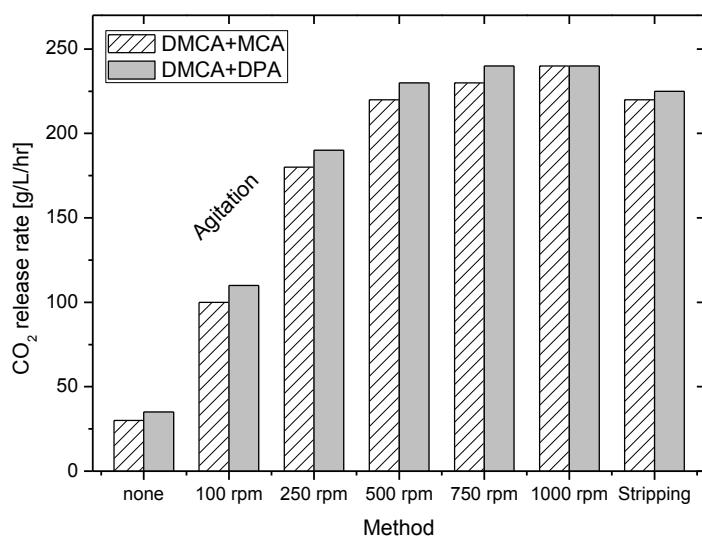
Figure 52. Enhancement of solvent regeneration by agitation

According to the calculation method described by Geuzebroek et al. (2009) and Oexmann et al. (2008 and 2010), the total energy consumption in agitated desorption for TBS system is estimated to be only less than 2.0 MJ/kg_{-CO_2}, which mainly includes 1.2 MJ/kg_{-CO_2} of reaction enthalpy, 0.14 MJ/kg_{-CO2} of agitation energy, 0.4 MJ/kg_{-CO_2} of sensible heat and 0.2 MJ/kg_{-CO_2} of heat loss. Compared to the MEA-based "state-of-the-art" technology with steam stripping (4.0 MJ/kg_{-CO_2}), it significantly limits the consumption of latent heat and saves half of the required desorption energy.

A comparison study between nucleation and agitation indicates that solvent regeneration has been intensified more deeply by agitation (see Figure 53), since a more effective mechanical force is involved for cavities formation. Nucleation is more suitable for solvents with more regeneration promoter, such as formulations DsBA+MCA+AMP (2+1+1 M) and DMCA+MCA+AMP (3+1+1 M), since they are more easily to be regenerated; while agitation is preferred for solvents with more

activators, due to their higher CO_2 loading capacity. Additionally, by combining agitation and nucleation, the regeneration rate were enhanced synergistically by 10-20%, compared to employing the measures individually.
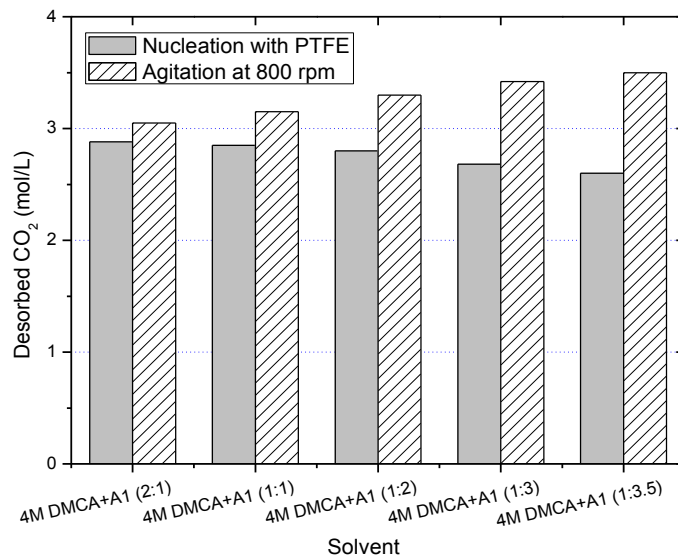
Figure 53. Comparison of nucleation and agitation for solvent regeneration at 80 °C

6.4 Ultrasonic desorption

Ultrasonic desorption has also been investigated for enhancing the solvent regeneration, using high frequency sound waves to agitate the aqueous solution and encourage bubble formation, since the compression waves in the liquid tears the liquid apart, leaving behind many millions of microscopic "*voids*" or "*partial vacuum bubbles*" – cavitations (Reidenbach, 1994). The ultrasonic cavitations create a population of seed bubbles above a critical radius and the bubbles expand and shrink in the ultrasonic field, which enables a biased transfer of dissolved gas (i.e., CO_2) into the bubble from solution by rectified diffusion and the grown bubbles are removed from the solution before dissolving back into the liquid (Salmon et al., 2012). The ultrasonic wave initiates microscopic cavities, which facilitates bubble formation and thus enhances CO_2 desorption only at moderate temperatures without steam stripping.

A positive influence of ultrasound on the CO_2 desorption rate is illustrated in Figure 54, where an economic Ultrasonic Bath was employed to degas the CO_2 from 40 mL loaded solvent. Although the rich solvent, for example MCA+DMCA, cannot be regenerated by nucleation or ultrasound as deeply as with gas stripping - typically 5-20% less - the regeneration rate is comparable or even faster than for N_2 stripping. Since

the frequency of ultrasonic wave was found to have minor influence on desorption (Gantert and Möller, 2011), a constant frequency was adopted in this study. The total energy consumption in ultrasonic desorption for TBS system is also around 2.0 MJ/kg-$_{CO2}$, where only 0.15 MJ/kg-$_{CO2}$ of ultrasonic energy is consumed.
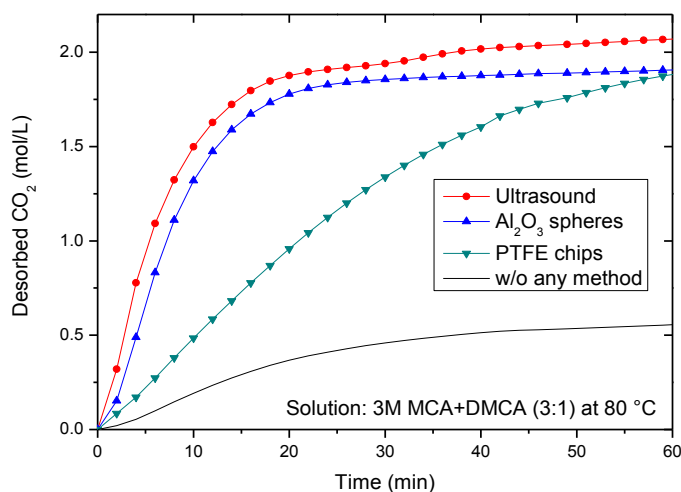
Figure 54. Intensification of CO_2 release with various methods

The bench-scale test was carried out in a bath unit equipped with an ultrasonic bath. The experimental measurements and detailed calculations were described in the paper from Gantert and Möller (2011). Figure 55 demonstrates the advantage of using biphasic solvent (5M DMCA+DPA+AMP, 3:1:1) in ultrasonic desorption, which exhibits a much faster CO_2 release rate and deeper regeneration compared to conventional alkanolamine solution (30 wt.% MEA+MDEA, 1:1).
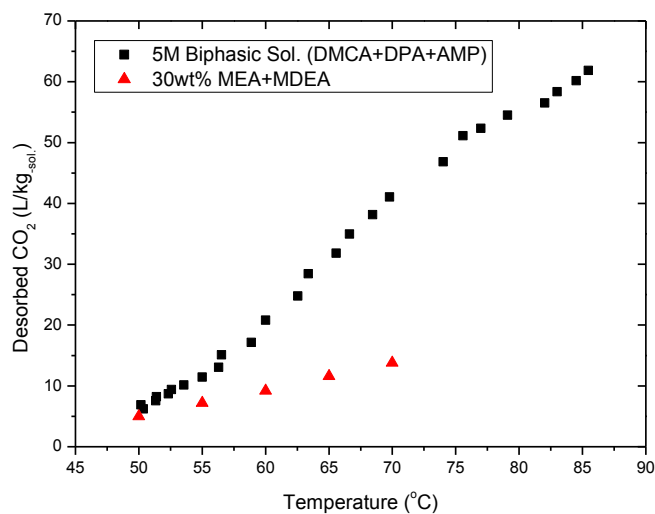
Figure 55. Ultrasonic desorption in bench-scale test

6.5 Hybrid technology

To further enhance the solvent regeneration, hybrid technologies with combination of two or more intensification methods has also been investigated in this paper. A glass cylinder desorber combining the nucleation and agitation has been designed and used in experimental study (see Figure 91C in Appendix). The initial CO_2 desorption rate in the combined method is faster that either, however the depth of regeneration is the same as that with the agitation technique, while nucleation only has limited contribution to the overall CO_2 desorption. Table 21 summarises the principle and features of those techniques; enhanced bubble formation and accelerated CO_2 desorption are their common characteristics.

The design of hybrid technologies in solvent regeneration is dependent on the application of CO_2 capture for the particular industrial process; for example, the combination of nucleation and agitation methods is suitable for a refinery and that of nucleation and stripping can be employed for a power plant due to the availability of proper energy sources for thermal regeneration. The detailed processes are discussed in section 9.1 presenting various flowsheets.

Table 21. Comparison of intensified regeneration techniques

Method	Equipment	Principle	Features
Nucleation	Fixed bed reactor	Add porous particles with active nucleation sites to lower surface energy and facilitate bubble formation	Accelerate CO_2 desorption No power consumption
Agitation	Stirred tank	Break the surface tension and increase the cavitation level to enhance bubble formation	Accelerate CO_2 desorption Deep regeneration
Ultrasound	Ultrasonic bath	Create voids for cavitation to encourage bubble formation	Accelerate CO_2 desorption regeneration
Nucleation + Agitation			Further enhance desorption rate with deep regeneration
Nucleation + Ultrasound			Same as above

6.6 Summary

The objective of regeneration intensification was to accelerate desorption by physical means, e.g. nucleation, agitation and ultrasonic desorption instead of gas stripping, which involves an additional downstream separation. The regeneration temperature required for TBS system is much lower than for conventional solvents, only at 80-90 °C, which enables the implementation of such techniques and the use of low-value heat from other industrial processes to reduce operational costs. Laboratory tests of those methods have all achieved comparable solvent regenerability and significant energy savings compared to the stripping process. These measures provide a great potential to intensify the CO_2 desorption process and to integrate heat recovery networks for developing a low-cost CO_2 capture technology.

7 Extractive solvent regeneration

7.1 Concept of extractive regeneration

Since gas stripping by N_2 is not feasible in industrial applications, a novel technology using additional hydrophobic solvents to extract loaded amines from the aqueous phase into the organic phase was investigated for enhancing the CO_2 release and further reducing the regeneration temperature for desorption (Agar et al., 2008b; Misch, 2008). Figure 56 illustrates the solvent regeneration process with inert solvent addition. It commences with CO_2 absorption into the biphasic lipophilic amine solution forming a homogeneous loaded amine solution. The extractive regeneration of the loaded solution is carried out by addition of an inert solvent, which is insoluble in water, with simultaneous CO_2 release. Due to the similar hydrophobic properties, the inert solvent acts as an extracting agent removing the lipophilic organic from the loaded solution and thus displacing the prevailing chemical equilibrium within it. CO_2 desorption from the loaded solution will consequently be enhanced. Moreover, the mixture of the extracted lipophilic amine and inert solvent can be separated by a variety of fluid separation techniques, with distillation being the preferred option (Tan, 2010).
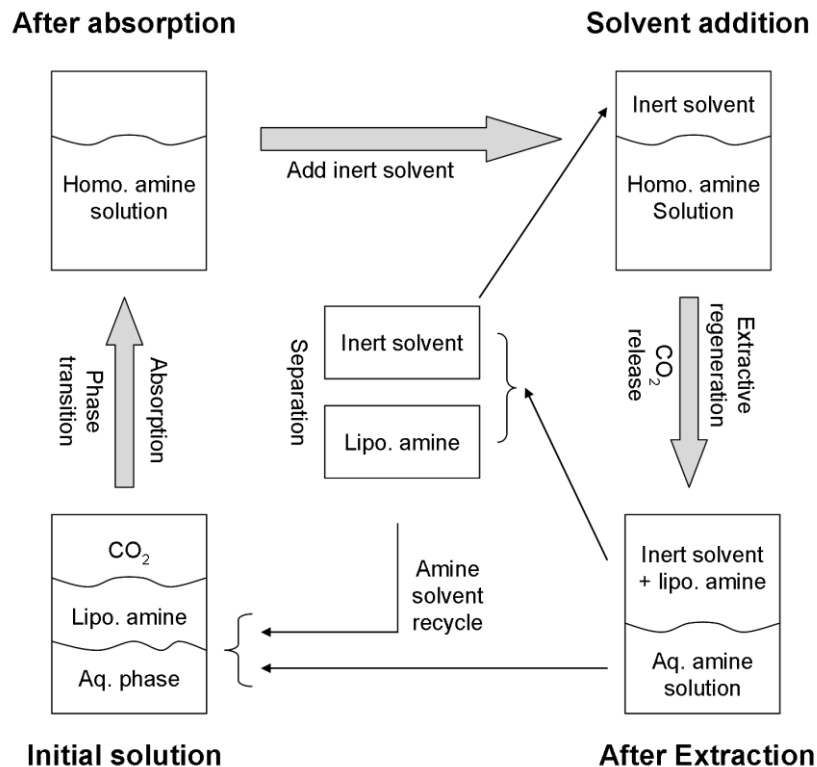
Figure 56. Concept of CO_2 absorption with extractive regeneration

The criteria for inert solvent selection are (1) *molecular polarity* - similar to the lipophilic amine, leading to highly selective extraction; (2) *thermal separability* - the inert solvent should have a boiling point at least 50 °C lower than the lipophilic amine; (3) *chemical inertness* - minimal influence on the overall absorption process if residual trace amounts are present in amine solution; (4) *chemical stability* - no side reactions and minimal solvent degradation.

Table 22. Solubility parameters of various inert solvents

Compounds	δ_D MPa$^{0.5}$	δ_P MPa$^{0.5}$	δ_H MPa$^{0.5}$	V_m [b] cm^3/mol	δ_T [c] MPa$^{0.5}$
n-Butane	14.1	0	0	101.4	14.1
n-Pentane	14.5	0	0	116.2	14.5
Cyclopentane	16.4	0	1.8	94.9	16.5
Cyclopentene	16.7	3.8	1.7	89.0	17.2
2-Methyl butane	13.7	0	0	117.4	13.7
2-Methyl-2-butene	14.3	2.0	3.9	106.7	15.0
n-Hexane	14.9	0	0	131.6	14.9
Cyclohexane	16.8	0	0.2	108.7	16.8
3-methyl pentane	14.7	0	0	130.0	14.7
n-Heptane	15.3	0	0	147.4	15.3
Methyl-tert-butylether	14.8	4.3	5.0	119.8	16.2
Dichloromethane	18.2	6.3	6.1	63.9	20.2
n-Decane	15.7	0	0	195.9	15.7
n-Dodecane	16.0	0	0	228.6	16.0
DPA	15.3	1.4	4.1	136.9	15.9
MCA [a]	17-18	2-3	5-6	-	18.3
DMCA [a]	16-17	1-2	3-4	151.5	17.8
MEA	17.0	15.5	21.2	59.8	31.3
CO_2	15.7	6.3	5.7	38.0	17.9
Water	15.5	16.0	42.3	18.0	47.8

[a] Estimated according to influence of function group on solubility parameters
[b] Molar volume of the pure solvent
[c] Total solubility parameter $\delta_T = (E_{vap}/V_m)^{0.5} = (\delta_D^2 + \delta_P^2 + \delta_H^2)^{0.5}$

The crucial issue in the extractive regeneration is to select solvents with polarities similar to those of the lipophilic amines, since this promotes amine solubility in the inert solvent and increases both the selectivity and capacity of the process (Bart, 2001). The solubility parameter (δ), reflecting the energy needed to separate molecules in a fluid and create 'cavities' to accommodate solute molecules (Reichardt, 2003), is used for solvent characterisation purposes. It considers cohesive, adhesive and hydrogen bonding interaction contributions (Barton, 1991). The cohesion is the dominant effect in determining the solubility, since it is derived from the energy needed to convert a liquid

to a gas, i.e. the latent heat of evaporation (E_{vap}), viz. that holding the liquid molecules together (Hildebrand and Scott, 1962). There are three major types of interaction parameters in common organic solvents: dispersion solubility parameter - δ_D, polar solubility parameter - δ_P and hydrogen bonding solubility parameter - δ_H (Hansen, 2000). According to the basic principle for predicting the solvent solubility "like dissolves like", the miscible solvents should have similar solubility parameters. Based on this criterion and a detailed literature survey, more than ten inert solvents were selected for further experimental investigation. Their solubility parameters, as well as those of the lipophilic amines, are given in Table 22. Since most selected solvents have similar dispersion solubility parameters, the polar and hydrogen bonding solubility parameters become the decisive factors.

7.2   Experiment: Extraction

CO_2 loaded amine standard solutions for extractive regeneration tests were initially prepared in a 500 mL glass bubble column at 30 °C. The screening tests on inert solvents for extractive regeneration were carried out in a 150 mL double-wall glass reactor from 25 to 70 °C. The experimental setup of the inert solvent screening unit is shown in Appendix B.4. To improve the capture efficiency, three- and four-stage extractions were used for lipophilic amine regeneration. To minimise inert solvent vaporisation, pressurised extraction was applied in further studies.

7.3   Inert solvent selection

Based on the prerequisites given above, the inert solvent selection was first conducted by theoretical study. Butane and Heptane, as well as their isomers, were eliminated in a preliminary screening due to their boiling points, which were either too low or too high. The screening tests for the potential inert solvents were carried out with saturated and unsaturated hydrocarbons having a carbon number of 5 or 6, for a variety of structures and functional groups. Preloaded 3M lipophilic amine solutions a-DMCA (DMCA+MCA at 3:1) were used as a standard for purposes of comparison. Figure 57 illustrates the performance of the inert solvents determined in a single-stage-equilibrium extractive regeneration at 40 °C. The solubility interaction alone could be used to regenerate the loaded amine solution with the release of more than 35% of the CO_2 at only 40 °C.
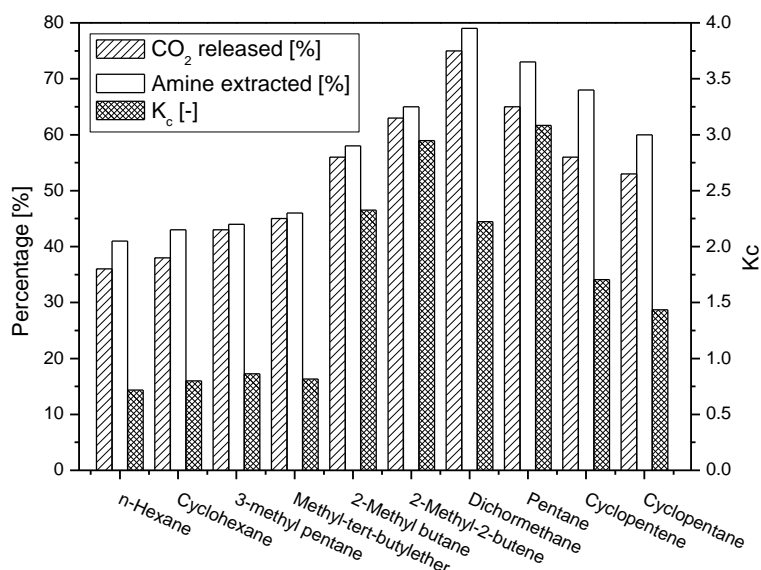
Figure 57. Single-stage extractive regeneration by various inert solvents

Dichloromethane is very reactive under basic conditions and is not inert toward amine solutions, because it can react with the lipophilic amines through a nucleophilic substitution mechanism to form mixtures of amines with various states of alkylation (Clayden et al., 2005); although its extractive behaviour is much better than for the other inert solvents, recovering 80% amine from aqueous phase in a single equilibrium, by virtue of its small molar volume and similar hydrogen bonding solubility parameter to lipophilic amines. Ethers with comparable polar and hydrogen bonding solubility parameters to lipophilic amines have outstanding extraction efficiency, but also proved somewhat unsuitable, since the ether group is chemically unstable during the subsequent thermal separation, resulting in solvent oxidation and formation of explosive vapour mixtures. A single alkenyl function group has positive influence on the extraction effect, but the unsaturated carbon-carbon bond might cause unexpected reactions such as oligomerisation and electrophilic addition (McMurry, 1999). Consequently, alkanes with their high chemical stability were selected for extraction. In particular, pentane, which performed best in the screening tests based upon its extraction properties and chemical stability, was chosen for further study. Hexane exhibits almost equivalent solubility parameters to those of pentane, but its performance in the extractive regeneration is much inferior to that of pentane. This is probably primarily a consequence of the critical condition of pentane at the experimental temperatures around its boiling point, which creates larger free volume in the inert solvent and enhances its solubilisation properties.

80

The extractive regeneration of 3M loaded aqueous DMCA solution was also carried out at 40-50°C, with the results acquired showing a 5% difference from the comparable values for the solution a-DMCA. Due to the weak polarity of the DMCA molecule, it preferentially dissolves in pentane and performs a little better than DPA and MCA in extraction. Moreover, an increase in temperature at first improved the extraction of lipophilic amines resulting in greater CO_2 liberation (see Figure 58). However, a further increase of the temperature above 60°C is not advisable, due to the high volatility of the inert solvent while reducing temperatures to 30 °C also has a negative impact on the extraction efficiency and regeneration rate. A reasonable operating temperature for the extractive regeneration process was thus stipulated to be 40-50°C, which is also a typical operating temperature for conventional CO_2-absorbers (Kohl and Nielsen, 1997) and the optimal temperature in lipophilic amine absorption systems.
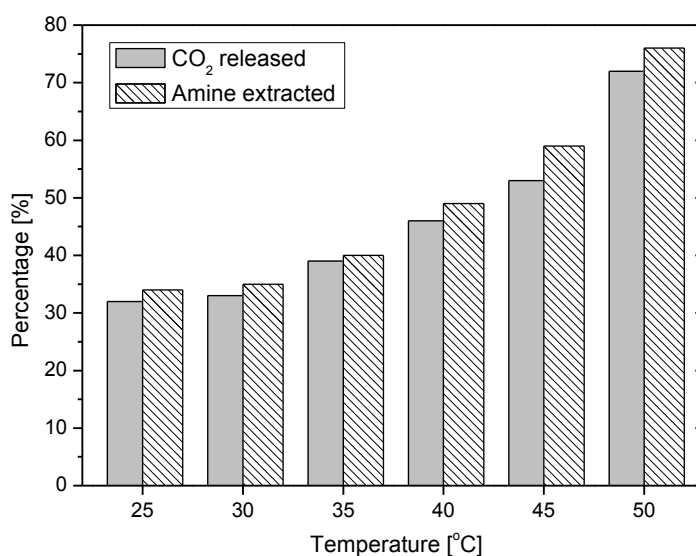
Figure 58. Single-stage extractive regeneration by pentane at various temperatures
($V_{pentane}$:V_{amine}=1:2)

7.4 Multi-stage test

In order to improve the depth of solvent regeneration, multiple-stage extraction systems were assessed in the experimental work. Figure 59 and Figure 60 illustrate the performance parameters of cross-current extractions using pentane for the blended lipophilic amine solutions DMCA+MCA (3M, 3:1) and DsBA+MCA (3M, 3:1). Due to the volatile loss of inert solvents i.e. pentane, the volume ratios of the extract and the initial amine raffinate solution (V_{inert}/V_{aq}) used for calculation were 4:5 (initial value 1:1) in the three-stage extraction and only 1:5 (initial value 1:3) in the four-stage

81

extraction. Following extraction, the inert solvent and amines without CO_2 were found in the extract while the raffinate was comprised of fully loaded amines, water and physically absorbed CO_2. Since the physical absorption is so weak at atmospheric pressure and only contributes to less than 5% of the total CO_2 capture, more than 90% of CO_2 can be released, while more than 95% of the lipophilic amines are regenerated by extraction into the inert solvent. Together with optimisation of the operating temperature (ca. 40-50 °C), these results underpin the economic and technical viability of scaling-up an extractive regeneration to reduce the exergy requirement.
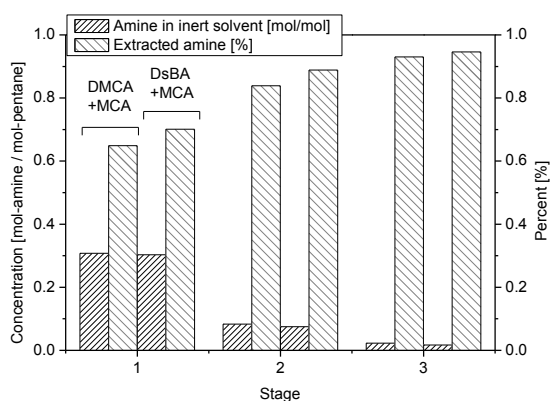
Figure 59. Three-stage cross-flow extractive regeneration
(volume ratio $V_{pentane}$:V_{amine}=4:5 in each stage)
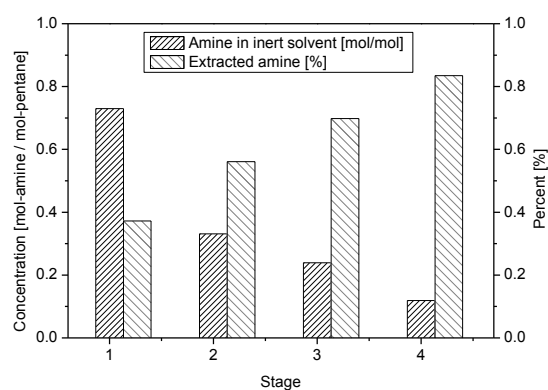
Figure 60. Four-stage cross-flow extractive regeneration
(volume ratio $V_{pentane}$:V_{amine}=1:5 in each stage)

For large-scale operation and more efficient use of the solvent, counter-current mixer-settlers or columns would usually be employed for such an industrial liquid-liquid extraction. According to the experiment results, the partition coefficient (K_c) of lipophilic amines measured lies around 3.0 at 40 °C (see Eq. 7.1). The extraction coefficient (E) is proportional to volume ratio of extract and raffinate in a given system (see Eq. 7.2). On this basis, the process was predicted to achieve an extraction of 95% of the lipophilic amine and release 90% of the CO_2. An analytical calculation was used to estimate the performance of the counter-current extraction and the number of stages (n) was calculated by the Kremser formula in Eq. 7.3 (Müller et al., 2005). Table 23 indicates that only 4 stages would be required to extract a-DMCA from the loaded aqueous amine solutions using pentane.

$$K_c = \frac{c_{a\,min\,e,inert}}{c_{a\,min\,e,aq}} \qquad\qquad \text{Eq. 7.1}$$

$$E = \eta \cdot K_c \cdot \frac{V_{inert}}{V_{aq}} \qquad\qquad \text{Eq. 7.2}$$

$$\frac{c_{a\,min\,e,feed}}{c_{a\,min\,e,exhaust}} = \frac{E^{n+1} - 1}{E - 1}$$

Eq. 7.3

Table 23. Performance of inert solvents for extractive regeneration

Inert solvent	Atmospheric pressure				Elevated pressure (≈3 bar)			
	Partition coefficient	Volatile loss	Required stages*	T	Partition coefficient	Volatile loss	Required stages*	T
	mol/mol	%		°C	mol/mol	%		°C
Pentane	3.2	45	4.5	40	2.1	20	6.0	60
Hexane	3.5	4	4.3	60	1.8	<1	7.0	70
Cyclohexane	3.6	2	4.2	60	1.9	<1	6.6	70
Iso-hexane	3.0	10	4.6	60	-	-	-	-

* calculated by Eq. 7.3 for counter-current extraction with 96% amine recovery and $V_{inert}=V_{amine}$.

7.5 Inert solvent loss and its reduction

Inert solvent loss via vaporisation was found to be significant during extractive regeneration, due to the low boiling point of the inert solvents employed. A cooling water condenser (15°C) was hence used to reduce the volatility losses, recovering over 50% of the vaporised solvent. The residual vapour can subsequently be scrubbed out with high boiling point hydrophobic solvents, e.g. n-decane, n-dodecane, or even higher alkanes. In experiments, it has proven possible to recover more than 90% pentane by a scrubber with Diphyl (from Lanxess) in three equilibrium stages. Since the boiling point of Diphyl is very high ≈257 °C, the separation of inert solvent from Diphyl is very easy. Another alternative would be to use other inert solvents with a slightly higher boiling point, such as cyclopentane and hexane. The volatility losses could thus be significantly reduced by more than 80%, but the extraction efficiency would decrease by 20-55%, which would have to be compensated for by additional extraction stages.
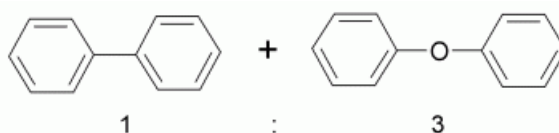
Figure 61. Composition of Diphyl

7.6 Pressurised extraction test

To achieve fast absorption kinetics, lipophilic activator is includes in most of the TBS solutions, but they are only partially regenerated without steam stripping at 80 °C.

Therefore, extractive regeneration with inert solvent was developed to improve performance. Inert solvents, such as pentane, hexane and cyclohexane, were selected for achieving an extensive regeneration at temperatures well below 70 °C, giving more degrees of freedom for integrating waste heat sources from industrial energy recovery networks in the solvent regeneration process. However, the large amount of inert solvent involved in the regeneration process may cause problems such as negative environmental impact and additional heat demand. The extraction process and operating parameters must be optimised.

In the system examined, an aqueous MCA+DMCA solution (4M, 3:1) was used as the activated solvent. A high proportion of MCA was present in order to increase the absorption rate and capacity; a small amount of DMCA ass incorporated to decrease the LLPS temperature to 80 °C. The loaded solution was separated into two phases in the pre-regeneration stage. More than 50% of the amines were recovered and an organic lean phase was formed. The organic phase was recycled to the absorber. The CO_2 is highly concentrated in the aqueous rich phase. As shown in Figure 62, this was passed to the extraction unit with an inert solvent. Compared to the previous extraction method (cf. Figure 56), the developed process reduced both inert solvent requirement and energy consumption in desorption. But vaporisation loss of inert solvent was found to be a significant drawback.
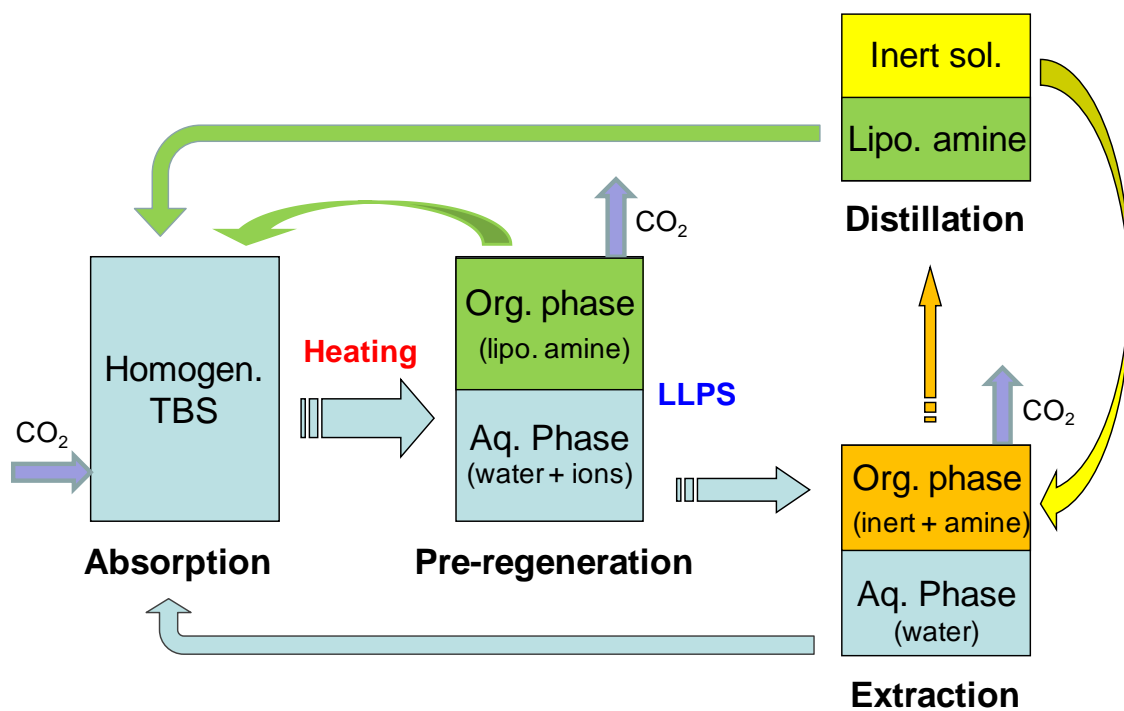
Figure 62. Concept of LLSP with inert solvent extractive regeneration

In order to reduce the volatile losses of the inert solvent, the system pressure at regeneration was increased to up to 3 bar at 50-70 °C. Due to the different miscibility properties of the solvent system, lipophilic amines were preferably dissolved in the organic phase, the residual amine was thus extracted by the inert solvent with simultaneous CO_2 release. The desorbed CO_2 from the pre-regenerator and extractor can be compressed for storage; the lean aqueous phase from the extractor was recycled to the absorber and the organic phase containing inert solvent and lipophilic amines was sent to a low temperature distillation unit. Since the boiling point of the inert solvent is lower than 70 °C and for lipophilic amine is higher than 130 °C, the thermal separation is very easy. Following separation, the recovered lipophilic amines can be recycled to the absorber and the inert solvent can be recycled to the extraction unit.

One of the key tasks in this extractive regeneration is the selection of appropriate inert solvent. Pentane with an excellent partition coefficient was initially employed, but the significant volatile losses represent a major weakness. Other organic solvents such as hexane, cyclohexane and isohexane were further evaluated. Using less volatile hexane can effectively reduce the vaporisation loss, but the partition coefficient is inferior. This shortcoming can be overcome by increasing the extraction temperature and the number of stages. Since the carbon capture technology is being developed to mitigate global climate change, a negative environmental impact of the CO_2 capture process should be avoided. Therefore, a high boiling point hydrophobic solvent scrubbing unit is employed to remove the low boiling point inert extracting agent vapour. Table 23 demonstrates the practicability of using inert solvent extraction at an elevated pressure for CO_2 regeneration in 4M loaded DMCA+A1 (3:1) solution.

7.7   Summary

Extractive regeneration using foreign hydrophobic inert solvents has been proposed to reduce the regeneration temperature for CO_2 desorption still further for facilitating the use of waste heat. More than 95% of lipophilic amine recovery can be achieved by a multi-stage extraction process and the extracted amine can subsequently be recovered from the inert solvent by low temperature (<80 °C) distillation. This measure offers a more flexible and expedient thermal integration of CO_2 desorption system into the low-value heat recovery network to regenerate CO_2 from loaded solutions at only 50-70 °C. However, volatile loss of low boiling point extractants becomes the major weakness.

Elevation of extraction pressure and use of less volatile inert solvent reduce vaporisation loss but depress the partition coefficient, however, this drawback can be overcome by increasing the extraction temperature and the number of stages. Additional distillation processes required for separation of amine and extractant together with a solvent scrubbing process to recover the significant foreign solvent loss via vaporisation lead to some extra costs; however, they are minor compared to steam stripping. To adapt such technology for CO_2 capture, inert solvent loss must be well controlled, and it still has potential to achieve a better saving than a conventional stripping process, since waste heat at temperatures of 80 °C is available in most process heat network systems.

8 Packing wettability test

To observe the characteristics of the fluid dynamics of the packed column in the absorption process, basic parameters, such as pressure drop, liquid hold-up and flooding point, were measured in the bench-scale experiment and some physical properties, e.g. density, viscosity, surface tension and contact angle of lean and rich solvent, were also determined for a better understanding of the fluid dynamics in CO_2 absorption.

8.1 Experiment: Bench-scale test

The experiments were performed in a glass column with 0.04 m inner diameter and a packed height of 1 m at 30 °C and atmospheric pressure. As shown in Table 24, Raschig rings with different materials, e.g. ceramic (C), plastic (P) and stainless steel (M), were investigated in this work. Water and amine solutions were used as the liquid phase. 10-75 L/min (containing 15 mol% CO_2) of gas and 60-200 mL/min of liquid flow were applied. Liquid leaving the column outlet at the phase separator was collected and weighed on a balance to determine the dynamic liquid hold-up. The pressure drop across the packed bed was detected with differential pressure transducers connected at different positions between the top and the bottom of the column. The experimental data were collected by a system-design platform National Instruments LabVIEW 8.5 installed on a PC. The detailed setup is demonstrated in Appendix B.5.

Table 24. Specification of random packings

Type	Code	Material	Diameter	Specific surface area	Porosity
			mm	m^2/m^3	m^3/m^3
Raschig Ring	RR-3-G	Glass	3	1571	0.411
	RR-5-M	Metal	5	1012	0.857
	RR-6-M	Metal	6	859	0.877
	RR-6-P	Plastic	6	779	0.666
	RR-6-C	Ceramic	6	850	0.362
	RR-8-C	Ceramic	8	514	0.589
Wilson Ring	WS-3-M	Metal	3	1918	0.662
Berl-Saddle	BS-5-C	Ceramic	5	572	0.593
Raschig Super Ring	RS-10-M	Metal	10	451	0.956

8.2 Pressure drop

As a major criterion to evaluate the packing performance in an absorption column, the pressure drop through various random packings was experimentally measured in the glass column (Misch, 2010; Hussain, 2012). The calculations followed the instructions from the textbooks (Behr et al., 2010; Billet, 1995; Hölemann and Górak, 2006; Górak, 2006; Maćkowiak, 2003; Walzel, 2006).

To control the experiment conditions, a blank test using N_2 with various gas load factors (F_G) against dry packings was initially conducted. As seen from Figure 63, the influence factor of those packings on pressure drop is in the order of RR-6-C > RR-6-P > RR-6-M, primarily due to their different porosities. To validate the measurement of the gas-liquid system, a benchmark test using N_2 and water with various packings was also carried out. Figure 64 shows the specific pressure drop ($\Delta p/H$) with varying gas load factors and the pressure drops are in the same order as the previous results in the dry packing test. The flooding points were observed at $F_G = 0.35$ for RR-6-C (low porosity) with 200 mL/min of liquid flow and at $F_G = 0.8$ for RR-6-M (high porosity) with 100 mL/min of liquid flow.
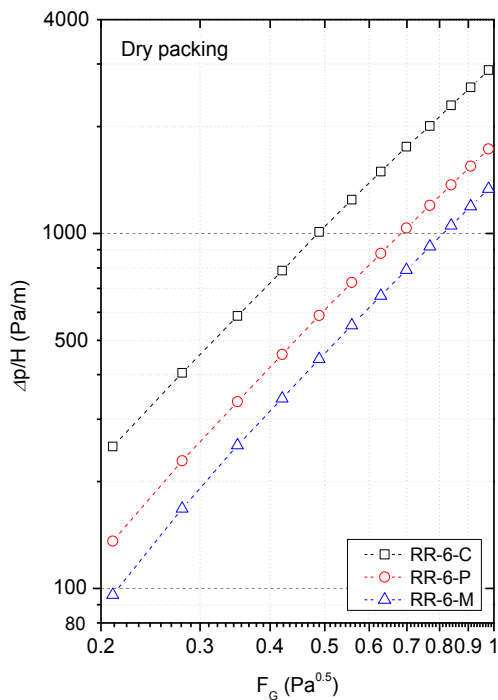
Figure 63. Pressure drop with dry packing
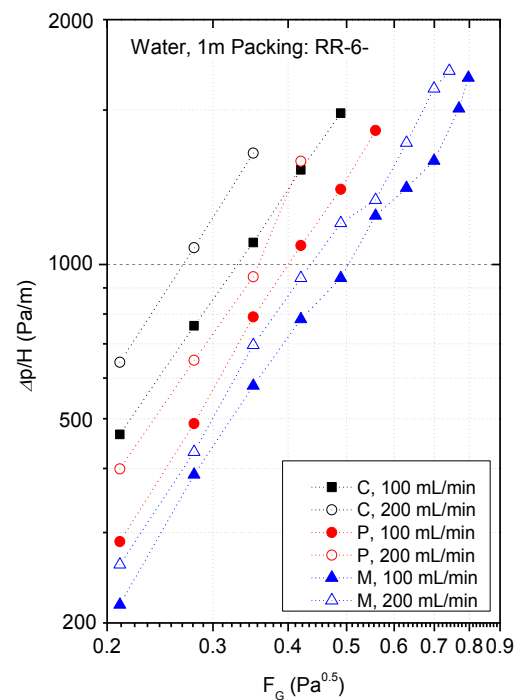
Figure 64. Pressure drop with water

88

8. Packing wettability test

Further tests were performed with the CO_2-N_2-Amine-Water system, compared to MEA solution, MCA has created higher pressure drop at the same experimental conditions and its flooding point also appears at a lower gas load factor (see Figure 65 and Figure 66). It is primarily due to the higher viscosity of the MCA solution.
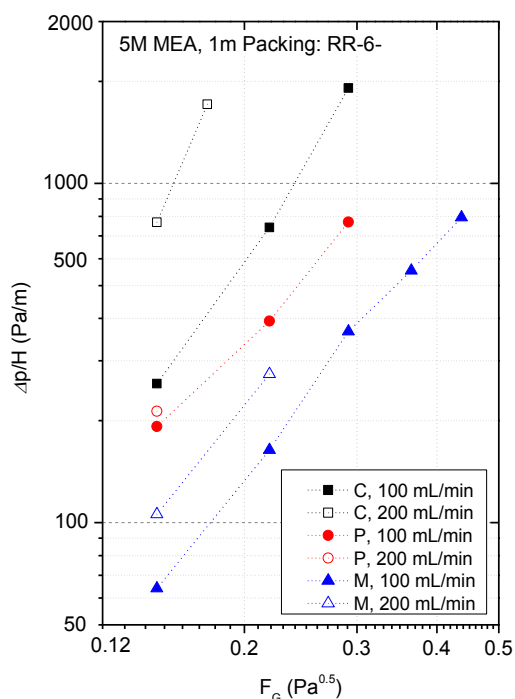
Figure 65. Pressure drop with 5M MEA
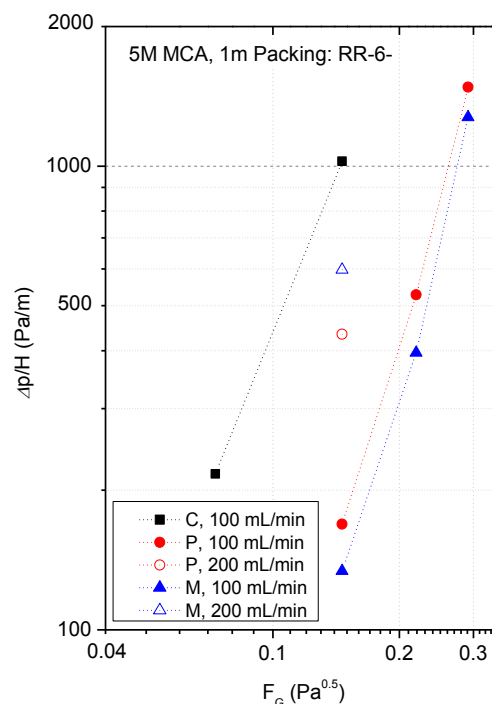
Figure 66. Pressure drop with 5M MCA

The advanced test was carried out with the blended solvent DMCA+MCA+AMP (3+1+1.5M). The pressure drop in such blend amine solution is even higher than that in the MCA solution. As shown in Figure 67, unloaded solvent ($\alpha_{-CO_2} = 0$) was used at the 1st run, the pressure drops were relative low; at the 2nd run, lean solvent ($\alpha_{-CO_2} = 0.12$) was applied, the pressure drops were significantly increased; at the 3rd run, the pressure drops were even higher, when the rich solvent ($\alpha_{-CO_2} = 0.20$) was employed. This is mainly due to the viscosity enhancement by CO_2 loading in solvent.

The viscosity of lipophilic amine solution is considerable higher than that of alkanolamine solution and the values of pressure drops for lipophilic amine solution are higher, higher porosity packings are suggested to be applied to reduce the pressure drop and eliminate the negative effect. As illustrated in Figure 67, by increasing the diameter of the metal Raschig ring, the pressure drop was prominently decreased. Increase of

packing porosity can also obtain large operation range, because the flooding point was found at $F_G = 0.3$ for 6mm metal Raschig ring, while it was observed at $F_G = 0.35$ for 8mm metal Raschig ring.
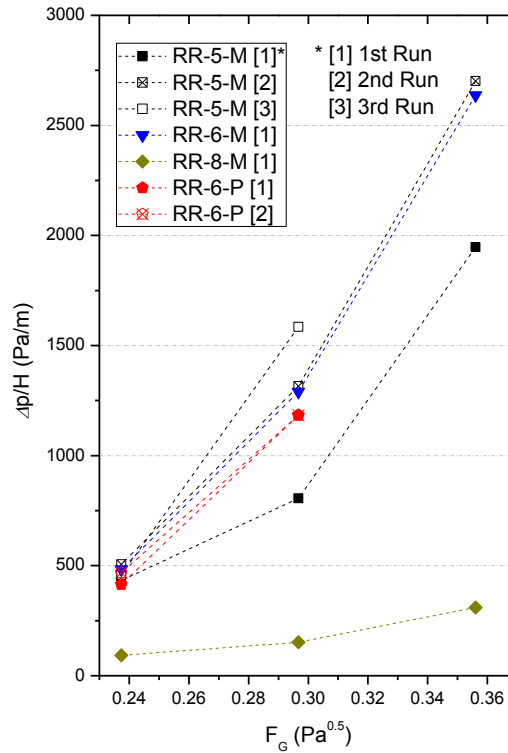
Figure 67. Pressure drop with blended solvent

8.3 Liquid hold-up

To study another important parameter for the fluid dynamics in the absorption column, the dynamic liquid hold-up (h_{dyn}) was measured in bench-scale experiment with varying random packings. Metal Raschig rings with different diameters of 5 mm, 6 mm and 8 mm, respectively, as well as 6 mm plastic and ceramic Raschig rings in the packing height of 1 m were employed.

In the control test, water was initially employed to validate the measurement method and apparatus. Figure 68 shows the results with various materials of 6 mm Raschig rings below the flooding point. Both the liquid velocity and gas velocity have influence on the dynamic liquid hold-up: the h_{dyn} increases by increase of the gas velocity or by decrease of the liquid velocity.
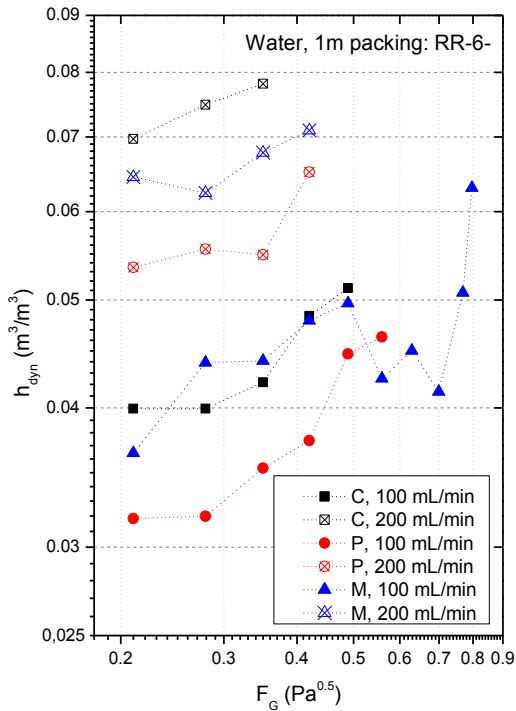
Figure 68. Liquid hold-up with water
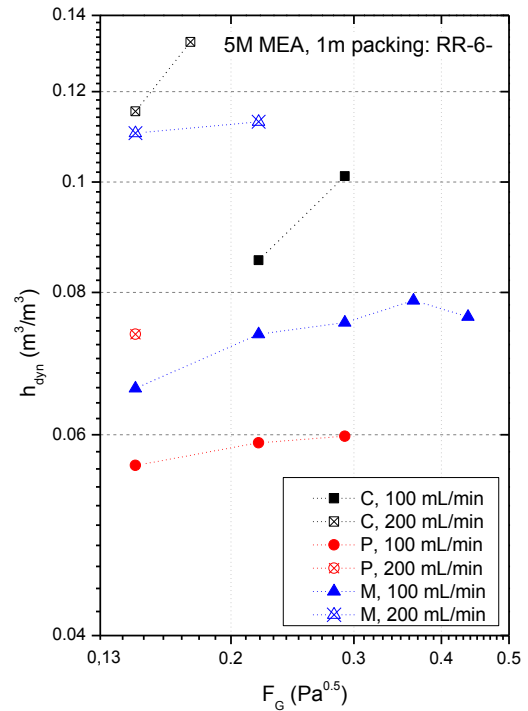
Figure 69. Liquid hold-up with 5M MEA

Further investigation with MEA solution exhibited a higher dynamic liquid hold-up compared to water (see Figure 69). The dynamic holdup is primarily a function of the liquid flow rate and the gas/liquid system properties, while the static hold up is dependent upon the packing surface area, the roughness of the packing surface and the contact angle between the packing surface and the liquid. However, in the experimental results, the packing material also showed a minor influence on the dynamic hold-up, which is in the order of: Ceramic > Metal > Plastic.

The advanced tests were conducted with the biphasic solutions. Figure 70 and Figure 71 presents the even higher dynamic liquid hold-ups of the MCA and DMCA+MCA+AMP solutions compared to MEA. It is mainly due to the higher viscosity and lower contact angle of the biphasic solutions. These indicate a better wettability of biphasic solvent on packing surface in the CO_2 absorption. However, the flooding point of the biphasic solvent system was observed at lower gas and liquid velocities, which limits the operation range of the absorption process. Therefore, high efficient packings should be studied in future tests.
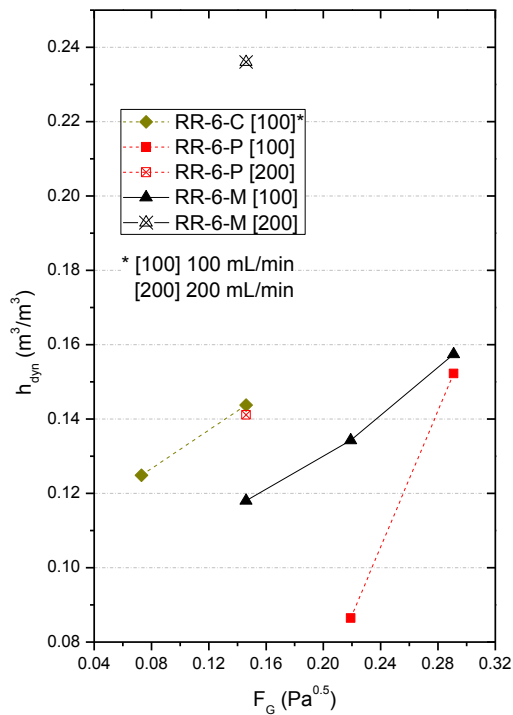
Figure 70. Liquid hold-up with 5M MCA
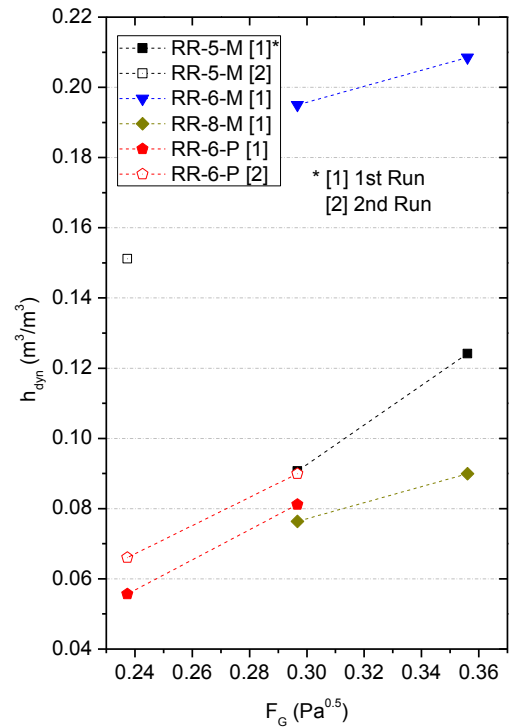
Figure 71. Liquid hold-up with blended solvent

8.4 Physical properties

Physical properties were found to be important for amine scrubbing, for example, density, viscosity and surface tension are essential parameters for the calculation of fluid dynamics as well as the selection of absorber packings, and contact angle advises the use of packing materials. Such fundamental parameters are hence studied in experiments with various apparatus.

8.4.1 Density

The density was measured in a DIN standard pycnometer (DURAN) with a determined volume at room temperature. It was initially verified by determining the densities of deionised water with varying temperatures at atmospheric pressure. Then, the densities of pure amines and their lean aqueous solutions were measured in the temperature range of 25 to 60 °C. Samples with varying CO_2 loadings (α) from the absorption experiment were also determined at 30 °C. The detailed experimental method is presented in Appendix E.1.

8. Packing wettability test

According to the operation conditions, the density of amine solvents was measured with varying temperatures (30-60 °C) and CO_2 loadings (0-2.5 mol/L). Figure 72 shows the density decreases by the increase of temperature and Figure 73 illustrates it increases with enhancing CO_2 loadings. The influence of CO_2 loading on the density of rich amine solutions is a linear equation, since the effect of CO_2 dissolution into aqueous solution on liquid volume is negligible at low temperatures. The tendency of the density of lipophilic amines with varying CO_2 loadings is the same as that of alkanolamines. Table 25 presents both the values for lean and rich solvents. Lipophilic amine solutions typically exhibit a slightly lower density compared to alkanolamine solutions.
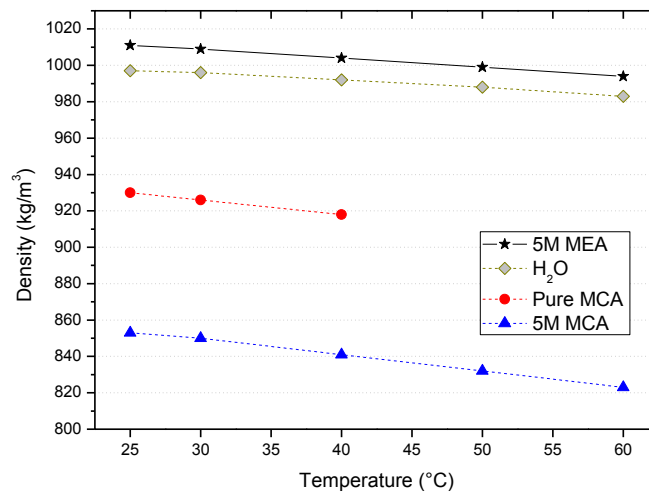
Figure 72. Influence of temperature on solvent density
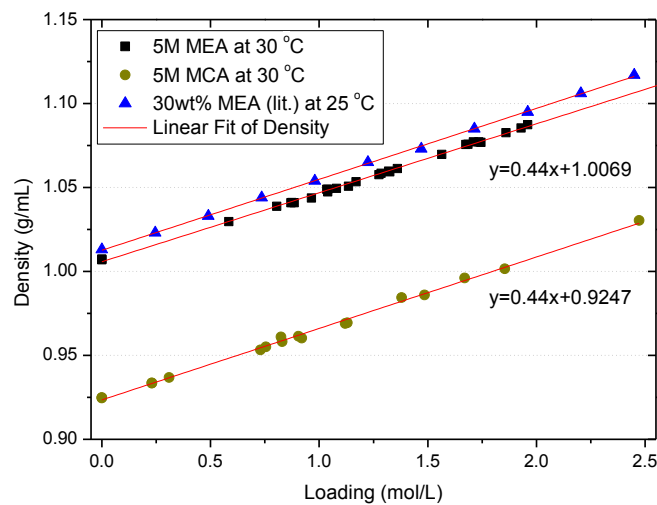
Figure 73. Influence of CO_2 loading on solvent density
(lit.: Weiland et al., 1998)

Table 25. Density of lean and rich solutions at 30 °C

Absorbent	α mol/L	ρ kg/L	Absorbent	α mol/L	ρ kg/L
5M MEA	0	1.007	DMCA+MCA+AMP (3+1+1.25M)	0	0.926
	2.5	1.117		2	1.014
5M MCA	0	0.925	DMCA+MCA+AMP (3+1+1.5M)	0	0.924
	2.5	1.035		2	1.012

8.4.2 Viscosity

8.4.2.1 Literature review of viscosity

The viscosity of aqueous amine solutions was extensively studied in literatures listed in Table 26, but very few have presented the values with CO_2 loadings. The measurement techniques mainly include capillary and rotational methods. Due to unfavourable bubble formation at high temperatures, the measurement is typically below 80 °C.

Table 26. Literature review of viscosity measurement for amine solutions

Author	Year	Amine	Method	T (^{o}C)	α_{-CO2}
Rinker et al.	1994	MDEA, DEA	capillary	20-100	-
Li et al.	1994	MEA, MDEA, AMP	capillary	30-80	-
Hsu et al.	1997	Blends: MEA, DEA, MDEA, AMP, 2-PE	capillary	30-80	-
Weiland et al.	1998	MEA, DEA, MDEA	capillary	25	0-0.64
Park et al.	2002	AHPD	capillary	30-70	-
Mandal et al.	2003	Blends: MDEA, AMP, MEA, DEA	capillary	25-50	-
Paul et al.	2006	MDEA+PZ, AMP+PZ	capillary	15-60	-
Rebolledo-Librers et al.	2006	Blends: MDEA, DEA, AMP	capillary	30-70	-
Murshid et al.	2011	AMP	capillary	25-60	-
Amundsen et al.	2009	MEA	rotational	25-80	0-0.5
Freeman et al.	2011a	PZ	rotational	20-60	0-0.53
Song et al.	2011	amino acid salts	rotational	25-80	-
Aronu et al.	2012	amino acid salts	rotational	20-70	-
Fu et al.	2012	MDEA, MEA	rotational	20-70	0-0.5
Fu et al.	2013	MDEA+DEA	rotational	20-70	0.25-0.5
Zhao et al.	2010	ionic liquids	falling ball	30-70	-

8.4.2.2 Viscosity of amine solutions

The kinematic viscosity (*v*) was initially measured by a certified Ubbelohde viscometer (SCHOTT) with glass capillaries sizes I and II for samples in the ranges of 1.2-10 mm^2/s and 10-100 mm^2/s. The viscometer was initially verified by measuring the viscosity of deionised water at various temperatures, and then the viscosity of pure amine substances and their aqueous solutions with varying temperatures and CO_2 loadings were further studied. The dynamic viscosity (*μ*) was calculated by the multiplication of the kinematic viscosity and density. The detailed experimental setup is shown in Appendix E.2.

The measured viscosity of pure solvents is in the order of MEA > MCA > Water, but that for the lean solutions is [MCA+Water] > [MCA+Water] > Water (see Table 27). A particular behaviour was found in the MCA solution, since the viscosity of the binary [MCA+Water] solution is higher than both pure MCA and water. This can be explained by the interaction of the molecules (refer to Section 2.1.1), principally because the dissolution of MCA in water destroys the initial hydrogen bonds between water molecules and reforms new hydrogen bonds between MCA and water at low temperatures so as to prolong the molecular chains and enhance the interaction between MCA and water molecules.

Table 27. Dynamic viscosity of lean solutions at 25-60 °C

(Unit: mPa·s)

T (°C)	H_2O	MEA	MCA	5M MEA	5M MCA	5M MEA (ref.)*
25	0.99	19	1.5	2.5	6.5	2.48
30	0.80	15	1.3	2.2	5.3	/
40	0.66	9.8	1.0	1.7	3.8	1.67
50	0.55	7.6	0.8	1.4	/	1.33
60	0.48	5.5	0.7	1.1	/	1.08

* Data from Amundsen et al. (2009).

Figure 74 indicates the viscosity of amine solutions is increased by CO_2 loading after absorption. The values for the dynamic viscosity of CO_2 dissolved solutions were fitted by Eq. 8.1 from the study of Weiland et al. (1998) and the calculation parameters are listed in Table 28.

$$\frac{\mu_{sol.}(T)}{\mu_{H_2O}(T)} = \exp\frac{[(a \cdot w_{Am} + b) \cdot T + (c \cdot w_{Am} + d)] \cdot [X_{CO_2} \cdot (e \cdot w_{Am} + f \cdot T + g) + 1] \cdot w_{Am}}{T^2} \qquad \text{Eq. 8.1}$$

Table 28. Parameters for calculation of the dynamic viscosity of amine solutions

Solution	Parameter							Source
	a	b	c	d	e	f	g	
MEA	0	0	21.186	2373	0.01015	0.0093	-2.2589	Weiland
MCA	-0.0376	0.00067	21.186	2320.411	0.01047	0.01093	-2.2589	this work
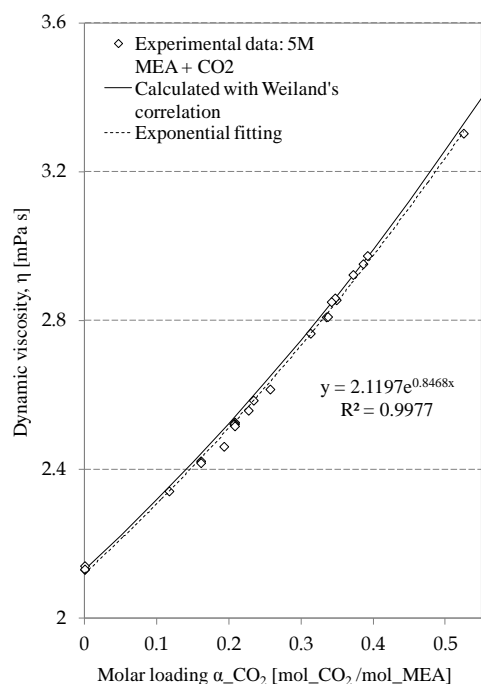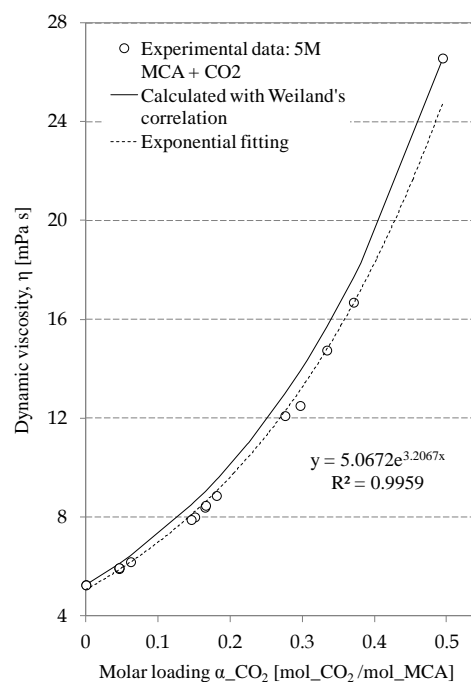
(A) 5M MEA   (B) 5M MCA

Figure 74. Dynamic viscosity of amine solutions with varying loadings at 30 °C

The Weiland's correlation was developed with conventional alkanolamines and has exhibited a good agreement with experimental data in MEA solutions with varying CO_2 loadings at 25-80 °C (see Figure 75), as well as for DEA and MDEA solutions. However, the deviation was increased while applying it for TBS system. As presented in Figure 74, for a specific solvent with certain temperature and definite concentration, an exponential function can be adapted to fit the measured values with the influence of CO_2 loading. Due to the significant effect of CO_2 dissolution, the viscosity of MCA solution increases rapidly with CO_2 loading (see Figure 74B) and value for rich TBS solutions is much higher than for MEA (see Table 29), which becomes a challenge for the pump and piping systems and it is also suggested to increase the porosity of the packings to reduces the pressure drop along the absorption column.
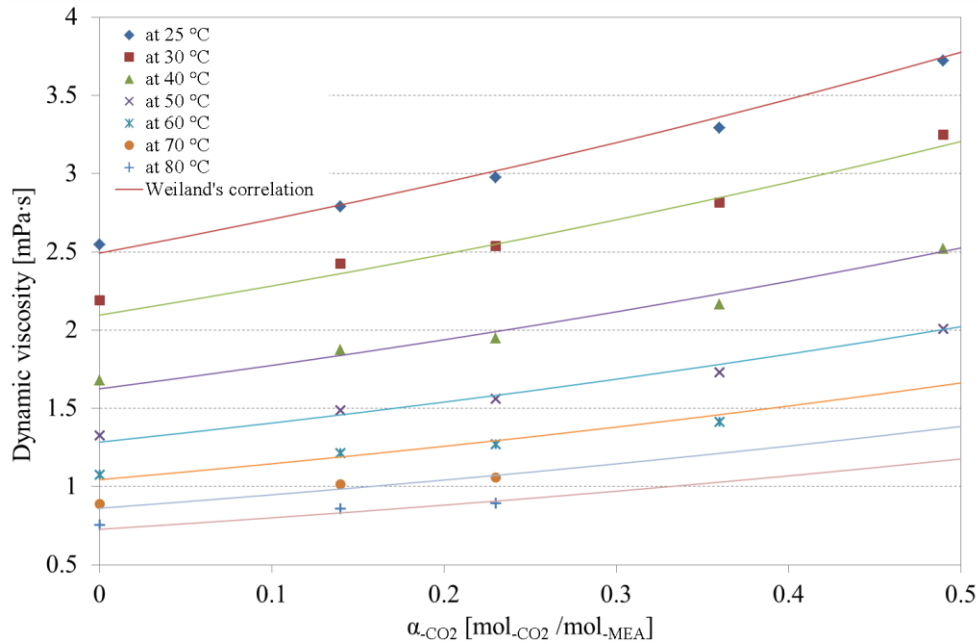
Figure 75. Dynamic viscosity of 30wt% MEA fitted with Weiland's correlation

Table 29. Viscosity of lean and rich solutions at 30 °C

Absorbent	α mol/L	μ mPa·s	Absorbent	α mol/L	μ mPa·s
5M MEA	0	1.5	4M DMCA+MCA (1:3.5)	3	17.5
	2.5	5.5	4M DMCA+MCA (2:1)	2.5	20.1
5M MCA	0	5.2	3M DMCA+MCA (2:1) + 5g AMP	2.4	13.5
	2.5	15.0	4M DMCA+MCA (2:1) + 4g AMP	2.6	16.4
3M DMCA	0	1.3	DMCA+MCA+AMP (3+1+1.5M)	0	7.4
	2	6.9		2	11.8

8.4.3 Surface tension

8.4.3.1 Literature review of surface tension

The surface tension for amine solutions has typically been measured by the Wilhemy plate, capillary rise and pendant drop methods (see Table 30). There are few literatures that have studied the influence of CO_2 loadings and the temperature was also limited up to 60 °C for rich solvents. A theoretical model was proposed by Fu et al. (2012b) to fit the experimental data, but large deviations were observed and a polynomial function was presented Jayarathna et al. (2013a) to correlate the measured values for CO_2 loaded amine solutions, but it is only validated with MEA.

Table 30. Literature review of surface tension measurement for amine solutions

Author	Year	Amine	Method	T (^{o}C)	α_{-CO2}
Rinker et al.	1994	MDEA, DEA	Wilhemy plate	20-80	-
Vazquez et al.	1997	MEA, AMP	Wilhemy plate	25-50	-
Alvarez et al.	1998	MDEA, MEA, DEA, AMP	Wilhemy plate	25-50	-
Fu et al.	2012b	MDEA+PZ	Wilhemy plate	20-50	0-0.8
Fu et al.	2013b	MDEA+MEA	Wilhemy plate	20-50	0-0.5
Maham et al.	2001	MEA, DEA, TEA, MDEA, DMEA	capillary-rise	25-55	-
Aguila-Hernandez et al.	2001	DEA, MDEA	capillary-rise & pendant drop	20-90	-
Aguila-Hernandez et al.	2007	MDEA, AMP, DEA	pendant drop	20-70	-
Alvarez et al.	2003	Blends: AP, MIPA, DEA, TEA, AMP	pendant drop	20-50	-
Murshid et al.	2011	AMP	pendant drop	25-60	-
Han et al.	2012	MEA	pendant drop	30-60	-
Jayarathna et al.	2013a	80 wt% MEA	pendant drop	40-70	0-0.5
Jayarathna et al.	2013b	20-70 wt% MEA	pendant drop	30-60	0-0.5
Sanchez et al.,	2007	Ionic liquids	Du Noüy ring	20-70	-
Song et al.	2011	amino acid salts	max. bubble pressure	25	-

8.4.3.2 Surface tension of amine solutions

The surface tension measurement was conducted with the maximum bubble pressure method using a capillary tensiometer equipped with a precisely adjusted distance gauge and a U-tube manometer was used for measuring the dynamic surface tension of various solutions. The detailed measuring technique is illustrated in Appendix E.3.
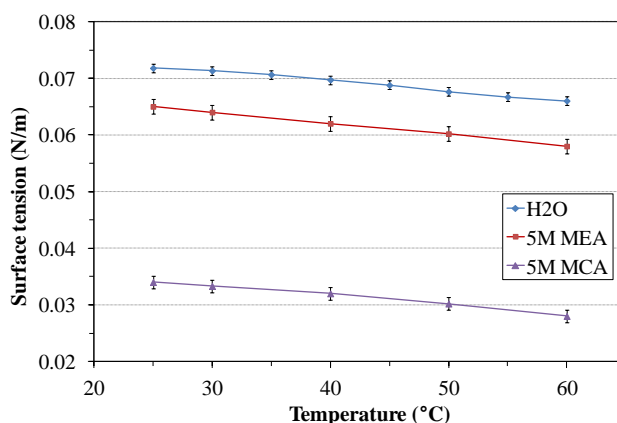
Figure 76. Surface tension of water and amine solutions at various temperatures

The apparatus is initially validated with the measurement of deionised water at various temperatures from 25 to 60 °C (see Figure 76). Amine solutions with varying temperatures and CO_2 loadings were further tested. Table 31 shows the surveyed values of the lean solutions are in the order of Water > [MEA+Water] > MEA > [MCA+Water] > MCA. The lower surface tension has important positive influence on the mass transfer in the absorber (Tsai et al., 2009), which is an advantage of TBS systems.

Table 31. Surface tension of lean solutions at 25-60 °C

(Unit: mN/m)

T (°C)	Water	MEA	MCA	5M MEA	5M MCA	MEA (ref.)*
25	72	50	30	65	34	49
40	69	48	28	62	32	46
60	65	45	26	58	28	-

* Data from Vázquez et al. (1997).

As illustrated in Figure 77 and Figure 78, the MCA solution presents a much lower surface tension compared to MEA, at both lean and rich CO_2 loadings. Surface tension of amine solutions is increased by CO_2 dissolution or by a decrease in temperature.
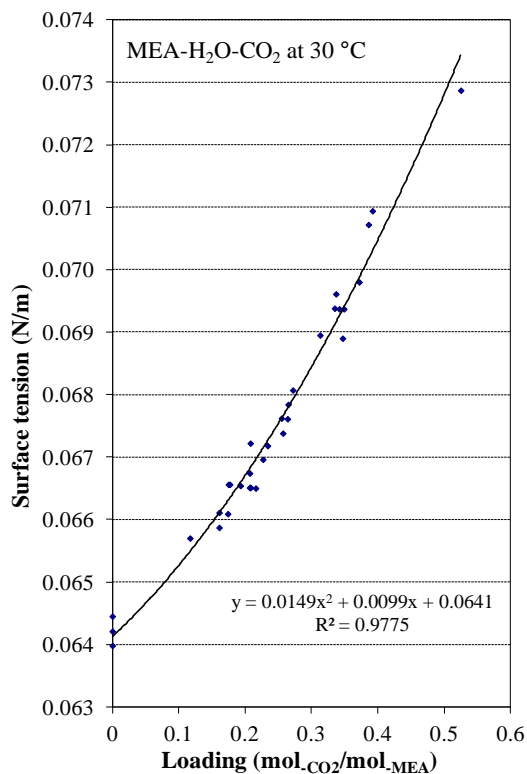
Figure 77. Surface tension of MEA solution with varying loadings at 30 °C
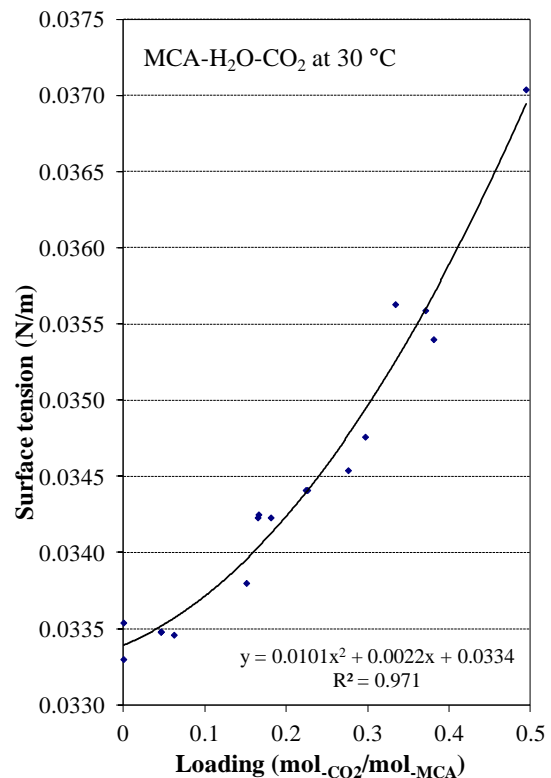
Figure 78. Surface tension of MCA solution with varying loadings at 30 °C

8.4.4   Contact angle

Contact angle (θ) is a quantitative measure of the wetting of a solid by a liquid. It is defined geometrically as the angle formed by a liquid at the three phase boundary where a liquid, gas and solid intersect as shown in Figure 79. A low value of θ indicates that the liquid spreads, or wets well, while a high contact angle indicates poor wetting. If $\theta <$ 90 degrees the liquid is wet the solid. If $\theta >$ 90 degrees it is non-wetting. A zero contact angle represents complete wetting.
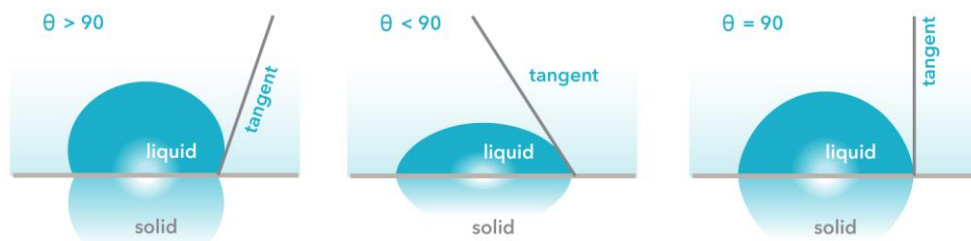
Figure 79. Illustration of contact angle for liquid samples (AttensionLab)

It is very difficult to find a literature which studies the contact angle of amine and packing material in CO_2 capture. Some investigations of the contact angle of water, MEA and DEA solution on polypropylene hollow fibre membranes for CO_2 absorption were presented by Lv et al. (2012) and Wang et al. (2004).

The measurement of contact angle was conducted with sessile drop method using a Krüss G40 analytical system at room temperature. Various metal and plastic materials were tested with the lean and rich solutions. The goniometer is shown in Appendix E.4.

The contact angle directly indicates the wettability of column packing with amine solvent. Figure 80 together with Figure 81 proves the values of the tested packing materials for example steel and aluminium are more wettable to lipophilic amine than for alkanolamine. Especially, the plastic material PE-HD (high-density polyethylene) has exhibited a good wettability for both the lean and rich MCA solutions. As seen in Figure 81, the contact angle is generally increased by CO_2 loading. Other plastic materials such as H-PVC (hard polyvinyl chloride) and PP-H (polypropylene homopolymer) exhibit comparable values with metal for lean lipophilic amine solutions but become less wettable for rich solutions. However, the contact angle of both alkanolamine and lipophilic amine solutions on PTFE (polytetrafluoroethylene) is much higher than for other tested materials.
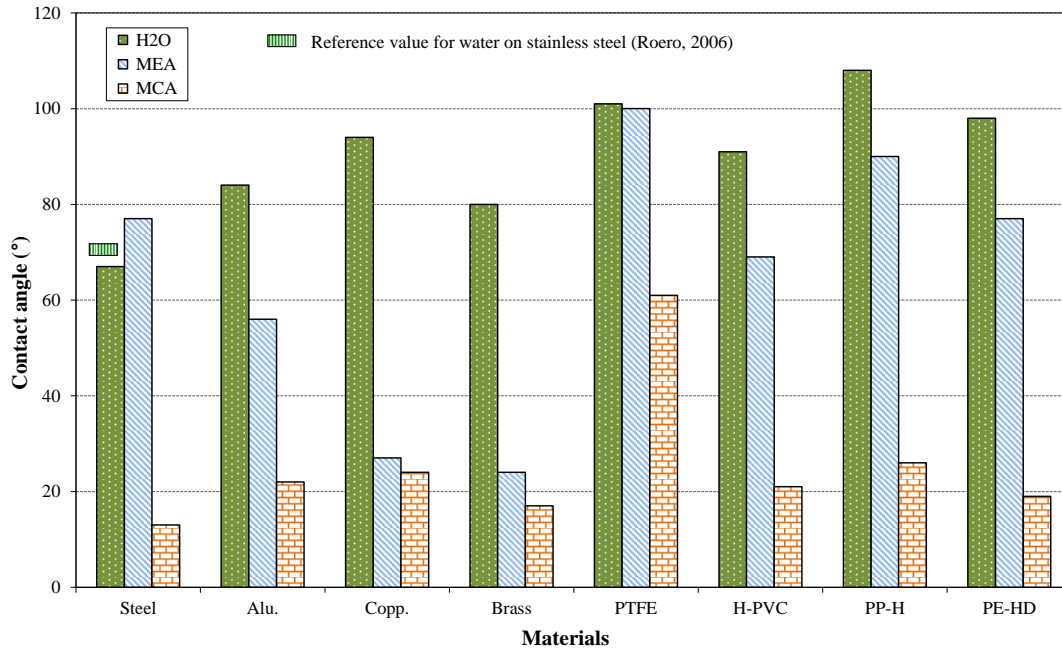
Figure 80. Contract angle of water, MEA and MCA solutions on various materials

(H-PVC = hard polyvinyl chloride, PE-HD = high-density polyethylene,
PP-H = polypropylene homopolymer, PTFE = polytetrafluoroethylene.)
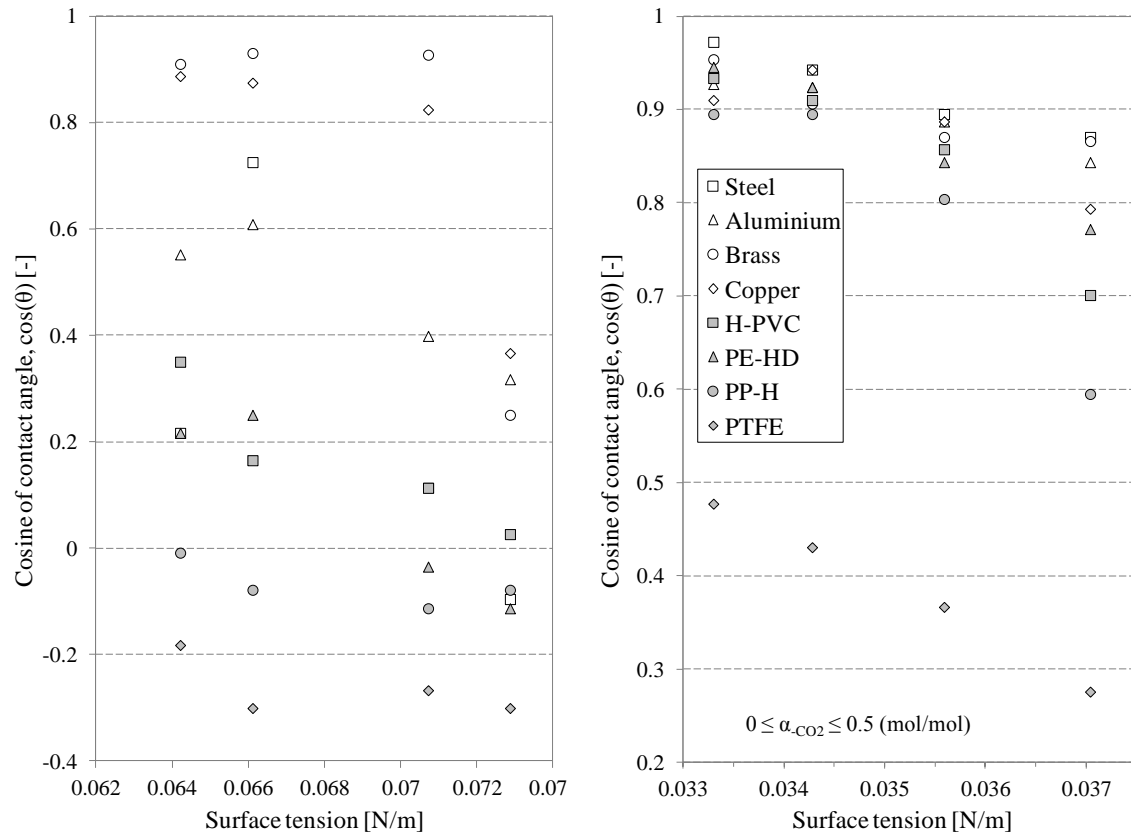
(A) 5M MEA solution

(B) 5M MCA solution

Figure 81. Contact angle of CO_2 loaded amine solutions on various materials

8.5 Summary

Compared to conventional MEA solvent, higher pressure drop has been observed in biphasic solvents, which is mainly caused by the higher viscosity of CO_2 loaded solutions. Packings with higher porosity were thus recommended to be used in the bottom section of column. Lower surface tension, smaller contact angle and higher liquid hold-up indicate the better wettability of packing materials to biphasic solvents, and plastic packings such as PE-HD can also be employed to reduce the capital cost and Fe-catalysed degradation as well as corrosion issues.

9　Process development

Since an innovative concept with a new type of amine was studied in this work, novel CO_2 capture processes were proposed in order to adapt the characteristics of the new TBS system. Compared to a conventional alkanolamine based process, the modified lipophilic amine based process should be more economic and efficient.

9.1　Novel TBS processes

9.1.1　Flowsheet for CO_2 capture from refinery

The initial purpose of the process flow sheet design is to fit the biphasic system for CO_2 capture from a refinery where there exists a lot of waste heat <100 °C, thus the regeneration temperature was set at 90 °C and the reboiler was not considered for solvent regeneration. In place of steam stripping, other techniques such as nucleation, agitation and extraction have been proposed.

According to the concept of phase change and low temperature regeneration, the major modifications of novel TBS process were found in the desorption technology. The regenerated TBS solution becomes homogeneous upon cooling to the lower critical solution temperature (LCST) of 30-40 °C, and the loaded solution separates into two immiscible phases upon heating to ca. 80 °C. In the improved TBS process (see Figure 82), deep regeneration is enhanced by the liquid-liquid phase separation (LLPS), which permits the exploitation of the low value heat at 85-95 °C from the other processes and cuts the energy consumption by more than 35% compared to the conventional alkanolamine monoethanolamine (MEA) based solvent system.
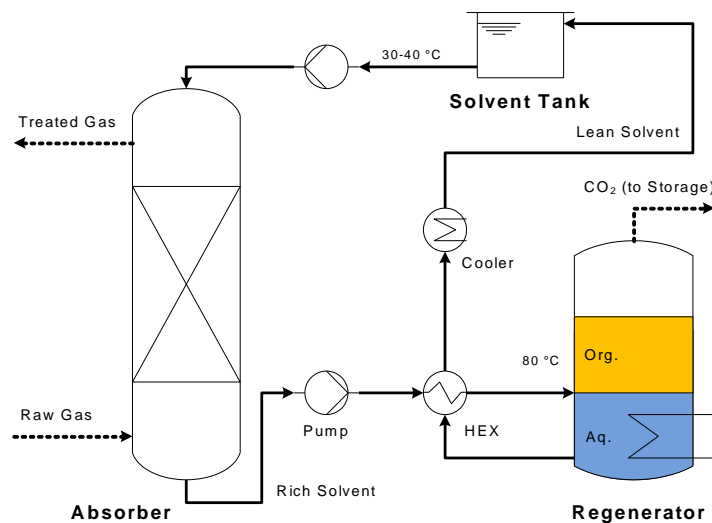
Figure 82. Simplified TBS process flow scheme

To intensify CO_2 regeneration from the loaded solvent, improved methods such as agitation and phase split were employed. In the agitated regeneration (Figure 83), A continuous stirred-tank reactor (CSTR) was applied for desorption purpose, in place of conventional steam stripping. Porous particles can be placed in the regenerator to accelerate CO_2 release by nucleation. Due to the difficulty of heating the rich solvent in the CSTR unit, a pre-heater must be installed for the rich stream before filling into the regenerator. Because of the high volatility of lipophilic amines, washing units were employed for the treated gas stream from the absorber and CO_2 stream from the regenerator to recover the vaporised amines. Since the CO_2 absorption is an exothermic reaction, the temperature in the absorption column will be increased, inter-stage cooling (refer to Figure 2) is recommended to improve the CO_2 loading capacity and to reduce the solvent vaporisation loss. In this case, the total heat requirement, i.e. the heat duty of the pre-heater, will be slightly increased, but only waste heat is used in this regeneration process.
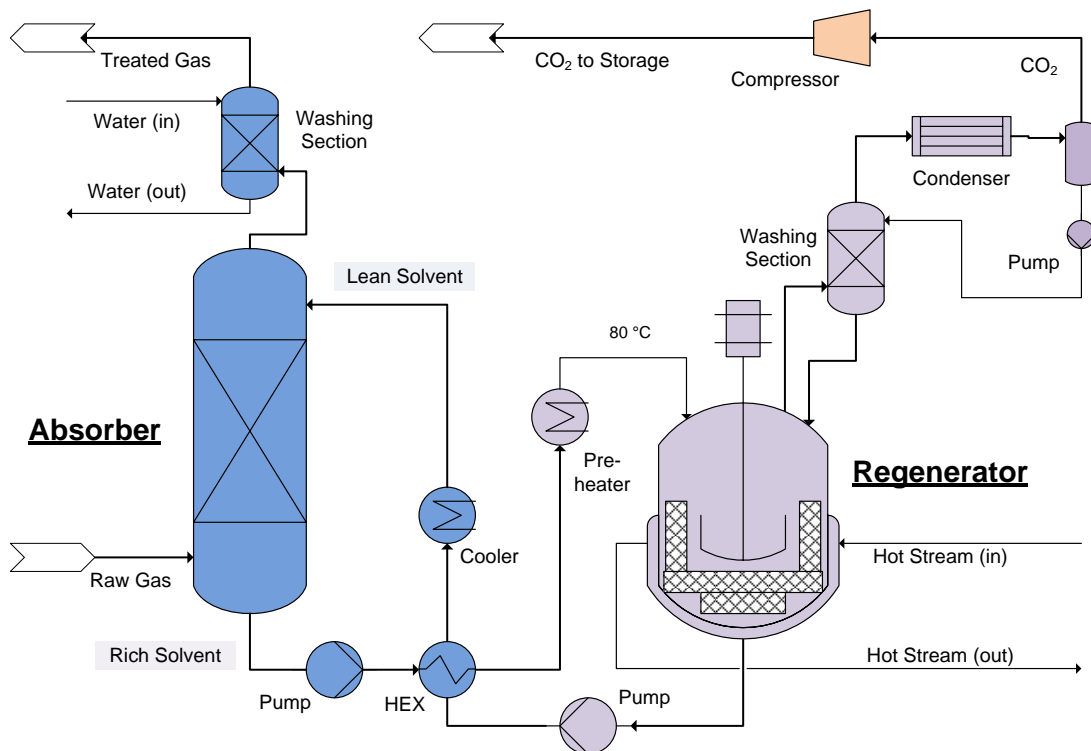
Figure 83. TBS process flowsheet with agitation

Another alternative is introducing a phase separator with preheat device before regeneration. As illustrated in Figure 84, the loaded rich solvent is preheated by the hot lean stream from the regenerator and pre-regenerated by nucleation in the phase separator at ca. 60 °C. A supernatant organic phase containing recovered lipophilic amines can be formed, which can directly be recycled to absorption after cooling, with simultaneous partial CO_2 release; the remaining aqueous phase comprising concentrated rich solvent can be forwarded to the regenerator for deep desorption. Such a process with additional phase split can reduce the energy consumption still further.
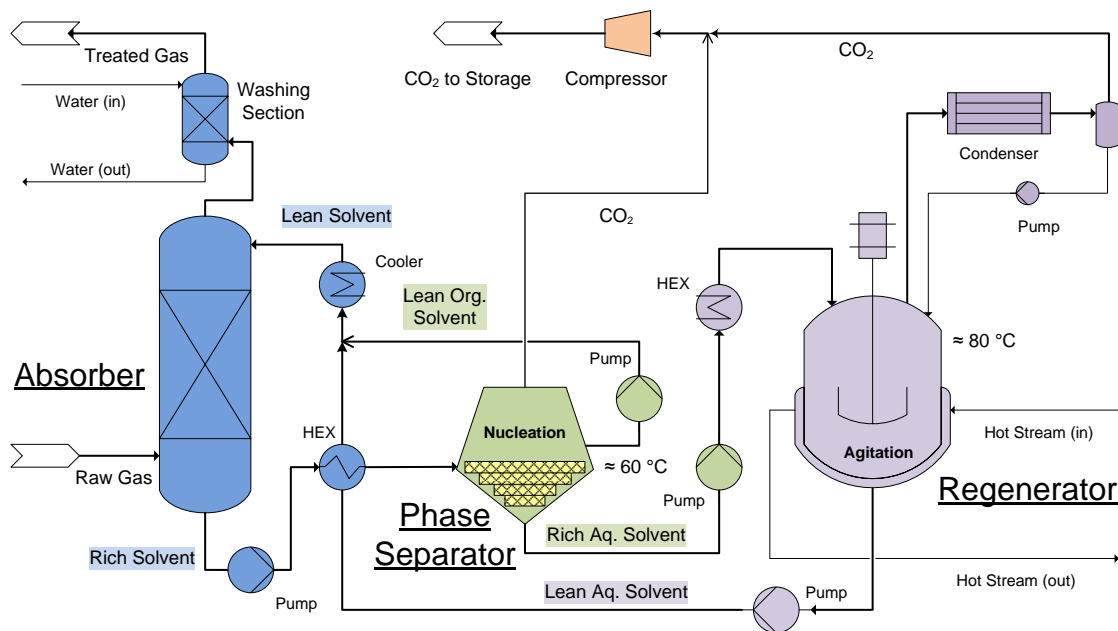
Figure 84. TBS process flowsheet with phase split and agitation

Figure 85 shows that the extractive regeneration process involves extraction, inert solvent / amine separation and vaporised inert solvent recovery units. Compared to the conventional regeneration technologies, the extractive regeneration requires additional inert solvent recovery processes, which consumes more heat, and the whole extractive regeneration process hence has a relatively high energy requirement of 3.5 GJ/t$_{-CO2}$, but it enables using waste heat at temperatures of 60-70 °C for CO_2 desorption, which can integrate the industrial energy recovery networks to the solvent regeneration system. The operating costs can thus be significantly reduced.
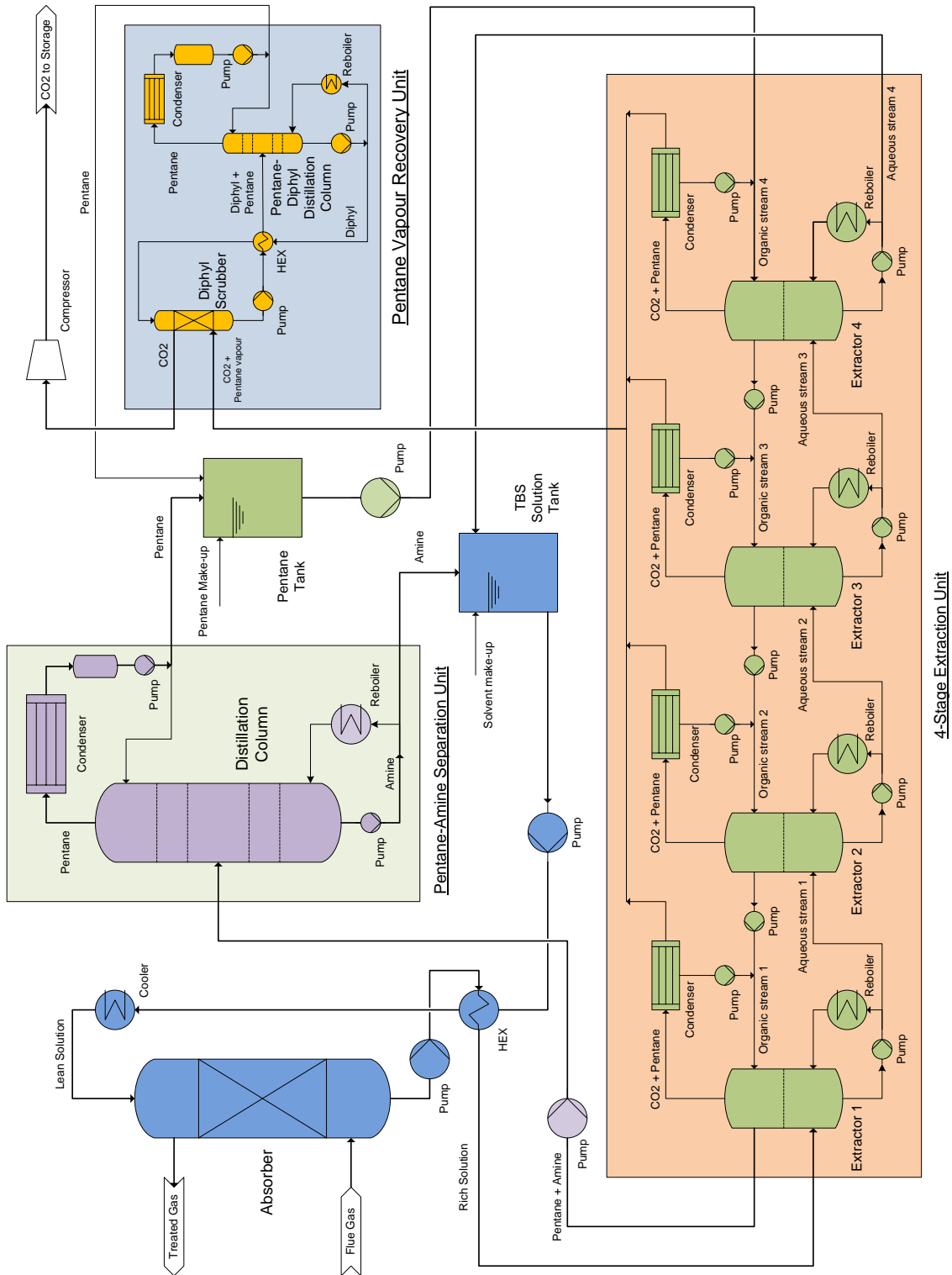
Figure 85. Flowsheet of an extractive regeneration process

9.1.2 Flowsheet for CO_2 capture from power plant

Since CO_2 emission from fossil fuel fired power plant is the largest source, a modified flowsheet is also designed for the post-combustion capture (PCC) from power plant, where existing internal steam from boiler. Figure 86 presents a flow scheme with phase split for rich solvent stream: after nucleation or/and agitation in the phase separator, the loaded solvent was separated into two phases – the supernatant organic phase mainly contains the recovered lipophilic amines which can recycled to the absorber, the lower aqueous phase comprises the protonated amine, carbamate and bicarbonate which should be sent to the stripper for deep regeneration. The stream split reduces the rich solvent flow fed into the stripper; it reduces both the stripping column size and steam requirement. Since the operating temperature in the stripper at ~120 °C is higher than that using other intensification methods at ~90 °C, the temperature in the phase separator is also elevated and more than half of the loaded amines can be regenerated; by control of the pressure of outlet gas (minor CO_2 stream), the concentration of CO_2 in the aqueous phase will be enhanced. This enables a higher operating pressure in the stripping column and saves the power consumption of the compressor.

Figure 86. Process flowsheet with phase split and stripping

This flow sheet is very similar to the DMX^{TM} process (Raynal et al., 2011a), however, nucleation is considered to accelerate the phase separation in the TBS system rather

than the high speed agitation which was employed in the DMX^{TM} process. Further energy save can be achieved, since nucleation doesn't consume any electrical power. In addition, the t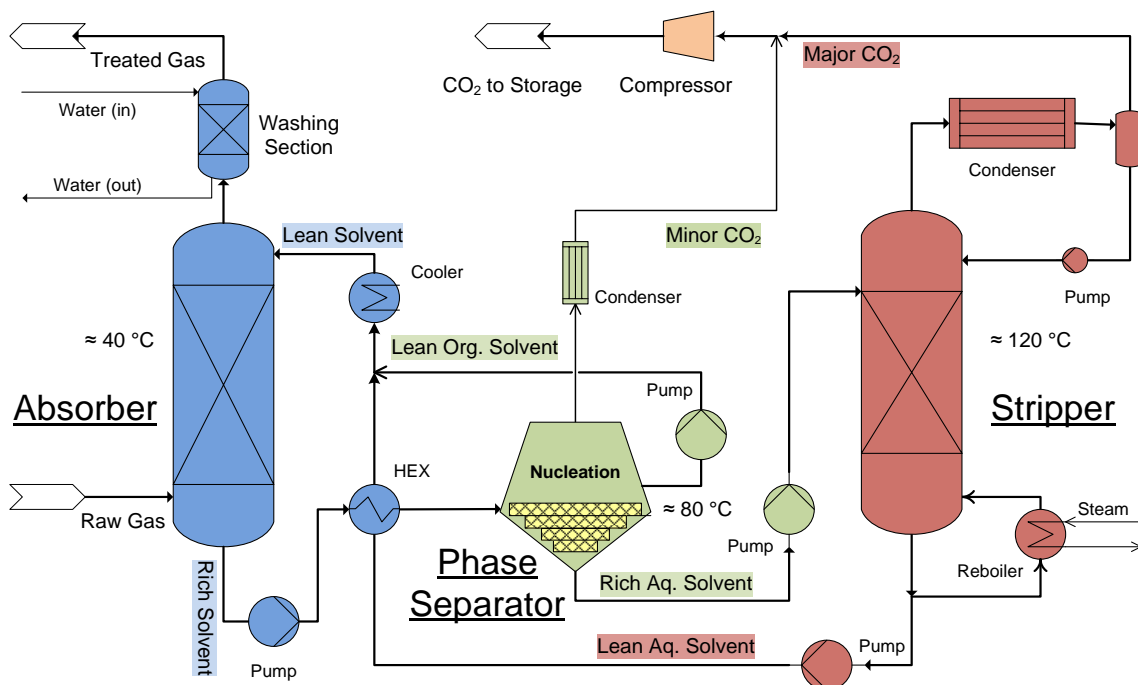emperature required for phase separation in the TBS system is only 70-80 °C, while it is 90 °C in the DMX^{TM} process. This proves a higher feasibility of integrating the process heating networks for the TBS process.

9.2 Estimation of energy consumption

Improved alkanolamine-based solvents have reduced the energy consumption by 22-27% in comparison to conventional 30 wt.% MEA (Rochelle, 2009). However, the TBS system has proved itself to be a promising advanced absorbent for CO_2 capture, since it is chemically very stable and exhibits low degradation rates, due to the lower operating temperature, and reduces the regeneration energy consumption still further by ≈40%, down to ca. 2.5 GJ/t$_{CO_2}$, compared to the MEA process (see Table 32). This is mainly owing to the energy saving in sensible heat by avoiding steam stripping. However, it requires additional mechanical or electrical power for regeneration if agitation or ultrasound is employed, but such energy consumption is minor, only ca. 0.15 GJ/t$_{CO_2}$. The extractive regeneration process still consumes relatively high energy, ca. 3.5 GJ/t$_{CO_2}$, which is primarily caused by the additional distillation processes used for separating amine from inert solvent and vaporised inert solvent recovery from Diphyl scrubbing. But it permits the use of low grade heat for solvent regeneration, which can cut the exergy demand.

Table 32. Estimation of regeneration energy consumption

(Unit: GJ/t$_{CO_2}$)

	Sensible heat	Heat of reaction	Stripping energy	Heat loss	Total
MEA	0.9	1.8	1.1	0.2	4.0
TBS-1[a]	0.5	1.6	0.3	0.1	2.5
TBS-2 + Agitation	0.4	1.35	0.15 *(Mechanical energy)*	0.1	2.0
TBS-1 + Extraction	0.6	1.6	0.9 + 0.2 *(Distillation energy*[b]*)*	0.2	3.5

[a] TBS-1 using MCA as principal component, TBS-2 using DMCA as principal component;
[b] Separation of inert solvent and amine by waste heat & recovery of inert solvent from Diphyl.

The equations for calculating the required heats are shown in the following and the major parameters are listed in Table 33.

Sensible heat	$Q_{sen} = F_{sol} \cdot C_p \cdot \Delta T$	Eq. 9.1
Heat of reaction	$Q_r = F_{CO_2} \cdot \Delta_r H$	Eq. 9.2
Stripping energy	$Q_{str} = F_{steam} \cdot L_v$	Eq. 9.3
Heat loss	$Q_{los} = \phi \cdot \Delta T \cdot A$	Eq. 9.4
Distillation energy	$Q_{dis} = F_{inert} \cdot \Delta_v H$	Eq. 9.5

where F is the specific mass flow, C_p is the heat capacity, ΔT is the temperature difference, $\Delta_r H$ is the reaction enthalpy, L_v is specific latent heat for vaporisation, Φ is the heat loss coefficient, A is the heat transfer surface area, $\Delta_v H$ is the specific vaporisation enthalpy.

In the regeneration for TBS, the power (P) of agitation can be calculated using the following Equation:

$$P = Ne \cdot n^3 \cdot d^5 \cdot \rho$$
Eq. 9.6

where Ne is the Newton number; n is the stirrer speed; d is the stirrer diameter; ρ is the density. The Reynolds number is determined first and the corresponding value of Ne can be read from the chart of power characteristics of the stirrer types (Zlokarnik, 2005).

Table 33. Parameters for calculation of energy consumption

Solvent	c_{am}	$C_{p,mix}$	ΔT_1	ΔT_2	$\Delta \alpha$	$\Delta_r H$	R	T_{des}	p_{vap}
	mol/L	kJ/(kg K)	°C	°C	mol_{CO_2}/kg_{sol}	kJ/mol_{CO_2}		°C	kPa
MEA solution	5	3.9	15	90	1.5	80	2	120	200
Previous TBS	3	3.6	15	50	2.8	70	1	90	70
Improved TBS	5	3.1	20	50	3.2	60	0.6	80	47

($\Delta_v H$=25.8 $kJ/mol_{pentane}$)

Since the heat of reaction typically contributes roughly half of the energy consumption for regeneration in the CO_2 capture process, it represents an important parameter in assessing the overall heat requirement. The absorption enthalpies of CO_2 and lipophilic amines were measured by means of the van't Hoff thermodynamic equation at TU Dortmund and the data were also confirmed with using a reaction

calorimeter at Shell Global Solutions International B.V. in Amsterdam, NL and at Thermal Hazard Technology (THT) in Bletchley, UK. As discussed in section 3.5.4, the reaction enthalpies for lipophilic amines lie between those of the conventional alkanolamine solutions MEA and MDEA. Notz et al. (2007) introduced a thermodynamic method for solvent comparison by ranking of solvent flow rate and desorber vapour flow rate in relation to MEA. According to this evaluation technique, the energy consumption can be cut by 30-35% compared to the benchmark aqueous absorbent MEA (see Figure 87). In addition, the low regeneration temperature required for TBS system enables the use of waste heat for CO_2 desorption, which makes it one of the most potential technologies get through the economic evaluation for the next generation CO_2 capture processes.
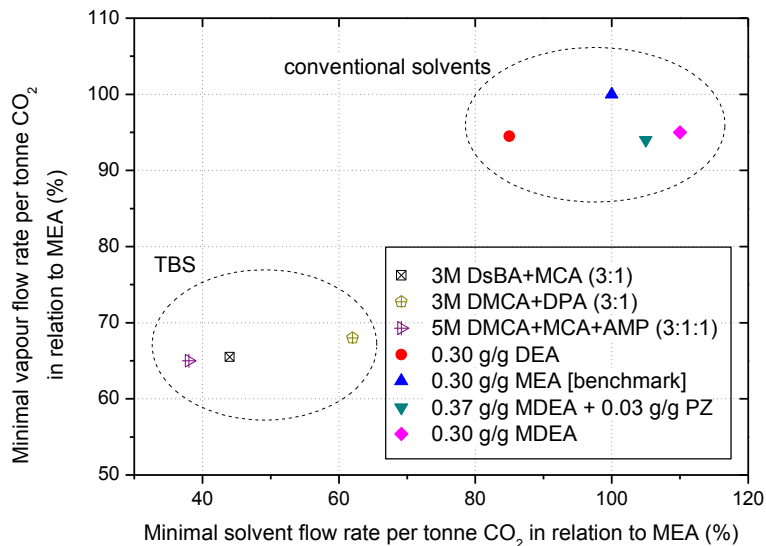
Figure 87. Theoretical solvent evaluation with a thermodynamic method

10 Conclusions and outlook

A new CO_2 absorption system with thermal-induced liquid-liquid phase change has been developed in this work. The TBS absorbents comprising lipophilic amines as activating components potentially enable an extensive regenerability over 90% at 75-85 °C without gas stripping, when other alternative process intensification measures are adopted, thus permitting a more flexible and expedient thermal integration for the CO_2 capture process. The performance of TBS observed is comparable, if not superior, to that of conventional alkanolamines such as MEA. In particular, the cyclic loading capacity (40-85°C: 3.5 mol_{CO_2}/kg_{5M-TBS}) is markedly improved compared with the benchmark amine solvent (40-120°C: 1.6 $mol_{CO_2}/kg_{30wt\%-MEA}$).

To optimise the solvent recipe, more than 60 lipophilic amines were screened in the experiment. The selected amines were classified into two categories: (A) absorption activator due to its rapid reaction kinetics, and (B) regeneration promoter according to the outstanding regenerability. Blended amine solvents were formulated to combine the advantages of both and thus to achieve high net CO_2 capacity and fast absorption rate as well as low degradation. Additionally, solubiliser was also introduced to regulate the lower critical solution temperature (LCST) for attaining desired phase change behaviours: it was converted to homogeneous at 30-40 °C at lean conditions and separated to two phases at 70-80 °C at rich conditions.

Lipophilic amines exhibited a more significant vaporisation loss compared to MEA. This loss however can be substantially reduced by 80% or even more using a chilled water or hydrophobic solvent scrubber. Foaming is another disadvantage for DMCA-based solvents, but it can be well controlled or eliminated by means of a liquid spray, foam breakers, water scrubbing and solubiliser addition. Irreversible chemical degradation of optimised TBS absorbents is less than for MEA. Both the aqueous chemistry of the oxidative reaction and the lower operating temperature contribute to the improved chemical stability, one of the major unresolved weaknesses of conventional amines in the CO_2 separation from flue gases.

Several potential intensified regeneration techniques were investigated to replace the conventional steam stripping method. Nucleation accelerates CO_2 desorption without further mechanical or electrical energy consumption; agitation and ultrasound enhance solvent regeneration in both the rate and depth of desorption; extractive regeneration with low boiling point foreign hydrophobic solvents reduces the regeneration temperature still further down to 50-70 °C and offers a higher freedom for the use of waste heats in desorption.

The lean TBS solution shows a lower viscosity compared to the MEA solution, but it becomes much more viscous after CO_2 loading, and leads to a higher pressure drop and lower flooding point in the absorption column. Both the surface tension and contact angle of TBS are lower than for MEA at various CO_2 loadings and on different packing materials. It indicates a better wettability of packing materials with lipophilic amines and results in a higher liquid hold-up. Due to the rapid rise in viscosity along the absorption column, higher porosity packings are suggested to be applied at the bottom of the absorber. According to the good wettability, plastic packings such as PE-HD can also be used to reduce the corrosion and degradation.

Since the reaction enthalpy of lipophilic amines is not lower than for conventional alkanolamines, savings in total energy consumption are mainly contributed by reducing sensible heat and getting rid of steam stripping. The lower desorption temperature provides further degrees of freedom to cut the exergy demand and thus to improve the technical feasibility of using waste heat for CO_2 regeneration. Such an intensified TBS process offers significant advantages for enhancing the efficiency of CO_2 capture and reducing the process costs due to the rapid reaction kinetics, high loading capacity, moderate regeneration temperature, excellent regenerability and low energy consumption.

However, volatile loss is still the most significant challenge for lipophilic amines. It is better to develop a non-volatile solvent than to use an additional scrubbing process to recover the vaporised amines. New TBS absorbents are therefore expected to be developed, which should not be restricted to only lipophilic amines but also some blends comprising well performed aqueous soluble amines with a small amount of lipophilic additives. The vaporisation loss thus can be reduced. For a better understanding of the phase change behaviour, more thermophysical data such as the heat capacity of TBS and demixing enthalpy of lipophilic amine and water are required to be measured.

To deploy the CO_2 absorption process using TBS system, a further scaled-up work is expected to be conducted. Using a steel absorption column to determine the corrosion and Fe-catalysed oxidations is important to adapt such solvent for industrial applications. More efficient structured packings can be employed in the absorber to further study the influence of lipophilic amines on packing wettability. Thermodynamic modelling can also be carried out to predict the column dynamics for CO_2 absorption with Novel TBS system after acquiring sufficient experimental data.

References

Agar, D.W.; Tan, Y.; Zhang, X., **2008**a, CO$_2$ removal processes by means of absorption using thermomorphic biphasic aqueous amine solutions. *Patent* WO 2008/015217.

Agar D.W.; Tan, Y.H., **2008**b, Extractive regeneration of loaded amine solutions at very low temperature. *Patent* DE 10 2008 007 087.4.

Aleixo, M.; Prigent, M.; Gibert, A.; Porcheron, F. et al., **2011**, Physical and chemical properties of DMX^{TM} solvents. *Energy Procedia*, 4, 148-155.

Amundsen, T.G.; Øi, L.E.; Eimer, D.A., **2009**, Density and viscosity of monoethanolamine + water + carbon dioxide from (25 to 80) °C. *J. Chem. Eng. Data*, 54, 3096-3100.

Aroonwilas, A., **2004**, Evaluation of split-flow scheme for CO$_2$ absorption process using mechanistic mass-transfer and hydrodynamic model. presented in *7th International Conference on Greenhouse Gas Control Technologies*, September 2004, Vancouver, Canada.

Astarita, G., **1983**. *Gas Treating with Chemical Solvents*. Wiley-Interscience Publication: New York.

Bart, H.J., **2001**, *Reactive extraction*, Springer-Verlag: Berlin.

Barton, A.F., **1991**, *CRC Handbook of Solubility Parameters and Other Cohesion Parameters*, 2nd ed., CRC Press, Inc.: Boca Raton.

Behr, A.; Agar, D.W.; Jörissen, J., **2010**, Thermische Trennverfahren II - Absorption und Extraktion, in *Einführung in die Technische Chemie*, Spektrum Akademischer Verlag: Heidelberg, pp. 93-106.

Bello, A.; Idem, R.O., **2006**, Comprehensive study of the kinetics of the oxidative degradation of CO$_2$ loaded and concentrated aqueous monoethanolamine (MEA) with and without sodium metavanadate during CO$_2$ absorption from flue gases. *Ind. Eng. Chem. Res.*, 45(8), 2569-2579.

Billet, R. **1995**, *Packed Towers*. VCH Verlag: Weinheim.

Bouillon, P.A.; Jacquin, M.; Raynal, L., **2010**a, Gas deacidizing method using an absorbent solution with demixing control. *US Patent* 0104490.

Bouillon, P.A.; Jacquin, M.; Methivier, A., **2010**b, Gas deacidizing method using an absorbent solution with demixing during regeneration. *US Patent* 0132551.

Bruder, P.; Svendsen, H.F., **2011**, Solvent comparison for postcombustion CO$_2$ capture. presented in *1st Post-Combustion Capture Conference*, May 2011, Abu Dhabi.

Cadours, R.; Carrette P.L.; Boucot, P., **2007**, Process for deacidification of a gas by means of an absorbent solution with fractionated regeneration by heating. *Patent* WO 2007/104856.

Carson, J.K.; Marsh, K.N.; Mather, A.E., **2000**, Enthalpy of solution of carbon dioxide in water + Monoehtanolamine or Diethanolamine or N-methyldiethanolamine at T = 298.15K. *J. Chem. Thermodyn.*, 32(9), 1285-1296.

Chi, Q.S., **2000,** Oxidative degradation of monoethanolamine. *MSc. Thesis*, University of Texas, Austin.

Chakraborty, A. K.; Astarita, G.; Bischoff, K. B., **1986**, CO$_2$ absorption in aqueous solutions of hindered amines. *Chem. Eng. Sci.*, 41, 997-1003.

References

Chen, X.; Freeman, S.A.; Rochelle, G.T., **2011**, Foaming of aqueous piperazine and monoethanolamine for CO_2 capture. *Int. J. Greenhouse Gas Control*, 5, 381-386.

Chowdhury, F.A.; Okabe, H.; Shimizu, S.; Onoda, M.; Fujioka, Y., **2009**, Development of novel tertiary amine absorbents for CO_2 capture. *Energy Procedia*, 1, 1241-1248.

Chowdhury, F.A.; Okabe, H.; Yamada, H..; Onoda, M.; Fujioka, Y., **2011**, Synthesis and selection of hindered new amine absorbents for CO_2 capture. *Energy Procedia*, 4, 201-208.

Clayden J.; Greeves, N.; Warren, S.; Wothers, P., **2005**, *Organic chemistry*. Oxford University Press: Oxford.

Cole, R., **1974**, Boiling Nucleation, *Adv. Heat Transfer*, 10, 85-166.

Cousins, A.; Wardhaugh, L.T.; Feron, P.H.M., **2011**, A survey of process flow sheet modifications for energy efficient CO_2 capture from flue gases using chemical absorption. *Int. J. Greenhouse Gas Control*, 5(4), 605–619.

Counsell, J.F.; Everett D. H.; Munn R.J., **1961**, Recent redeterminations of the phase diagram of the system: triethylamine + water, [online]
http://iupac.org/publications/pac/pdf/1961/pdf/0201x0335.pdf (accessed 31 August 2013).

Dang, H.Y.; Rochelle, G.T., **2003**, CO_2 Absorption rate and solubility in Monoethanolamine/Piperazine/Water. *Sep. Sci. & Technol.*, 38(2), 337-357.

Davis, J.; Rochelle, G., **2009**, Thermal degradation of monoethanolamine at stripper conditions. *Energy Procedia*, 1, 327-333.

Davis, J., **2009**, Thermal degradation of aqueous amines used for carbon dioxide capture. *Ph.D. Dissertation*, University of Texas, Austin.

Davison, R.R., **1968**, Vapor-liquid equilibria of Water-Diisopropylamine and Water-Di-n-propylamine. *J. Chem. Eng. Data*, 13(3), 348–351.

Eisenberg, B.; Johnson, R.R., **1979**, Amine regeneration process. *US Patent* 4152217 A1.

Estep, J.W.; McBride, J.T.; West, J.R., **1962**, *Advances in Petroleum Chemistry and Refining*, Vol. 6, Interscience Publishers: NY, pp. 315-466.

Feron, P.H.M, **2009**, The potential for improvement of the energy performance of pulverized coal fired power stations with post-combustion capture of carbon dioxide. *Energy Procedia*, 1, 1067-1074.

Freeman, S.A.; Rochelle, G.T., **2011**, Thermal degradation of piperazine and its structural analogs. *Energy Procedia*, 4, 43-50.

Gabrielsen, J.; Svendsen, H. F.; Michelsen, M. L.; Stenby, E. H.; Kontogeorgis, G. M., **2007**, Experimental validation of a rate-based model for CO_2 capture using an AMP solution. *Chem. Eng. Sci.*, 62(2), 2397-2413.

Gantert S.; Möller D., **2012**, Ultrasonic desorption of CO_2 - a new technology to save energy and prevent solvent degradation. *Chem. Eng. & Technol.*, 35(3), 576-578.

Geuzebroek, F.; Schneider, A.; Last, T.; Zhang, X., **2009**, Benchmark study on the energy consumption of novel solvents for CO_2 capture. presented at *5th Trondheim CCS Conference*, June 2009, Trondheim, Norway.

Goff, G.S.; Rochelle, G.T., **2004**, Oxidative degradation of aqueous monoethanolamine in CO_2 capture controlled by the physical absorption of O_2. *Ind. Eng. Chem. Res.*, 43, 6400-6408.

References

Goff, G.S., **2005,** Oxidative degradation of aqueous monoethanolamine in CO_2 capture processes: iron and copper catalysis, inhibition, and O_2 mass transfer. *Ph.D. Dissertation*, University of Texas at Austin, Austin.

Górak, A., **2006**, *Fluid Separation* (Lecture Notes), Technical University of Dortmund.

Goto, K.; Okabea, H.; Shimizua, S.; Onodaa M.; Fujioka, Y., **2009**, Evaluation method of novel absorbents for CO_2 capture. *Energy Procedia*, 1, 1083-1089.

Goto, K; Chowdhury, F.A.; Okabe, H.; Shimizu, S.; Fujioka, Y., **2011**, Development of a low cost CO_2 capture system with a novel absorbent under the COCS project. *Energy Procedia*, 4, 253-258.

Hagewiesche, D.P.; Ashour, S.S.; Al-Ghawas, A.A.; Sandall O., **1995**, Absorption of carbon dioxide into aqueous blends of monoethanolamine and N-methyldiethanolamine. *Chem. Eng. Sci.*, 50(7), 1071-1079.

Hamborg, E.S.; Derks, P.W.J.; Elk, van E.P. and Versteeg, G.F., **2010**, Carbon dioxide removal by alkanolamines in aqueous organic solvents: A method for enhancing the desorption process. *Energy Procedia*, 4, 187-194.

Hansen C.M., **2000**, *Hansen Solubility Parameters*. CRC Press: Boca Raton.

Hildebrand, J. and Scott, R.L., **1962**, *Regular Solutions*. Prentice-Hall: Englewood Cliffs, NJ.

Hölemann, K. and Górak, A., **2006**, Absorption, In: *Fluidverfahrenstechnik II* Goedecke, R., Ed.,Wiley-VCH: Weinheim, pp. 799-906.

Horng, S.Y.; Li, M.H., **2002**, Kinetics of absorption of carbon dioxide into aqueous solutions of monoethanolamine and triethanolamine. *Ind. Eng. Chem. Res.*, 41, 257-266.

Hu, L., **2005**, Phase enhanced gas-liquid absorption method. *US Patent 6969418.*

Hu, L., **2009**a, CO_2 capture from flue gas by phase transitional absorption. DOE Project Report, [online] http://www.netl.doe.gov/technologies/coalpower/ewr/co2/pubs/Phase%20Transitional%20AbsorptionNT42488FinalReport.pdf (accessed 31 August 2013).

Hu, L., **2009**b, Phase transitional absorption method. *US Patent 7541011*.

Hu, L., **2010**a, Methods and systems for deacidizing gaseous mixtures. *US Patent 7718151*.

Hu, L., **2010**b, Post-Combustion CO_2 Capture for Existing PC Boilers by Self-concentrating Absorbent. presented in *NETL CO_2 Capture Technology Meeting*, September 2010, Pittsburgh, PA.

Hussain, K., **2012**, Flowsheet development of a post-combustion carbon capture process using thermomorphic biphasic solvents. *Master's Thesis*, Technical University of Dortmund.

Jacquin, M. **2010**, Absorbent solution based on N,N,N',N'-tetramethylhexane-1,6-diamine and on one particular amine comprising primary or secondary amine functional groups and process for removing acid compounds from a gaseous effluent. *Patent WO 2010/012883*.

IPCC, **2005**, *IPCC Special Report on Carbon Dioxide Capture And Storage*, Cambridge University Press.

Ismael, M.; Sahnoun, R.; Suzuki, A. et al., **2009**, A DFT study on the carbamates formation through the absorption of CO_2 by AMP. *Int. J. Greenhouse Gas Control*, 3(5), 612-616.

Jou, F-Y; Mather, A.E.; Otto F.D., **1995**, The solubility of CO_2 in a 30 mass percent monoethanolamine solution. *Can. J. Chem. Eng*., 73, 140.

References

Kennard, M. L.; Meisen, A. **1985**, Mechanisms and kinetics of diethanolamine degradation. *Ind. Eng. Chem. Fundam.*, 24, 129-140.

Kennard, M. L.; Meisen, A., **1980**, Control DEA degradation. *Hydrocarbon Process., Int. Ed.*, 59, 103-106.

Kim, J.H.; Lee, J.H.; Lee, I.Y.; Jang, K.R. and Shim, J.G., **2011**, Performance evaluation of newly developed absorbents for CO_2 capture. *Energy Procedia*, 4, 81-84.

Klamt, A.; Eckert F.; Arlt, W., **2010**, COSMO-RS: An alternative to simulation for calculating thermodynamic properties of liquid mixtures. *Annual Review of Chemical and Biomolecular Engineering*, 1, 101-122.

Knudsen, J.N.; Vilhelmsen, P.J.; Jensen, J.N.; Biede, O., **2007**, First year operating experience with a 1 t/h CO_2 absorption pilot plant at Esbjerg coal-fired power plant. *Proceedings of the 6th European Congress of Chemical Engineering*, Copenhagen, September 2007.

Kohl, A.L. and Nielsen, R.B., **1997**, *Gas Purification*, 5th ed., Gulf Publishing Co.: Houston, Texas.

Laakkonen, M.; Moilanen, P.; Aittamaa, J., **2005**, Local bubble size distributions in agitated vessels, *Chem. Eng. J.*, 106: 133–143.

Lepaumier, H.; Grimstvedt, A.; Vernstad, K.; Zahlsen, K.; Svendsen, H.F., **2011**, Degradation of MMEA at absorber and stripper conditions. *Chem. Eng. Sci.*, 66(15), 3491-3498.

Lepaumier, H.; Martin, S.; Picq, D.; Delfort, B.; Carrette, P.L., **2010**, New amines for CO_2 capture. III. Effect of alkyl chain length between amine functions on polyamines degradation. *Ind. Eng. Chem. Res.*, 49 (10), 4553-4560.

Lepaumier, H.; Picq, D.; Carrette, P.L., **2009**a, New amines for CO_2 capture. I. Mechanisms of Amine degradation in the presence of CO_2. *Ind. Eng. Chem. Res.*, 48(20), 9061-9067.

Lepaumier, H.; Picq, D.; Carrette, P.L., **2009**b, New amines for CO_2 capture. II. Oxidative degradation mechanisms. *Ind. Eng. Chem. Res.*, 48(20): 9068-9075.

MacDowell, N.; Florin, N.; Buchard, A. et al., **2010**, An overview of CO_2 capture technologies. *Energy Environ. Sci.*, 3, 1645-1669.

Maćkowiak, J., **2003**, Fluiddynamik von Füllkörpern und Packungen - Grundlagen der Kolonnenauslegung, 2nd ed., Springer Verlag: Berlin.

Mandal, B.P.; Biswas, A.K.; Bandyopadhyay, S.S., **2003**, Absorption of carbon dioxide into aqueous blends of 2-amino-2-methyl-1-propanol and diethanolamine. *Chem. Eng. Sci.*, 58, 4137-4144.

Mandal, B.P.; Guha,M.; Biswas, A.K.; Bandyopadhyay, S.S., **2001**, Removal of carbon dioxide by absorption in mixed amines: modeling of absorption in aqueous MDEA/MEA and AMP/MEA solutions. *Chem. Eng. Sci.*, 56, 6217-6224.

Mangalapally, H.P.; Hasse, H., **2011**, Pilot plant experiments for post combustion carbon dioxide capture by reactive absorption with novel solvents. *Energy Procedia*, 4, 1-8.

Maruyama, S.; Kimura, T., **2000**, A molecular dynamics simulation of a bubble nucleation on solid surface. *Int. J. Heat & Technology*, 18, 69-74.

McMurry, J., **1999**, *Organic chemistry*, Brooks/Cole, Pacific Grove, California.

Meisen, A.; Kennard, M. L., **1982**, DEA degradation mechanism. *Hydrocarbon Process., Int. Ed.*, 61, 105-108.

References

Meldon, J.H., **2011**, Amine screening for flue gas CO_2 capture at coal-fired power plants: Should the heat of desorption be high, low or in between? *Current Opinion in Chemical Engineering*, 1, 55-63.

Misch, R., **2008**, Intensivierung der CO_2-Desorption aus lipophilen Aminlösungen durch extraktive Regeneration. *Studienabeit*, Technical University of Dortmund.

Misch, R., **2010**, Study on CO_2 absorption into lipophilic amine solution and packing wettability tests. *Diploma Thesis*, Technical University of Dortmund.

Monteiro, J.G.M.; Pinto, D.D.D.; Svendsen, H.F., **2011**, Phase change solvents. presented in *EU-China Workshop on Innovative CCS Technologies*, September 2011, Beijing.

Müller, E.; Berger, R.; Blass, E.; Sluyts, D.; Pfennig, A., **2005**, Liquid-Liquid Extraction. *Ullmann's Encyclopedia of Industrial Chemistry*, 7th ed., Wiley-VCH Verlag GmbH.

Nguyen, T.; Hilliard, M.; Rochelle, G.T., **2010**, Amine volatility in CO_2 capture. *Int. J. Greenhouse Gas Control*, 4: 707-715.

Nguyen, T.; Hilliard, M.; Rochelle, G.T., **2011**, Volatility of aqueous amines in CO_2 capture. *Energy Procedia*, 4, 1624-1630.

NIST Chemistry WebBook, [online] http://webbook.nist.gov/chemistry/ (accessed 31 August 2013).

Nwani, K., **2009**, Experimental study of the solvent losses in the amine-based carbon dioxide absorption processes. *Diploma Thesis*, Technical University of Dortmund.

Notz, R.; Asprion, N.; Clausen, I.; Hasse, H., **2007**, Selection and pilot plant tests of new absorbents for post-combustion carbon dioxide capture. *Chem. Eng. Res. Des.*, 85(4), 510-515.

Oexmann, J.; Hensel, C.; Kather, A., **2008**, Post-combustion CO_2 capture from coal-fired power plants: Preliminary evaluation of an integrated chemical absorption process with piperazine-promoted potassium carbonate. *Int. J. Greenhouse Gas Control*, 2(4), 539-552.

Oexmann, J.; Kather, A., **2010**, Minimising the regeneration heat duty of post-combustion CO_2 capture by wet chemical absorption: The misguided focus on low heat of absorption solvents. *Int. J. Greenhouse Gas Control*, 4(1), 36-43.

Phan, L.; Andreatta, J.R.; Horvey, L.K. et al., **2008**, Switchable-polarity solvents prepared with a single liquid component. *J. Org. Chem.*, 73, 127-132.

Pimentel, G.C., **1963**, *Chemistry: An Experimental Science*, 4th ed., W.H. Freeman & Co.: San Francisco.

Polderman, L.D.; Dillon, C. P.; Steele, A. B., **1955**, Why monoethanolamine solution breaks down in gas-treating service. *Oil Gas J.*, 54, 180-183.

Puxty, G.; Allport, A.; Attalla, M., **2009**, Vapour liquid equilibria data for a range of new carbon dioxide absorbents. *Energy Procedia*, 1, 941-947.

Rao, A.B.; Rubin, E.S., **2002**, A technical, economic, and environmental assessment of amine-based CO_2 capture technology for power plant greenhouse gas control. *Environ. Sci. Technol.*, 36(20), 4467-4475.

Raynal, L., Alix, P., Bouilon, P., et al., **2011**a, The DMX^TM process: an original solution for lowering the cost of post-combustion carbon capture, *Energy Procedia*, 4, 779-786.

References

Raynal, L.; Bouillon, P.; Gomez, A.; Broutin, P., **2011**b, From MEA to demixing solvents and future steps, a roadmap for lowering the cost of post-combustion carbon capture. *Chem. Eng. J.*, 171(3), 742-752.

Reichardt C., **2003**, *Solvents and Solvent Effects in Organic Chemistry*, 3nd ed., Wiley-VCH Verlag GmbH: Weinheim.

Reidenbach, F., **1994**, ASM Handbook, Vol. 5, Surface Engineering, 10th ed., ASM International: Materials Park, OH.

Riemer, P., **1996**, Greenhouse Gas Mitigation Technologies, an overview of the co2 capture, storage and future. *Energy Convers. Mgmt.*, 37(6-8), 665-670.

Rochelle, G.T., **2009**, Amine scrubbing for CO_2 capture. *Science*, 325: 1652-1654.

Rochelle, G.T.; Chen, E.; Freeman, S.; van Wagener, D.; Xu, Q.; Voice, A., **2011**a, Aqueous piperazine as the new standard for CO_2 capture technology. *Chem. Eng. J.*, 171(3), 725–733.

Rochelle, G.T.; Freeman, S.; Voice, A.; Closmann, F., **2011**b, Degradation of amines in CO_2 capture, presented at 6th Trondheim CCS conference, June 2011, Trondheim.

Rochelle, G.T., **2012**, Thermal degradation of amines for CO_2 capture. *Current Opinion in Chemical Engineering*, 1(2), 183–190.

Roero, C. **2006**, Contact angle measurements of sessile drops deformed by a DC electric field. High Voltage Laboratory, ETH, Zürich, Switzerland.

Rolker, J.; Arlt, W., **2006**, Abtrennung von Kohlendioxid aus Rauchgasen mittels Absorption. *Chemie Ingenieur Technik*, 78(4), 416-424.

Qiao, Y., **2011**, Development of thermomorphic biphasic solvent for CO_2 absorption with intensified regeneration. *Master's Thesis*, Technical University of Dortmund.

Salmon, S.; House, A.; Freeman, C.; et al., **2012**, Lab-scale assessment of a post-combustion carbon dioxide capture process enabled by a combination of enzymes and ultrasonics. presented in 29th International Pittsburgh Coal Conference, October 2012, Pittsburgh.

Sartori, G.; Ho, W.S.; Savage, D.W.; Chludzinski, G.R.; Wiechert, S., **1987**, Sterically-hindered amines for acid-gas absorption. *Sep. Purif. Meth.*, 16, 171-200.

Sexton, A.; Rochelle, G., T., **2006**, Oxidation products of amines in CO_2 capture. presented in 8th International *Conference* on Greenhouse Gas Control Technologies, June 2006, Trondheim.

Sexton, A.; Rochelle, G.T., **2009**, Catalysts and inhibitors for MEA oxidation. *Energy Procedia*, 1, 1179-1185.

Sexton, A., **2008,** Amine Oxidization in CO_2 Capture Processes, *Ph.D. Dissertation*, University of Texas, Austin.

Shoeld, M., **1934**. Purification and separation of gaseous mixtures. *US Patent* 1971798.

Singh, P.; Versteeg, G.F., **2008**, Structure and activity relationships for CO_2 regeneration from aqueous amine-based absorbents. *Process Safety and Environmental Protection*, 86(5), 347-359.

Singh, P.; Niederer, J.P.M.; Versteeg, G.F., **2007**, Structure and activity relationships for amine-based CO_2 absorbents – I. *Int. J. Greenhouse Gas Control*, 1(1), 5-10.

Singh, P.; Niederer, J.P.M.; Versteeg, G.F., **2009**, Structure and activity relationships for amine-based CO_2 absorbents – II. *Chem. Eng. Res. Des.*, 87(2), 135-144.

References

Singh, P.; Brilman, D.W.F.; Groeneveld, M.J., **2011**, Evaluation of CO_2 solubility in potential aqueous amine-based solvents at low CO_2 partial pressure. *Int. J. Greenhouse Gas Control*, 5(1), 61-68.

Steeneveldt, R.; Berger, B.; Torp, T.A., **2006**, CO_2 Capture and Storage Closing the Knowledge-Doing Gap, *Chem. Eng. Res. Des*., 84(A9), 739-763.

Stewart, E.J.; Lanning, R.A., **1994**, Reduce amine plant solvent loss. *Hydrocarbon Processing*, 73, 67-81.

Stolten, D. and Scherer, V. ed., **2011**, *Efficient Carbon Capture for Coal Power Plants*. Wiley-VCH Verlag: Weinheim.

Strazisar, B.R.; Anderson, R.R.; White, C.M., **2003**, Degradation pathways for monoethanolamine in a CO_2 capture facility. *Energy & Fuels*, 17(4), 1034-1039.

Straelen, van J.; Geuzebroek, F., **2011**, The thermodynamic minimum regeneration energy required for post-combustion CO_2 capture. *Energy Procedia*, 4, 1500-1507.

Supap, T.; Idem, R.; Tontiwachwuthikul, P.; Saiwan, C., **2011**, Investigation of degradation inhibitors on CO_2 capture process. *Energy Procedia*, 4, 583-590.

Supap, T.; Idem, R.; Veawab, A.; Aroonwilas, A.; Tontiwachwuthikul, P.; Chakma, A.; Brian D.; Kybett, B.D., **2001**, Kinetics of the oxidative degradation of aqueous monoethanolamine in a flue gas treating unit. *Ind. Eng. Chem. Res.*, 40(16), 3445-3450.

Svendsen, H.F.; Hessen, E.T.; Mejdell, T., **2011**, Carbon dioxide capture by absorption; challenges and possibilities. *Chem. Eng. J.*, 171 (3), 718-724.

Tan, Y., **2010**. Study of CO_2 absorption into thermomorphic lipophilic amine solvents. *Ph.D. Dissertation*, Technical University of Dortmund.

Telikapalli, V.; Kozak, F.; Francois, J., et al., **2011**, CCS with the Alstom chilled ammonia process development program – field pilot results. *Energy Procedia*, 4, 273-281.

Thitakamol, B.; Veawab, A., **2008**, Foaming behavior in CO_2 absorption process using aqueous solutions of single and blended alkanolamines. *Ind. Eng. Chem. Res.*, 47: 216-225.

Thitakamol, B.; Veawab, A., **2009**, Foaming model for CO_2 absorption process using aqueous monoethanolamine solutions. *Colloids and Surfaces A: Physicochem. Eng. Aspects*, 349, 125-136.

Thome, J.R., **2010**, Wolverine engineering data book III, Chapter 9. Boiling heat transfer on external surface, [online] http://www.wlv.com/products/databook/db3/DataBookIII.pdf (accessed 31 August 2013).

Tönnies, I.; Garcia, H.; Mangalapally, H.P. et al., **2011**, CO_2-Abtrennung aus Kraftwerksabgasen auf dem Weg von der Forschung und Entwicklung zur industriellen Anwendung. *Chemie Ingenieur Technik*, 83(7), 1005–1015.

Tsai, R.E.; Seibert, A.F.; Eldridge, R.B.; Rochelle, G.T., **2009**, Influence of viscosity and surface tension on the effective mass transfer area of structured packing. *Energy Procedia*, 1, 1197-1204.

Vázquez, G.; Alvarez, E.; Navaza, J.M.; Rendo, R.; Romero, E., **1997**, Surface Tension of Binary Mixtures of Water + Monoethanolamine and Water + 2-Amino-2-methyl-1-propanol and Tertiary Mixtures of These Amines with Water from 25 °C to 50 °C. *J. Chem. Eng. Data*, *42* (1), 57–59.

119

References

Veldman, R., **2000**, Alkanolamine solution corrosion mechanisms and inhibition from heat stable salts and CO_2. *Proceedings of NACE International - CORROSION 2000*, Conference Paper 00496, March 2000, Orlando, FL.

Versteeg, G.F.; Kuipers, J.A.M.; Beckum van, F.P.H.; Swaaij van, W.P.M., **1990**, Mass transfer with complex reversible chemical reactions. II: Parallel reversible chemical reactions. *Chem. Eng. Sci.*, 45(1), 183-197.

Walzel, P., **2006**, *Particle Technology* (Lecture Notes), Technical University of Dortmund.

Wang, M.; Lawal, A.; Stephenson, P.; Sidders, J.; Ramshaw, C., **2011**, Post-combustion CO_2 capture with chemical absorption: A state-of-the-art review. *Chem. Eng. Res. Des.*, 89(9), 1609–1624.

Wang, W., **2012**, Study on degradation of lipophilic amine solvents in post-combustion carbon capture process. *Master's Thesis*, Technical University of Dortmund.

Weiland, R.H.; Dingman, J.C.; Cronin, D.B.; Browning, G.J., **1998**, Density and viscosity of some partially carbonated aqueous. *J. Chem. Eng. Data*, 43, 378-382.

Woertz, B.B., **1966**, Process for removing acidic constituents from gaseous mixtures. *US Patent* 3266220 A1.

Yalkowsky, S.H., **1999**, *Solubility and Solubilization in Aqueous Media*, American Chemical Society: Washington, DC.

Yamada, H.; Matsuzaki, Y.; Higashii, T.; Kazama, S. **2011**, *J. Phys. Chem. A*. 115(14), 3079-3086.

Zhang, J., **2008**, Study of the influence of lipophilic amine structures on their CO_2 absorption properties with thermomorphic auto-extractive regeneration. *Master's Thesis*, Technical University of Dortmund.

Zhang, J.; Agar, D.W.; Zhang, X.; Geuzebroek, F., **2011**a, CO_2 Absorption in biphasic solvents with enhanced low temperature solvent regeneration. *Energy Procedia*, 4, 67-74.

Zhang, J.; Nwani, O.; Tan, Y.; Agar. D.W., **2011**b, Carbon dioxide absorption into biphasic amine solvent with solvent loss reduction. *Chem. Eng. Res. Des*., 89(8), 1190-1196.

Zhang, J.; Misch, R.; Tan, Y.; Agar. D.W., **2011**c, Novel biphasic amine solvent for CO_2 absorption and low temperature extractive regeneration. *Chem. Eng. & Technol.*, 34(9), 1481-1489.

Zhang, J.; Qiao, Y.; Agar, D.W., **2012**a, Improvement of lipophilic-amine-based thermomorphic biphasic solvent for energy-efficient carbon capture. *Energy Procedia*, 23, 92-101.

Zhang, J., Qiao, Y., Agar, D.W., **2012**b, Intensification of low temperature thermomorphic biphasic amine solvent regeneration for CO_2 capture, *Chem. Eng. Res. Des*., 90, 743-749.

Zhang, J., Qiao, Y., Wang,W., Misch, R., Hussain, K., Agar, D.W., **2013**, Development of an energy-efficient CO_2 capture process using thermomorphic biphasic solvents. *Energy Procedia*, 37, 1254-1261.

Zhang, X., **2007**. Studies on multiphase CO_2 capture systems, *Ph.D. Dissertation*, Technical University of Dortmund, VDI Verlag, Düsseldorf.

Zlokarnik, M., **2005**, *Ullmann's Encyclopedia of Industrial Chemistry: String*, Wiley-VCH, Weinheim.

Appendix

A List of screened amines

All the screened lipophilic amines and benchmark amines are listed in the following tables.
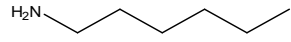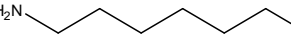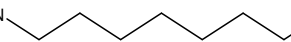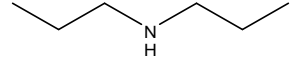
Table 34. List of chain amines
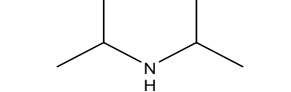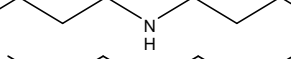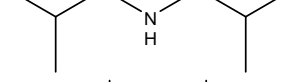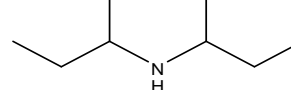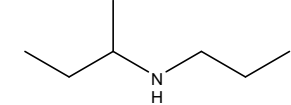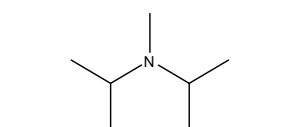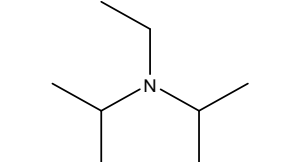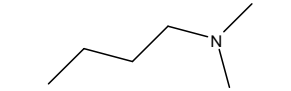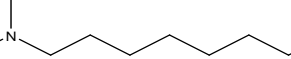
Chemical	Abbr.	CAS	Structure	Supplier
Hexylamine	HA	111-26-2		Merck
Heptylamine	HpA	111-68-2		Acros
Octylamine	OtA	111-86-4		Merck
Di-n-propylamine	DPA	142-84-7		Fluka
Diisopropylamine	DIPA	108-18-9		Merck
Di-n-butylamine	DBA	111-92-2		Merck
Diisobutylamine	DIBA	110-96-3		Acros
Di-*sec*-butylamine	DsBA (B1)	626-23-3		Aldrich
N-*sec*-Butyl-n-propylamine	SBPA	39190-67-5		ABCR
N,N-Diisopropyl methylamine	DIMA	10342-97-9		Fluka
N,N-Diisopropyl ethylamine	DIEA	7087-68-5		Acros
N,N-Dimethyl butylamine	DMBA	927-62-8		Fluka
N,N-Dimethyl octylamine	DMOA	7378-99-6		Acros

Table 35. List of cycloalkylamines
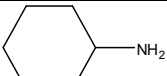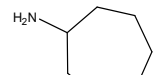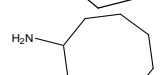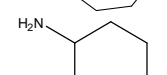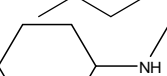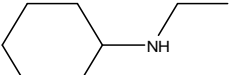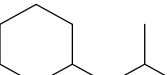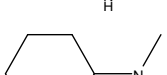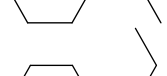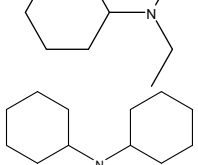
Chemical	Abbr.	CAS	Structure	Supplier
Cyclohexylamine	CHA	108-91-8		Merck
Cycloheptylamine	CHpA	5452-35-7		Fluka
Cyclooctylamine	COA	5452-37-9		Aldrich
2-Methylcyclohexyl amine	2MCA	7003-32-9		Fluka
N-Methylcyclohexyl amine	MCA (A1)	100-60-7		Acros
N-Ethylcyclohexyl amine	ECA	5459-93-8		ABCR
N-Isopropylcyclo hexylamine	IPCA	1195-42-2		Fluka
N,N-Dimethylcyclo hexylamine	DMCA	98-94-2		Merck
N,N-Diethylcyclo hexylamine	DECA	91-65-6		ABCR
Dicyclohexylamine	DCA	101-83-7		Acros

Table 36. List of aromatic amines
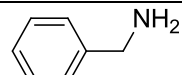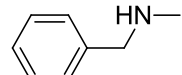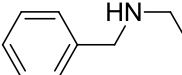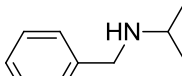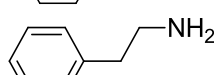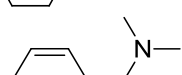
Chemical	Abbr.	CAS	Structure	Supplier
Benzylamine	BzA	100-46-9		Merck
N-Methylbenzyl amine	MBzA	103-67-3		Merck
N-Ethylbenzylamine	EBzA	14321-27-8		Merck
N-Isopropylbenzyl amine	IPBzA	102-97-6		Merck
Phenylethylamine	PhEA	64-04-0		Aldrich
N,N-Dimethyl benzylamine	DMBzA	103-83-3		Merck

Table 37. List of cyclic amines

Chemical	Abbr.	CAS	Structure	Supplier
2,6-Dimethylpiperidine	2,6-DMPD	504-03-0		Aldrich
3,5-Dimethylpiperidine	3,5-DMPD	35794-11-7		Acros
2-Methylpiperidine	2MPD	109-05-7		Aldrich
2-Ethylpiperidine	2EPD	1484-80-6		Aldrich
2,2,6,6-Tetramethyl piperidine	TMPD	768-66-1		Aldrich
N-Methyl piperidine	MPD	626-67-5		Acros
N-Ethyl piperidine	EPD	766-09-6		Fluka

Table 38. List of other amines

| Chemical	Abbr.	CAS	Structure	Supplier
Monoethanolamine	MEA	141-43-5		Merck
N-Methyldiethanolamine	MDEA	105-59-9		Merck
2-Amino-2-methyl-1-propanol	AMP	124-68-5		Merck
2-Amino-2-methyl-1,3-Propandiol	AMPD	115-69-5		Merck
N,N,N´,N´-Tetramethyl-1,6-hexane-diamine	TMHDA	111-18-2		Aldrich
N-Methylmorpholine	MMP	109-02-4		Merck
N,N-dimethyl-1,3-propyl-diamine	DMPDA	109-55-7		Fluka
Piperazine	PZ	110-85-0		Merck

B   Detailed experimental setups for CO_2 absorption and desorption

B.1   Test tube screening rig

The screening experiment was initially carried out in test tubes (Schott GL-18) with 18 mm O.D. and 180 mm length containing ≈6 mL aqueous amine solutions at varying concentrations from 0.9 to 4.2 M (see Figure 88). 1/16 inch PTFE tubing with 1 mm I.D. and 240 mm length were used as gas inlet pipe through the rubber septum.

Absorption was conducted in a water bath at 25 °C with CO_2 gas flow rate at 20 mL/min, saturated with water vapour, under atmospheric pressure. The weight of the test tube was measured every 5 min to observe the amount of absorbed CO_2, until the reaction was completely in equilibrium. The final CO_2 loading was determined by the barium chloride method with titration (Jou et al., 1995).

Desorption was carried out by heating in the thermal oil bath, regulated with a thermostat (HAAKE F3), stepwise from 40 to 90 °C with internal of 10 °C. In order to limit the effect of vaporisation, cotton sponge was applied as a demister for condensing water and volatile amine vapours. Magnetic stirrers were laid into each test tube to intensify CO_2 release and the oil bath to homogenise the temperature in the heating system. The weight was also measured stepwise to determine the mass of CO_2 desorbed.
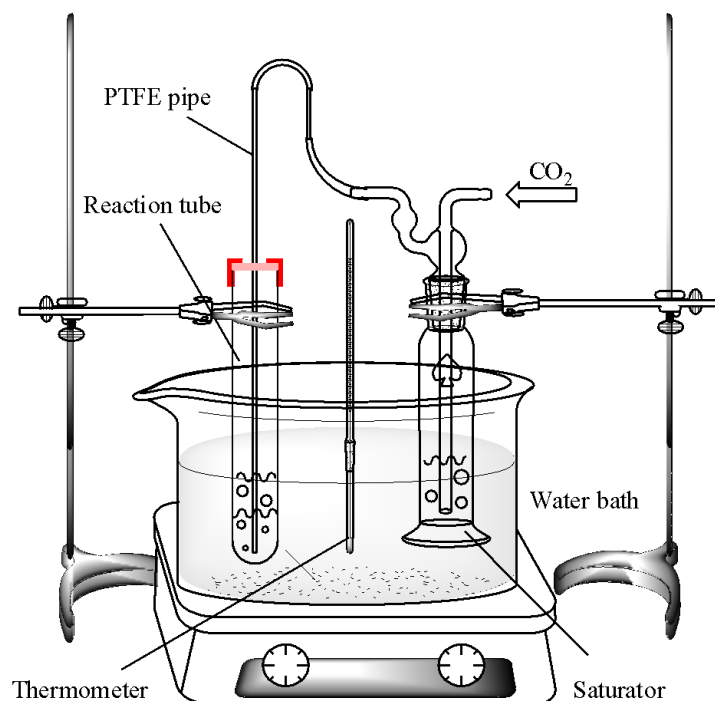
Figure 88. Experimental set-up for preliminary amine screening with a test tube

124

B.2   Bubble column screening rig

The absorption experiments for solvents selection were conducted in a 100 mL glass bubble column containing 40 mL of the aqueous amine solution at 40 °C (see Figure 89). Various amines with concentrations between 3-5 M and CO_2 partial pressures from 4 to 100 kPa were employed over contact times of 2-5 hours, to ensure that equilibrium was achieved. Desorptions were initially carried out by N_2 stripping and afterwards by magnetic agitation with PTFE coated round stir bar (30 mm length and 9 mm diameter) at 250-1000 rpm between 70-80 °C only in excess of the phase separation temperature of the corresponding solvent while N_2 was only used as a reference gas for online gas chromatography (GC) analysis. Both the feed and reference gas flows were saturated with water in order to make up the vaporisation loss and regulated by mass flow controllers (Bronkhorst EL-FLOW) so as to be constant in the absorption and desorption tests. During experiments, the outlet gas was monitored online by GC HP 6890 with GS-GasPro capillary column 30.0 m × 320 μm at an oven temperature 35 °C. After the reaction had been completed, the CO_2 loading was ascertained by the barium chloride method, total amine concentration was determined by acid-base titration and the blended amine compositions were determined by GC analysis with a J&W CP-Volamine capillary column 60.0 m × 320 μm and programmed oven temperatures from 60 to 260 °C. Figure 90 presents an example of good separation performance for CO_2, water and amines determination using GC analysis with a thermal conductivity detector (TCD).
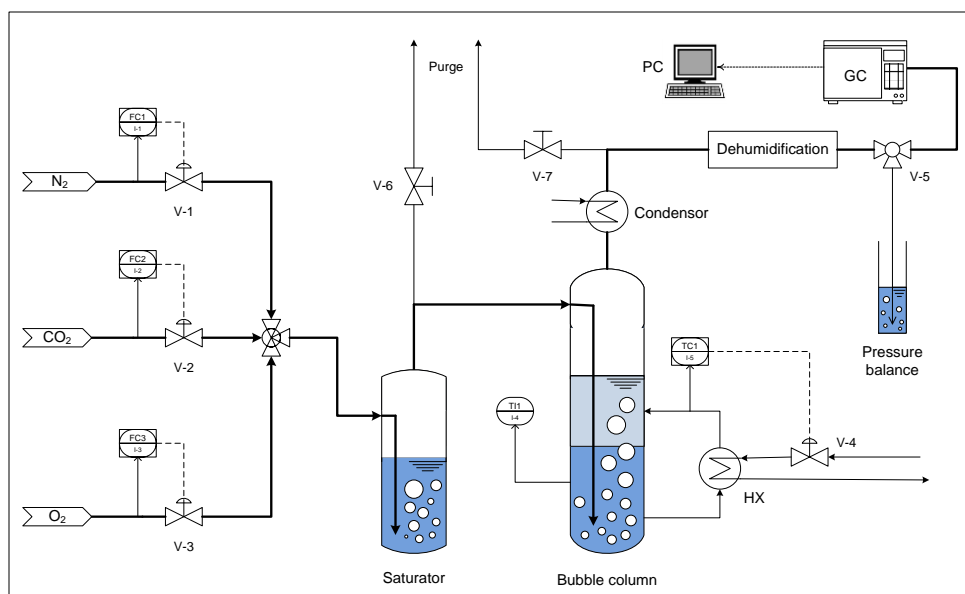
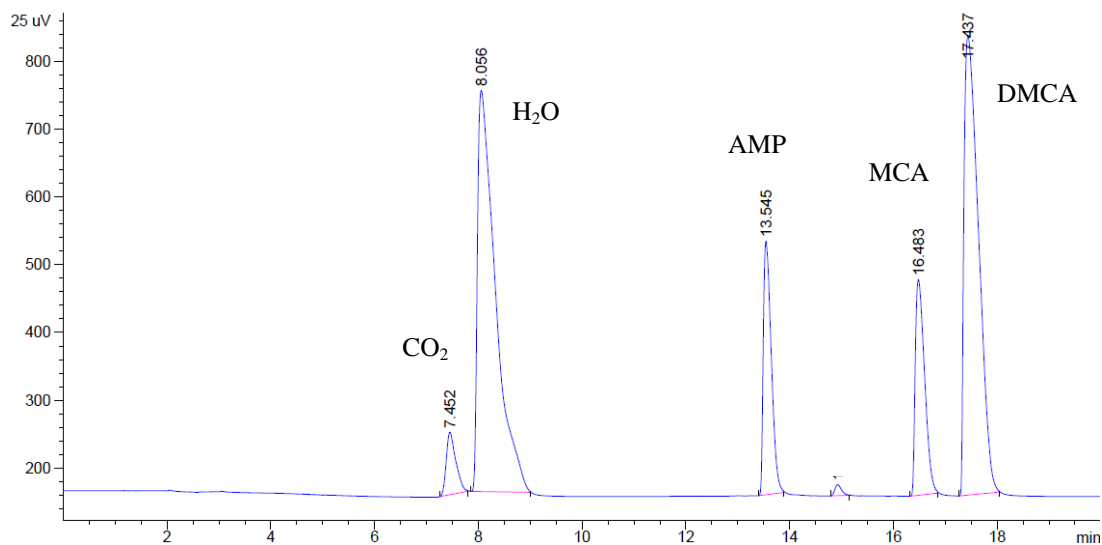**Figure 89**. Experimental set-up for solvent screening with a bubble column

Figure 90. GC chromatogram of a CO_2 rich amine solution

B.3 *Regeneration intensification experiments*

The CO_2 loaded amine standard solutions for regeneration experiments with intensified methods such as extraction, agitation, nucleation, ultrasound, etc., were prepared in a 500 mL glass bubble column with ca. 320 mL aqueous amine solutions and a gas flow comprising 15 mol% CO_2 balanced with N_2 at 30 °C. The feed gas was saturated with water vapour to prevent losses in the bubble column and the flow rate was regulated by mass flow controllers (Bronkhorst EL-FLOW) in order to be constant in the absorption and regeneration tests. A chilled-water condenser was employed to minimise the vaporisation loss of volatile lipophilic amines. Lipophilic amines with concentrations of 3-5 M were employed over contact times between 3-5 hours, to ensure that equilibrium was achieved.

Regeneration was carried out by nitrogen gas stripping or other intensive means in a 100 mL vessel with 50 mL CO_2 loaded solution at 70-85 °C (see Figure 91). For the intensification techniques, nitrogen was only used as a carrier gas and as a reference for online GC monitoring of the outlet gas after desorption. Agitation was carried out on a heating plate stirrer (RCT basic IKAMAG) with a magnetic stirring bar, laid at the bottom of the cylindrical glass reactor to agitate the loaded amine solution for accelerating the CO_2 desorption. The bath temperature was measured with a Pt1000 sensor and regulated by an integrated temperature control programme. After the ab/desorption had been completed, liquid samples were collected and analysed by the

same methods as presented in Appendix B.2 for ascertaining the CO_2 loading, the total amine concentration and the blended amine compositions.
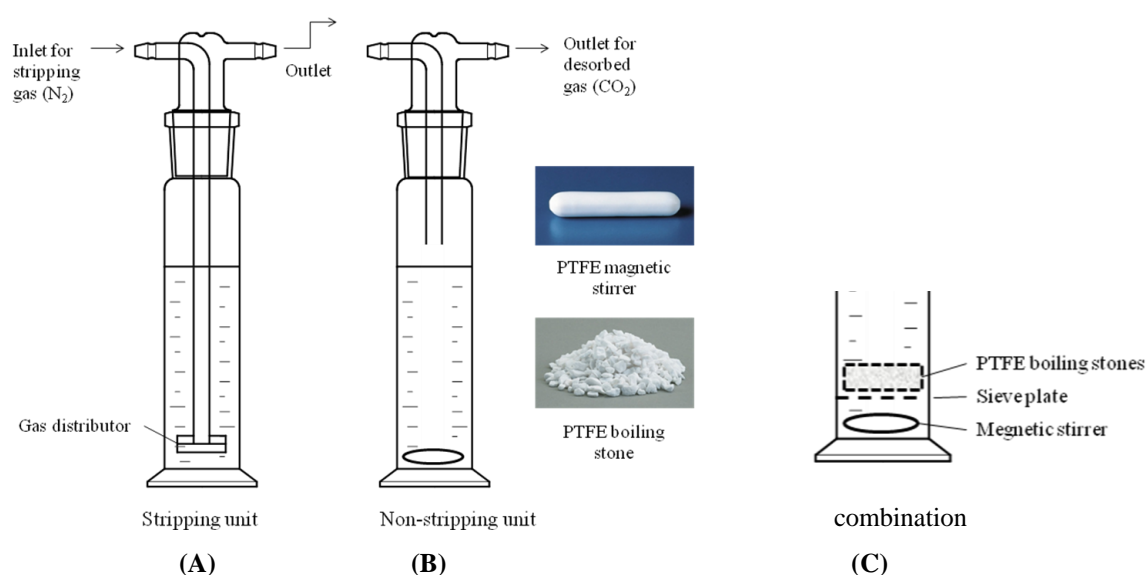
Figure 91. Sketch of regeneration reactors for gas stripping, nucleation and agitation

Nucleation was also performed in a 100 mL cylindrical glass reactor with different materials and various porous sizes, for instance, silica beads, aluminium oxide spheres, active carbon spheres, zeolite chips, PTFE boiling stones, ceramic Raschig rings, ceramic Berl-Saddle, molecular sieves, cotton fibre and wood fibre. Solid particles with various materials, shapes, sizes and diameter of pore openings (DPO) used for nucleation in the desorption are listed in Table 39. The same liquid solvent analysis method was adopted as before.

Table 39. Specification of solid particles

Particle	Specification	Supplier
Silica beads	0.2-0.5 mm with DPO 60 Å	Merck
Al_2O_3 spheres	≈3 mm	Degussa
Active carbon spheres	≈2.5 mm and ≈5 mm	Merck
Zeolite chips	≈4 mm	Merck
Polytetrafluoroethylene (PTFE) boiling stones	≈4 mm	Bola
Ceramic Raschig rings	5 mm	N/A
Ceramic Berl-Saddles	5 mm	N/A
SYLOBEAD molecular sieves	grade 562c, 3.2 mm and grade 564, 1.6 mm with DPO 3 Å	Grace
Cotton and wood fibres	N/A	N/A

The ultrasonic desorption was initially carried out in an Economic Ultrasonic Bath (Elmasonic E) with a constant wave frequency 37 kHz and the electronic energy consumption was measured by an ammeter. During desorption, a 20 mL test tube containing 10 mL of CO_2 loaded solution was immerse into the ultrasonic bath and maintained the solution level below the surface of the bath. Hot water at 70-80 °C was circulated in the ultrasonic bath to heat the amine solution. The same weight method as described in Appendix B.1 was used to determine the amount of desorbed CO_2.

A bench-scale ultrasonic-assisted desorption unit with batch systems as well as continuous flow devices was also employed for further investigation in the Brandenburg University of Technology Cottbus. This unit comprises an ultrasonic tube reactor and an ultrasonic bath (BANDELIN electronic GmbH). The cumulative volume of desorbed CO_2 was measured by a Remus 3 G1.6 gas meter (Contador). The temperature profiles were obtained using Pt100 sensors in connection with a data logger (Combilog) and the CO_2 loadings in lean and rich solvents were determined by the density measurement. The detailed experimental setup was described in Gantert and Möller's paper (2011).

B.4 Extraction reactor

The loaded lipophilic amine standard solutions for extractive regeneration tests were prepared in a 500 mL glass bubble column at amine concentrations between 3-4 M and a total gas supply of 300 mL/min, comprising 30 mol% CO_2 balanced with N_2 at 30 °C. The preloading of the amine solution is completed when the component of the outlet gas online measured by GC is constant. The screening tests of inert solvents for extractive regeneration were carried out in a 150 mL double-wall glass reactor and the temperature of the extraction was controlled using an external thermostat (HAAKE F3). During the extraction process, the solution was agitated by an externally driven magnetic stirrer (PTFE-coated cross-shaped bars) operated at a constant speed 600 rpm. 50 mL CO_2 loaded solution were extracted with the same volume of inert solvent for 2-4 hours. The extractor was connected to a reflux condenser operated at 15 °C to minimise the volatility losses of inert solvent. The components in the organic and aqueous phases were determined by analysis of the liquid phase using GC. The experimental setup of the inert solvent screening unit is shown in Figure 92.
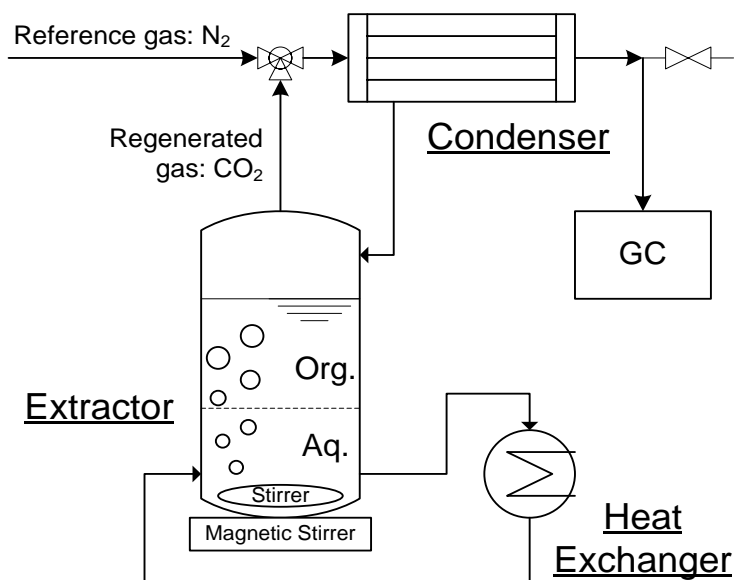
Figure 92. Experimental set-up for inert solvent screening

To improve the capture efficiency, three- and four-stage extractions were used for lipophilic amine regeneration. The experiment was carried out in the inert solvent screening unit. After a single stage extraction, the raffinate (aqueous phase) from the previous stage was separated from the extract (organic phase) and sent to the next stage. In each stage, the initial 75 mL of the CO_2 loaded solution was extracted with 75 mL or 25 mL of the corresponding inert solvent at 40 °C.

Table 40. List of inert hydrophobic solvent

Chemical	CAS	Structure	M_r (g/mol)	bp. (°C)
n-Pentane	109-66-0		72.15	36
Cyclopentane	287-92-3		70.10	49
n-Hexane	110-54-3		86.18	69
Cyclohexane	110-82-7		84.16	81
iso-Hexane	107-83-5		86.18	60

For minimising solvent vaporisation, pressurised extraction was applied for regeneration. It was conducted in a closed system at 3 (±0.2) bar and 50-70 °C. The liberated CO_2 was purged when the pressure in the extractor was in excess of 3.2 bar.

Agitation was also applied for intensifying mass transfer during extraction. The selected alkanes (purchased from Merck) used as inert hydrophobic solvents for extractive regeneration are listed in Table 40. For an easy separation of inert solvents from amines by distillation, the boiling points of the selected alkanes are all lower than 90 °C.
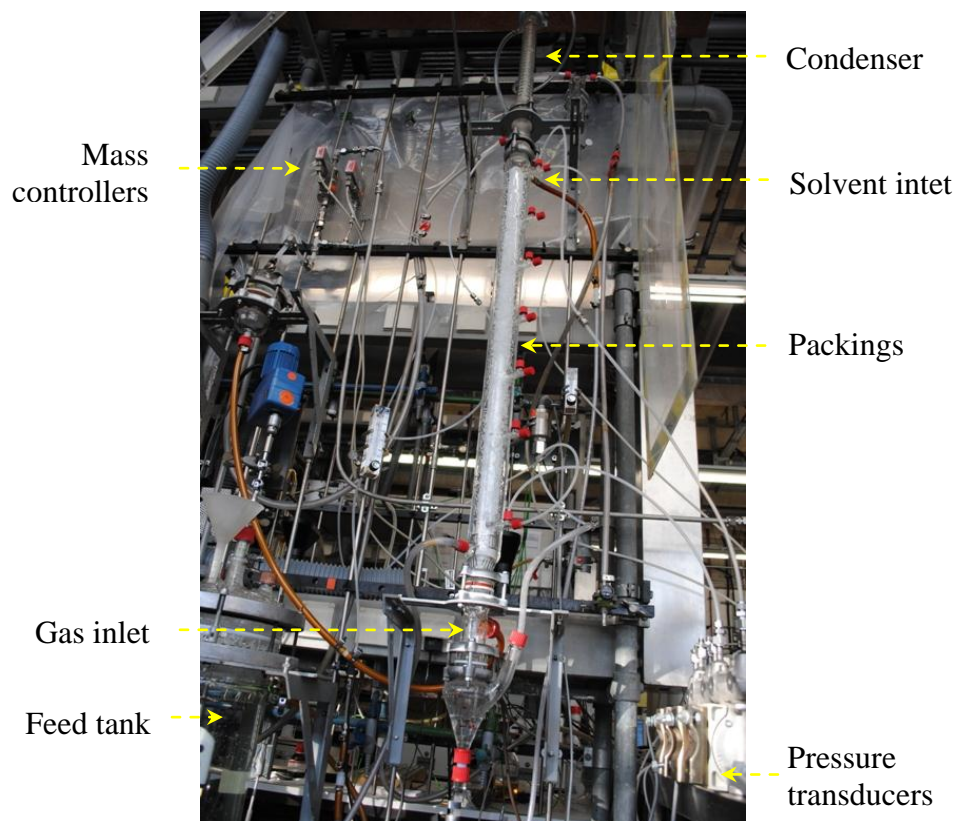
B.5 Bench-scale absorption column

The experiments were performed in a glass column of 0.04 m inner diameter and a packed height of 1 m at 30 °C and atmospheric pressure (see Figure 93). The packings mainly consisted of 5, 6 and 8 mm Raschig rings with varying materials such as ceramic, plastic and metal with the bed porosity of 0.36-0.88 (see Table 24).
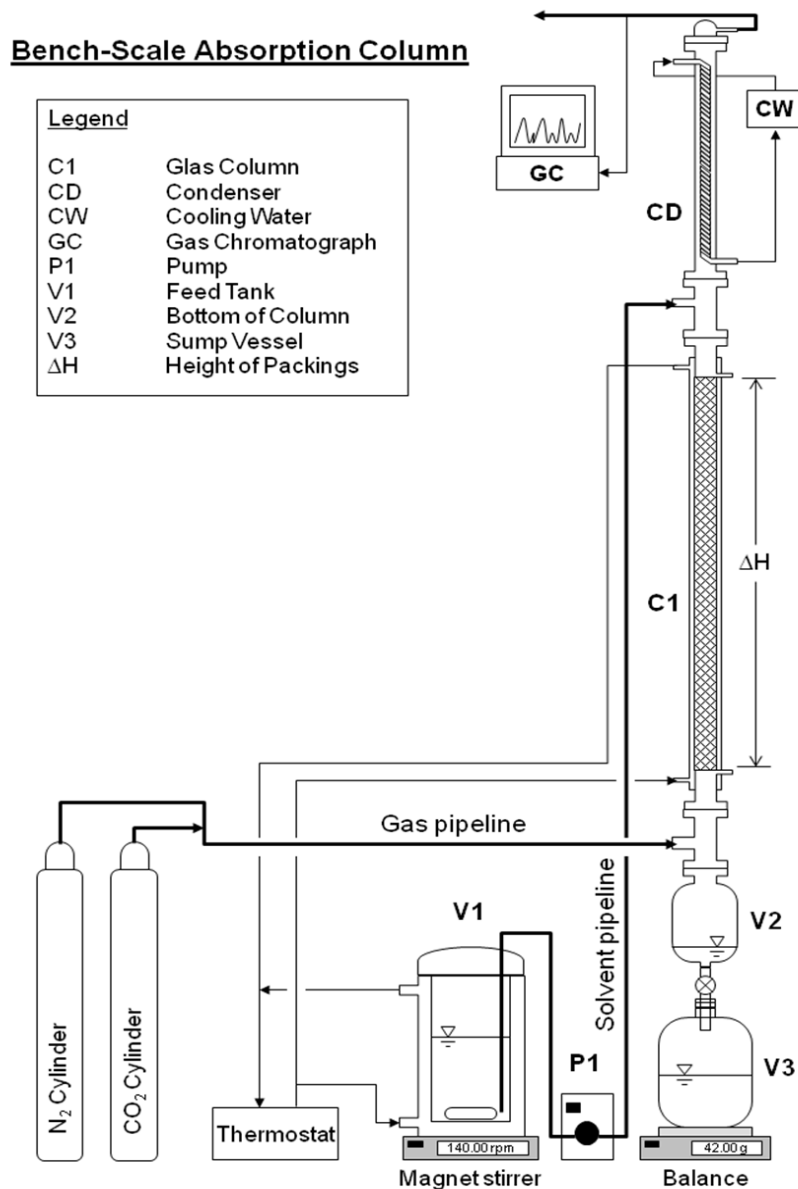
Figure 93. Experimental set-up of a bench-scale absorber

Figure 94. Bench-scale absorption column

Water, conventional 30 wt.% MEA ($\approx$ 5M), 5M MCA and 5.5 M blended DMCA+MCA+AMP (3:1:1.5) solutions were used as the liquid phase. Liquid surface tension was varied from 0.028 to 0.075 N/m for viscosity of 1-30 mPa·s. The gas and liquid mass flow rates applied ranged from 10 to 75 L/min (containing 15 mol% CO_2) and 60 to 200 mL/min, respectively. Gas flow rates were controlled by Bronkhorst EL-FLOW controllers and liquid flow rates were measured by Peltonturbine flowmeter (Flo-Sensor 101, McMillan). Liquid leaving the column outlet at the phase separator was collected and weighed on a balance (Sartorius 3862) to determine the dynamic liquid hold-up. The pressure drop across the packed bed was detected with differential pressure transducers (HBM PD1) connected at different positions between the top and the bottom of the column (see Figure 94).

The experimental data were collected by a system-design platform National Instruments LabVIEW 8.5 installed on a PC. Liquid samples from the bottom of column were taken at each run and were analysed by GC to check the amine concentration, CO_2 loading as well as the physiochemical properties presented in section 8.4. The treated gas was also monitored online by GC to observe the CO_2 removal ratio. The detailed analysis method has been elucidated in Appendix B.2.

## C   Influence of amine molecular structure on CO₂ absorption

The influence of amine molecular structure on absorption characteristics are illustrated in this section. The amines are classified according to the branch at the position of the carbon. Precipitation and salts formation are the most common but undesired phenomena found in the lipophilic amine solution during CO_2 absorption.
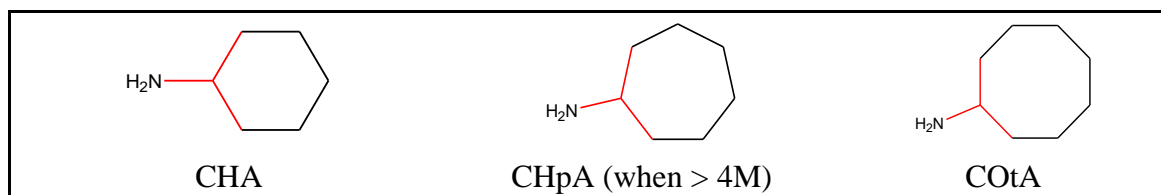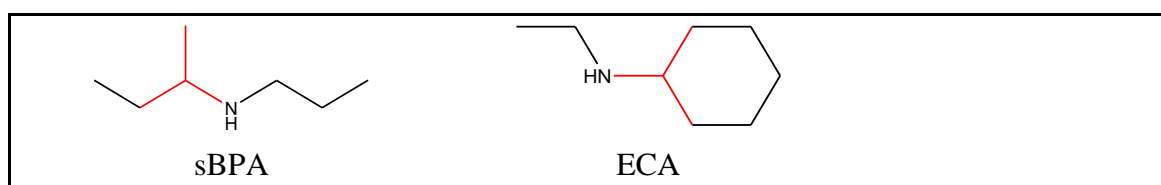
I. Branch at the α-carbon

<u>Single branch</u>
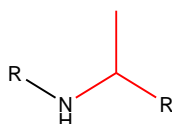
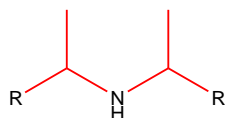(1) *Excellent performance*: fast reaction, high loading, no salts formation or precipitation

MCA   2MPD   2EPD
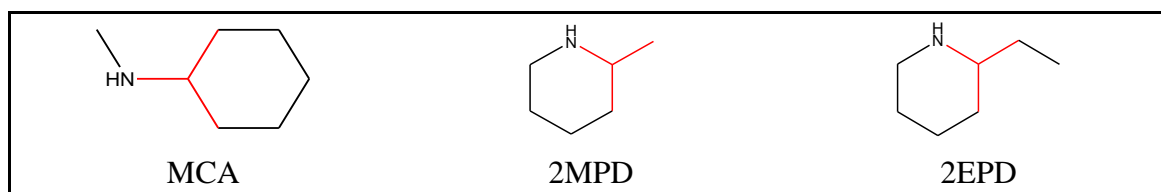
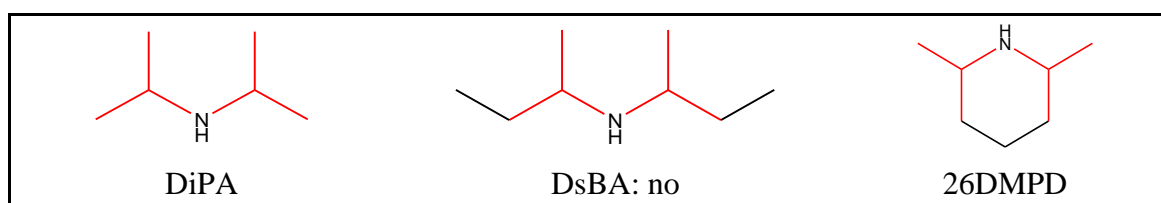(2) *Precipitation*: primary amines, ring structure

CHA   CHpA (when > 4M)   COtA

(3) *Salts formation*: secondary amines

sBPA   ECA

<u>Double branches</u>

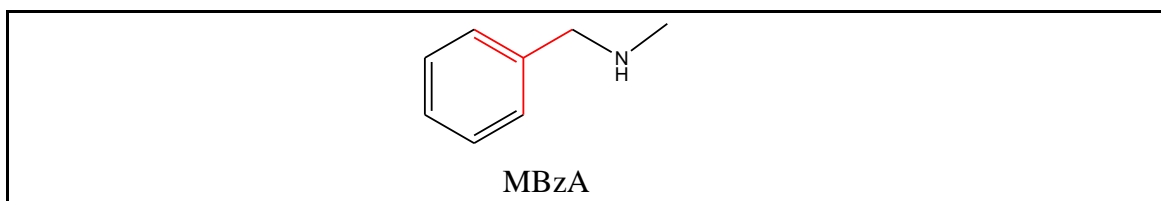*Salts formation* was found in all the follow amine solutions except DsBA.

DiPA   DsBA: no   26DMPD

iPCA   DCA   TMPD: gel
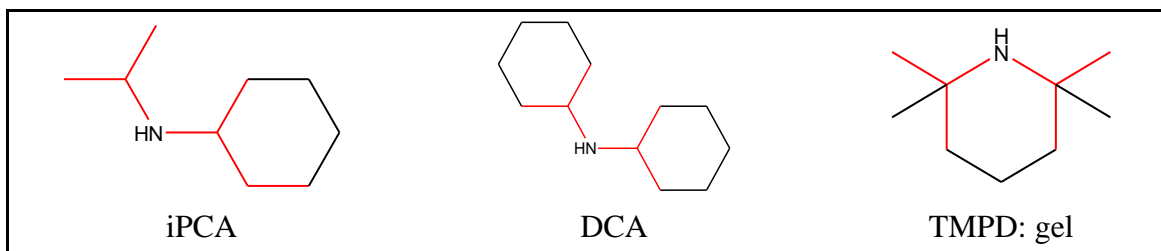
II. Branch at the β-carbon
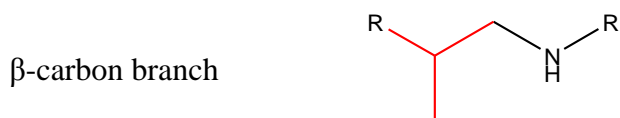
β-carbon branch

(1) *No salts formation or precipitation* was observed:

MBzA

(2) *Precipitation:*

BzA   EBzA

(3) *Salts formation*:

35DMPD   DiBA

III. Branches at both the α- and β-carbons
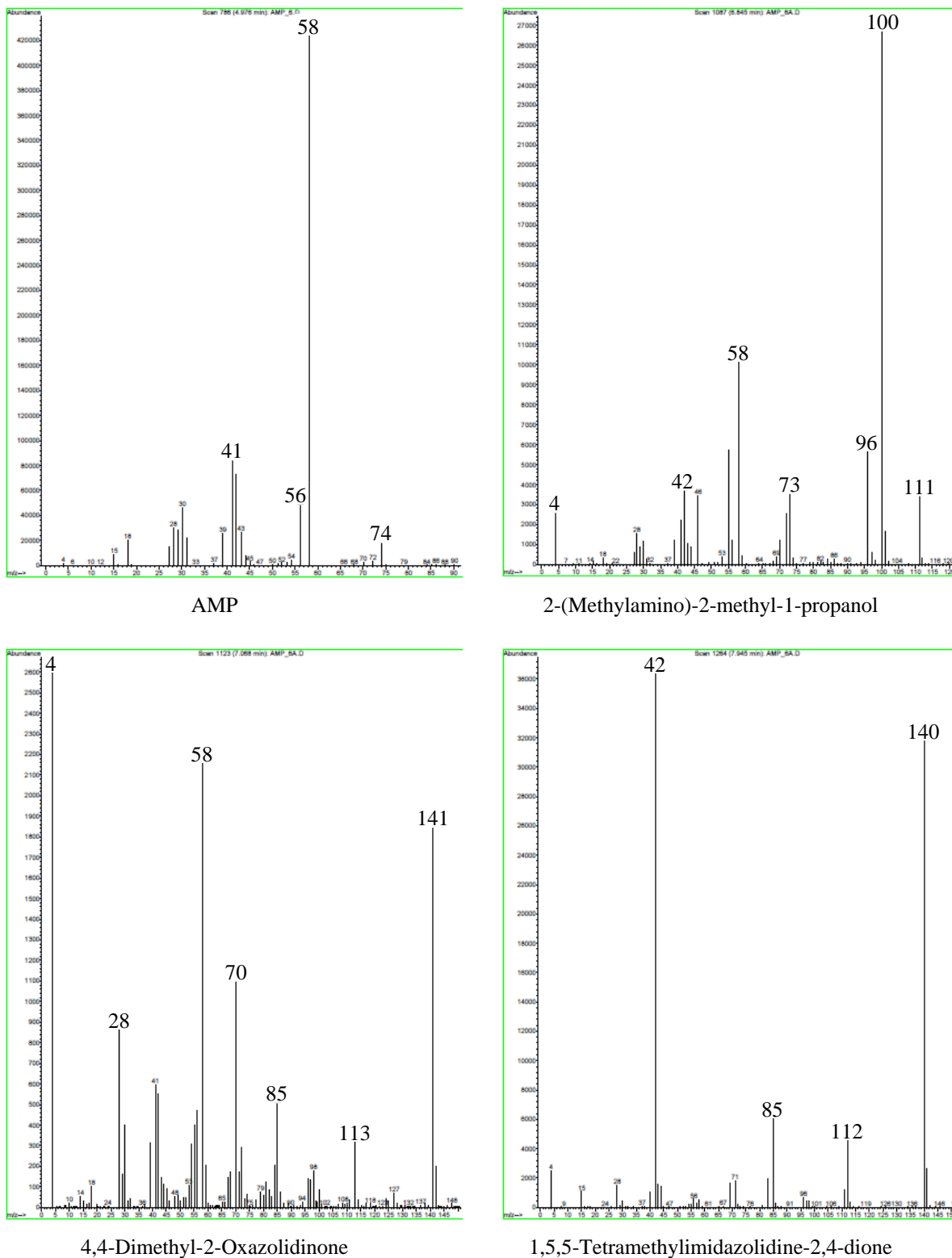
(3) *Salts formation*:

2MCA   iPBzA
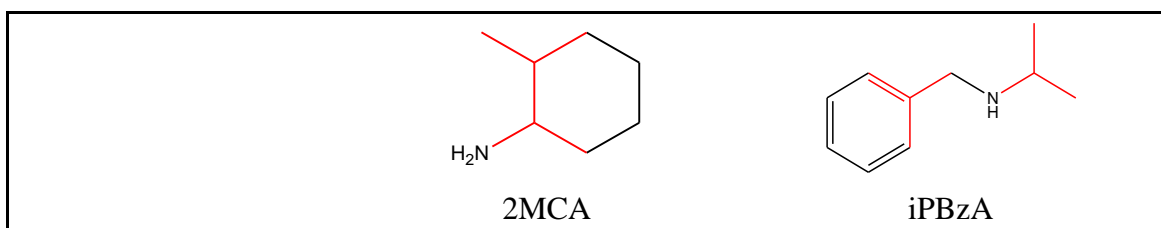
D MS spectra for main oxidative degradation products

D.1 Components from oxidation of alkanolamines

Corresponding to the GC-MS chromatogram of MEA shown in Figure 46 (A).

MEA

N-Methylformamide

Oxazolidin-2-one

4-Methylpiperazin-2-one
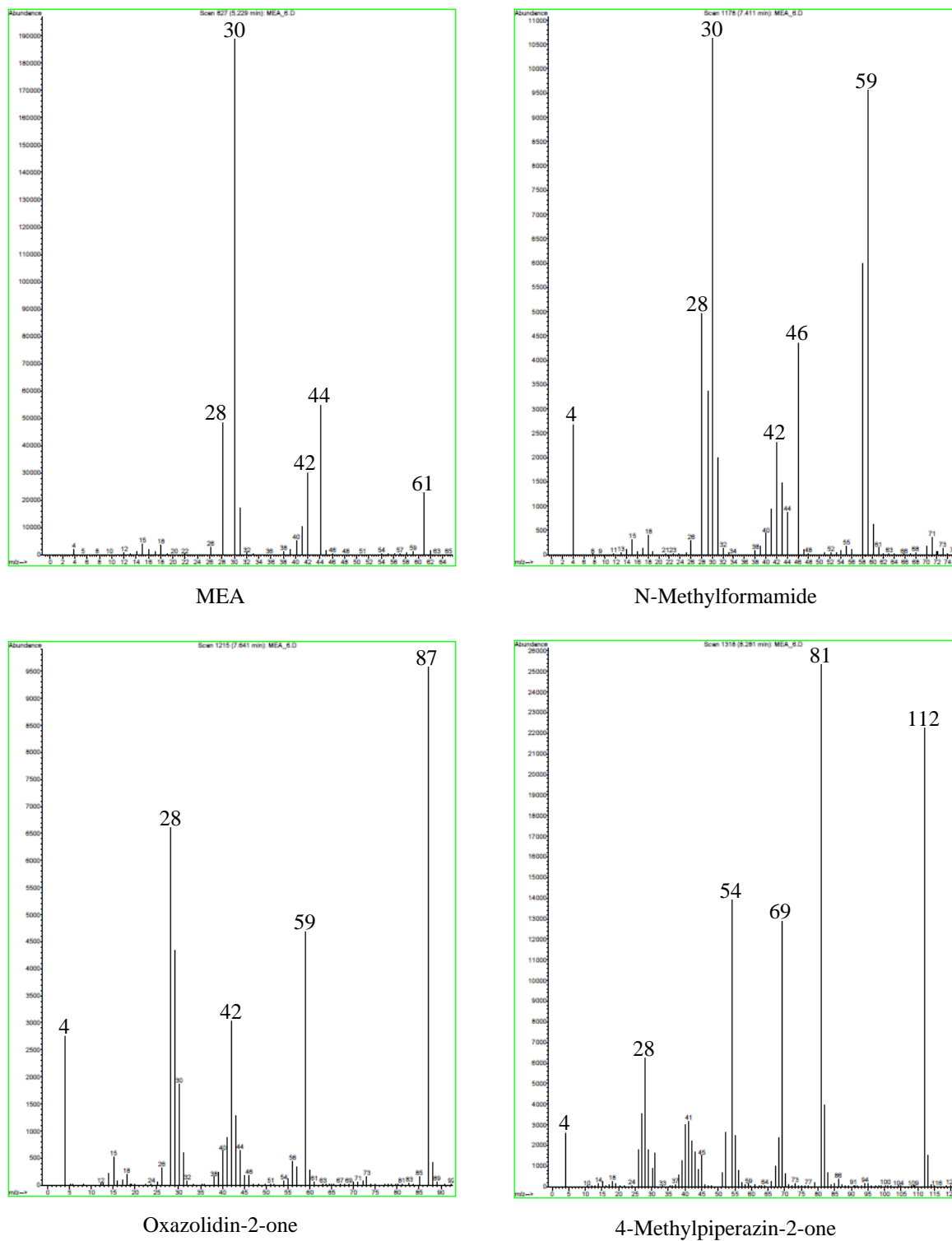
Figure 95. MS spectra for oxidative degradation products of MEA

Corresponding to the GC-MS chromatogram of AMP shown in Figure 46 (B).

AMP

2-(Methylamino)-2-methyl-1-propanol

4,4-Dimethyl-2-Oxazolidinone

1,5,5-Tetramethylimidazolidine-2,4-dione

Figure 96. MS spectra for oxidative degradation products of AMP

D.2 Components from oxidation of lipophilic amines

Corresponding to the GC-MS chromatogram of MCA shown in Figure 47 (A).

MCA

Cyclohexanone oxime

N-Isopropylcyclohexylamine

N-Methyldicyclohexylamine
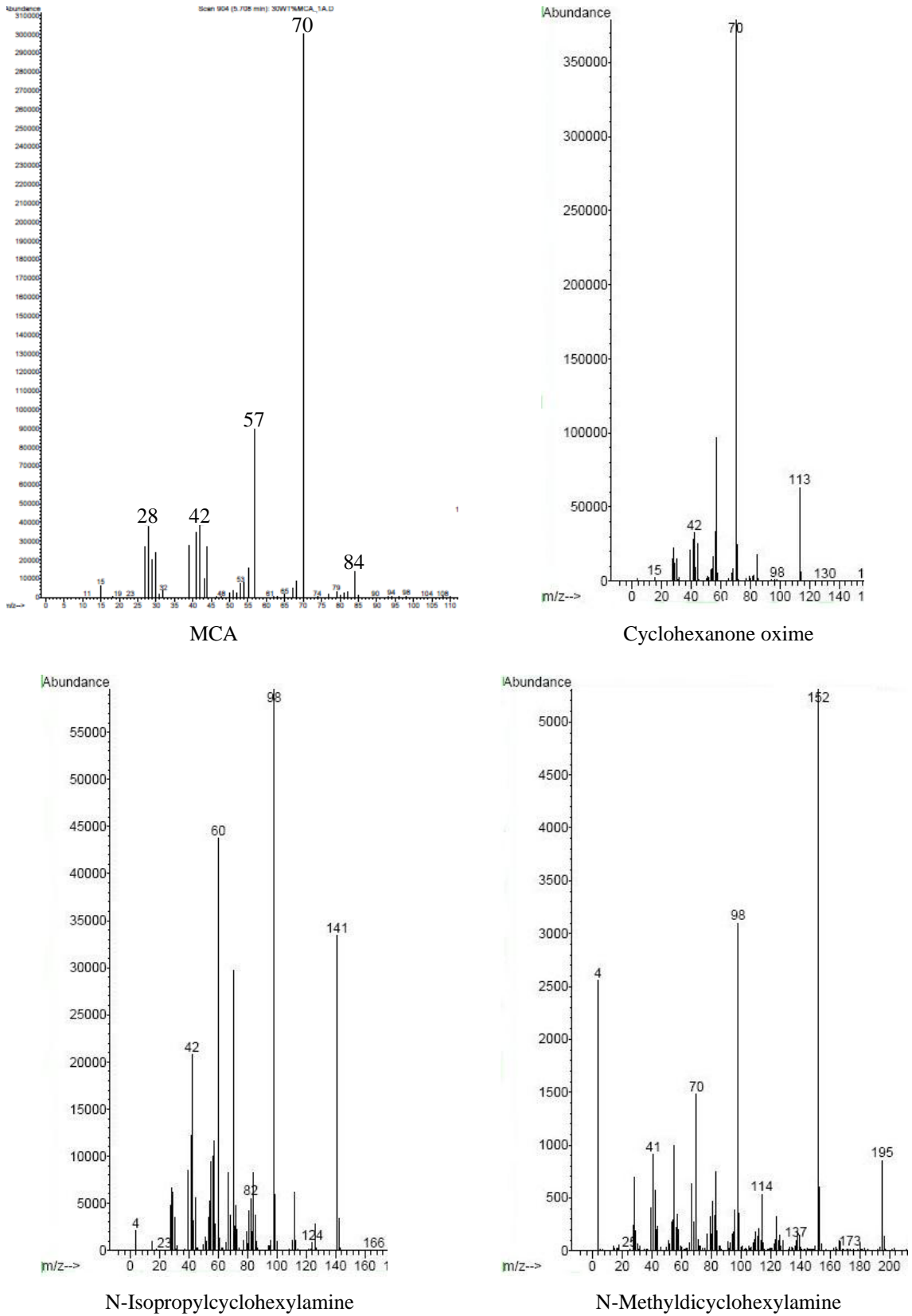
Figure 97. MS spectra for oxidative degradation products of MCA

Corresponding to the GC-MS chromatogram of DMCA shown in Figure 47 (B).

DMCA

CHA

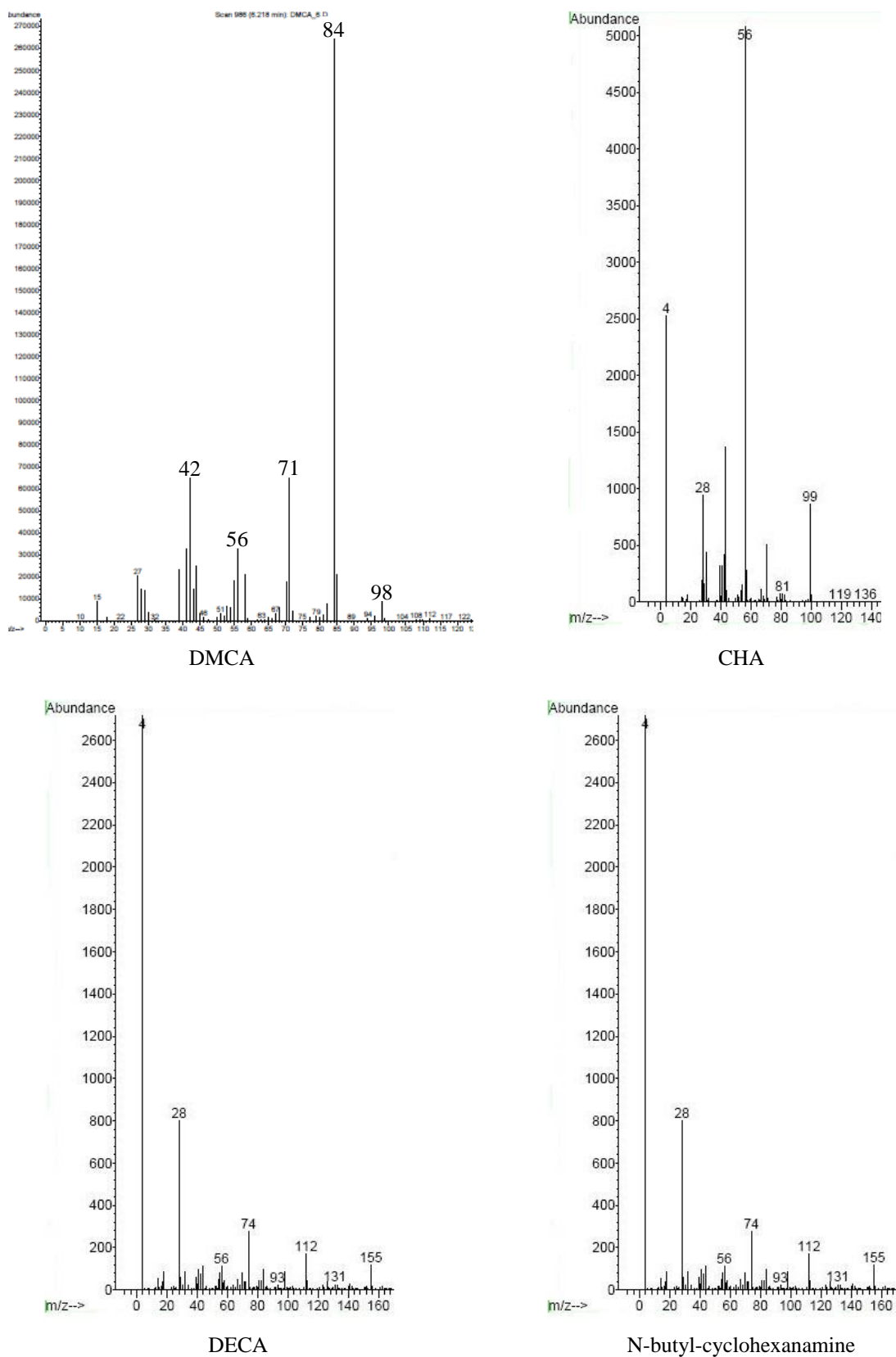DECA

N-butyl-cyclohexanamine

Figure 98. MS spectra for oxidative degradation products of DMCA

E   Measurement of physical properties

E.1   DIN standard Pycnometer

The density was measured by DIN standard pycnometers (DURAN) with determined volume of 25.268 and 52.486 cm^3 at room temperature (see Figure 99). The glass flask was filled with the liquid sample until approaching the neck of the flask and placed it in the water bath for a certain time to keep the sample at a desired temperature. Subsequently, a glass stopper with a capillary tube was placed in the neck and allowed the excess liquid to escape from the flask through the capillary tube. By weighing the unfilled and filled pycnometer, the density of sample can be determined with the following equation:

$$\rho_s(T) = \frac{m_{pyc,s} - m_{pyc,0}}{m_{pyc,w} - m_{pyc,0}} \cdot \rho_w(T) \qquad\qquad \text{Eq. A.1}$$

Figure 99. DIN standard pycnometer

E.2   Ubbelohde viscometer

The kinematic viscosity was initially measured by a certified Ubbelohde viscometer (SCHOTT) with glass capillaries sizes I and II for samples in the ranges of 1.2-10 mm^2/s and 10-100 mm^2/s (see Figure 100). After filling the viscometer with ca. 20 ml of sample, it was immersed into a water bath and an electronic timepiece ViscoClock (SCHOTT) was carefully installed. The measurement was conducted at least three times per sample when the thermostat (HAAKE F3) indicated a constant temperature for at least 10 minutes, and the measurement was carried out in the temperature range of 25-60 ^{o}C. The kinematic viscosity (v) was calculated with a capillary constant K, the

average value of the measured flow time t_m as well as the Hagenbach-Couette correction time t_H using the equation A.2. The dynamic viscosity (μ) was calculated by Eq. A.3 together with the previously determined densities ρ.

$$v = K \cdot (t_m - t_H)$$ Eq. A.2

$$\mu = v \cdot \rho$$ Eq. A.3

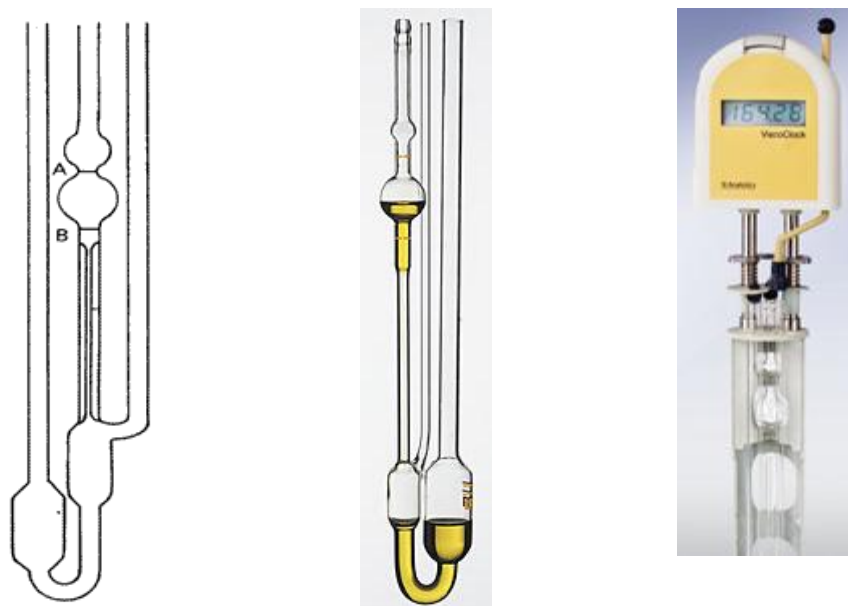$$t_H = \frac{E}{K \cdot t_m^{\,2}}$$ Eq. A.4

Figure 100. Ubbelohde viscometer with ViscoClock

E.3 Capillary tensiometer

The surface tension measurement was conducted with the maximum bubble pressure method in the laboratory of Physical Chemistry at TU Dortmund. A capillary tensiometer (see Figure 101) equipped with a precisely adjusted distance gauge and a U-tube manometer was used for measuring the dynamic surface tension of various solutions. After filling 30 ml of sample into the double-walled measuring vessel and heating it to a desired temperature, the capillary was immersed in the liquid sample at a constant distance (a = 6 mm in this experiment) above the distance indicator in each measurement. By opening the connection valve (V1), water flowed from the storage tube into the U-tube manometer. Simultaneously, bubbles continuously formed at the opening of the capillary and were broken at the maximum pressure drop (Δp_{max}), which was recorded by an analogue chart recorder with an electronic measuring device. Therefore, the dynamic surface tension can be calculated by Eq. A.5 and A.6.
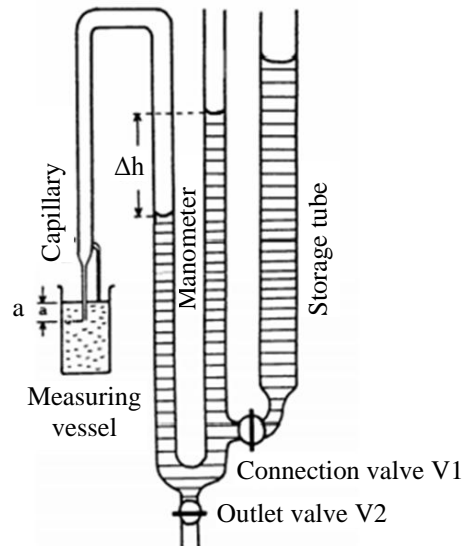
Figure 101. Apparatus for surface tension measurement

$$\frac{2\sigma}{r} = \Delta p_{max} - (\rho_s \cdot g \cdot a)$$ Eq. A.5

$$\Delta p_{max} = \rho_w \cdot g \cdot \Delta h$$ Eq. A.6

The measuring range of the recorder is 0 - 10 hPa and 100 scale divisions resulting in an accuracy of 10 Pa. In order to determine the radius (*r*) of the capillary, a control measurement with deionised water at 20 ° C was carried out using literature value $\sigma_w =$ 0.072736 N/m for calculation.

E.4 Goniometer

The contact angle was measured with the sessile drop method using a Krüss G40 analytical system (see Figure 102) at 20 °C in the Lehrstuhl für Biomaterialien und Polymerwissenschaften at TU Dortmund. Various metals such as stainless steel, aluminium, copper, brass, as well as plastics, e.g. hard polyvinyl chloride (H-PVC), polyethylene high-density (PE-HD), polypropylene homopolymer (PP-H) and Polytetrafluoroethylene (PTFE), were tested with the lean and rich solutions.

Figure 102. Krüss G40 analytical system

Declaration of Originality

I, Jiafei Zhang, hereby certify that this dissertation has been written by me, based on the original work conducted by me in the Department of Chemical Engineering at Technical University Dortmund between 2009 and 2012, except where specifically noted by citations in the text.

Jiafei Zhang

London, 02.12. 2013

CURRICULUM VITAE

Jiafei Zhang

Born in Hangzhou, 14 Nov. 1983

Since 2012	Postdoctoral Researcher in the Department of Chemical Engineering, Imperial College London, UK
2009 - 2012	Research Assistant and Ph.D. candidate in the Chair of Technical Chemistry B, Department of Biochemical and Chemical Engineering, Technical University of Dortmund (TU Dortmund), Germany
2006 - 2008	M.Sc. in *Chemical Engineering*, Department of Biochemical and Chemical Engineering, TU Dortmund, Germany
2002 - 2006	B.Sc. in *Applied Chemistry*, School of Chemical Engineering and Technology, China University of Mining and Technology, China
1999 - 2002	Hangzhou High School, Zhejiang Province, China